THE DETERMINATION OF MYOCARDIAL VIABILITY USING MAGNETIC RESONANCE IMAGING AND GD-DTPA

by

Raoul S. Pereira
Graduate Program in Medical Biophysics

Submitted in partial fulfilment
of the requirements for the degree of
Doctor of Philosophy

Faculty of Graduate Studies
The University of Western Ontario
London Ontario
August 1998

ABSTRACT

The non-invasive discrimination of viable from infarcted tissue after a heart attack is crucial for the proper management of patients. Recently, due to the use of new and effective therapies to restore flow to occluded coronary arteries, this has become even more important. Currently used imaging techniques lack the spatial resolution and/or specificity to accurately assess the extent of permanent tissue damage. It was postulated that the distribution volume (λ) of an extracellular MRI contrast agent (Gd-DTPA) would significantly increase in infarcted tissue due to damage of the myocyte cell membrane.

Using an animal model of ischaemia-reperfusion injury it was established that:

i) λ was inversely related to myocardial viability, *ie*: λ was greater in infarcted tissue with cell membrane damage

ii) λ was increased in damaged tissue as early as 1 minute to as late as 8 weeks post reperfusion

iii) λ could be accurately estimated *in vivo* using MR image signal intensities. This allowed us to follow λ *in vivo*. Previously, we determined λ using radioactive counting of ^{111}In-DTPA in excised tissue sections and blood samples.

Further, using an animal model of sustained coronary artery occlusion (without reperfusion) it was established that:

i) λ was increased in damaged tissue as early as 2 days post occlusion and may have been increased as early as 4 hours post occlusion.

Based on these encouraging results a limited clinical trial comparing contrast-enhanced MRI with rest-redistribution ^{201}Tl SPECT and dobutamine stress testing with cine MRI

functional assessment was performed. Analysis of the first 7 patients has established that:

i) increased signal intensity on MR images during a constant infusion of Gd-DTPA was indicative of infarcted tissue as determined by regions of decreased signal on ^{201}Tl SPECT images

ii) myocardial tissue with increased signal intensity failed to show increases in contractility with dobutamine, again indicating that these regions represent infarcted tissue.

iii) values of λ in damaged and normal tissue calculated *in vivo* were similar to those obtained in the animal studies.

Although additional animal and human work is needed to establish the relationship of increased distribution volume and myocardial tissue viability under all possible tissue states following ischemic injury, MRI with Gd-DTPA shows great promise in the non-invasive determination of myocardial viability

Key Words: myocardial infarction, magnetic resonance imaging, myocardial viability, Gd-DTPA, contrast-enhanced MRI

ACKNOWLEDGEMENTS

Although my name is on the front of this thesis there are many people who contributed to its completion. First and foremost I would like to thank my supervisor Frank Prato for his support, advice, guidance and friendship throughout the years. Jane Sykes has been an important part of this work providing technical support, help with experimental design, friendship and dedication beyond what could ever be expected of her. Gerry Wisenberg has been an integral part of this research, providing the 'clinical picture' which is so important in medical research. Dick Drost and Terry Thompson have provided encouragement, advice and technical support. Chris Ellis represented the 'non-MR' point of view, ensuring that my work was scientifically sound.

There are many others who contributed to this research both academically and also socially which was just as important. Although it may seem like a lot of people, I appreciated all of them and will try to list as many as possible but if I forget someone please accept my apologies. Eric Talman, with whom I participated in every sport I played and who was always a good friend; Andrew Farrall, my first friend at LRI; Baldev Ahluwalia, for his enthusiasm and friendship; John Potwarka, for always being willing to help out even with trivial problems; Keith St. Lawrence, for a lot of stuff Charlie McKenzie, my office partner for almost the last 5 years; Robert Stodilka; Rebecca Thornhill, who has only been here a short time but has made a big difference; Constance Campbell, my workout partner; Chun Y. (Edward) Tong; J Davis, for his invaluable computer support and interesting discussions; Suresh Pereira, my brother; Sara Edwards, who was an important part of much of the time I spent here. In addition: Cheryl McCreary, Dawn Kilkenny, Dan Hardy, Cynthia Maier, Peter Msaki, Dr. Z. Chen, Elizabeth Henderson, Dr. Kenneth Yvorchuk, all the people in the Department of Nuclear

Medicine, Robert Bartha, Brad Kemp, Greg Marsh, Pat McCabe, Chris Norley, Craig Jones, Dr. C.P.S. Taylor, Dr. Alan Groom, Dr. Ting Y. Lee, Alex Thomas, Michael Westmore, David Holdsworth, Dr. Brian Rutt, Michael Furmaniak, Dr. C. Rajgopal and all my soccer, ultimate frisbee, broomball, volleyball and baseball teams.

I would also like to thank those people who have guided me in the past. Dr. Ian MacDonald under whose guidance I undertook my first ever research project (and who has continued to help and support me throughout the years) and Drs. Marvin Sherebrin and Peter Canham who helped me during my undergraduate studies. Dr. J. Bryan Finlay who supervised my undergraduate research project (with the help of Dr. Robert Hardie and Boris Lysinski). Dr. Donald Dawson at the London Regional Cancer Centre who gave me my first exposure (ha ha) to medical physics. In addition, Drs. Rob Barnett, Peter Munro and Jerry Battista at the LRCC who showed me many things at the LRCC.

The work contained herein was supported by a grant from the Medical Research Council (MT-9467) to Drs. Prato, Wisenberg and Drost. Part of my support was provided by an Ontario Graduate Scholarship. In Chapters 2-5 I would like to acknowledge Berlex Canada (Lachine Quebec) for their donation of Gd-DTPA (Magnevist™ formulaton) and Dr. Richard Robb for the use of the 3D visualization software Analyze (in Chapters 3 and 5, AnalyzeAVW was used). For Chapter 2 I would also like to acknowledge Mr. Alex Thomas for statistical consultation. Siemens Canada and Dr. Orlando Simonetti are thanked for their hardware and software support.

Finally, I would like to thank my parents, Aubert and Phoebe, for always being supportive of everything I have done (whether successful or not) and for being so excited with all my successes. I hope I have made them proud and will continue to do so.

TABLE OF CONTENTS

LIST OF FIGURES

LIST OF TABLES

LIST OF APPENDICES

NOMENCLATURE

The following symbols and abbreviations were used in this thesis:

λ	Partition coefficient of tracer; ratio of concentration tissue to concentration in blood
β_{tissue}	Relaxivity of Gd-DTPA in tissue
β_{blood}	Relaxivity of Gd-DTPA in blood
$c_a(t)$	Concentration of tracer in arterial blood
$c_{tissue}(t)$	Concentration of tracer in myocardial tissue
E	Extraction fraction; percentage of tracer extracted during first pass of contrast agent
F	Regional myocardial blood flow
FOV	Field of view of MR image
Gd-DTPA	Gadolinium diethylenetriaminepentaacetic acid
LAD	Left anterior descending coronary artery
MRI	Magnetic resonance imaging
NMR	Nuclear magnetic resonance
PET	Positron emission tomography
R_1	Spin-lattice relaxation rate ($1/T_1$)
R_2	Spin-spin relaxation rate ($1/T_2$)
ΔS	Change in signal intensity from baseline
SPECT	Single photon emission computed tomography
T_1	Spin-lattice relaxation time constant
T_2	Spin-spin relaxation time constant
TE	Echo time
TR	Repetition time (magnetization recovery time)

1 Introduction

1.1 Overview of Thesis

The determination of myocardial viability after acute myocardial infarction (AMI) is very important clinically. This thesis deals with the development and validation of a diagnostic imaging test for infarcted myocardial tissue after AMI using magnetic resonance imaging (MRI) and the MR contrast agent gadolinium diethylenetriamine pentaacetic acid (Gd-DTPA). MRI offers better spatial resolution than any currently used technique for the determination of myocardial viability and this accurate assessment of the extent of infarcted tissue would aid greatly in patient management. We believed that at tissue equilibrium during an intravenous infusion of Gd-DTPA, regions of increased signal intensity would be indicative of infarcted or damaged myocardial tissue (and thus, regions of normal signal intensity would be viable). This introductory chapter outlines the importance of a high-resolution non-invasive diagnostic test for myocardial viability and provides an overview of currently used techniques. The central hypothesis of the thesis is then presented along with an outline of the thesis organization to show how the hypothesis was tested.

1.2 Impact of Ischemic Heart Disease

Ischemic heart disease, the presence of an atherosclerotic obstruction resulting in inadequate delivery of oxygen to heart muscle tissue either at rest or during exercise, is one of the largest causes of morbidity and death in North America. In 1995, 21% of all deaths in Canada were caused by ischemic heart disease and ½ of those were due to acute myocardial infarction, death of heart muscle resulting from a sudden reduction in blood flow by occlusion of a coronary artery with a thrombus or blood clot, usually

superimposed on a pre-existing atherosclerotic plaque. In 1995, cardiovascular diseases (including ischemic heart disease, stroke and other cardiovascular afflictions) accounted for $7.3 billion in direct health care costs: the costs of hospital expenditures, medical care, drugs and research. Indirect costs associated with loss of productivity due to illness or disability and the loss of future earnings due to premature mortality were estimated at $12.3 billion (1). Obviously, effective diagnosis and timely treatment of ischemic heart disease are clinically important.

1.3 Acute Myocardial Infarction

A heart attack or acute myocardial infarction (AMI) is caused by a sudden reduction in blood flow to heart tissue as a result of the blockage of a coronary artery which supplies blood to myocardial tissue. In the majority of AMI patients the coronary arteries are narrowed by atherosclerotic lesions. At the time of infarction, flow is suddenly stopped by an occlusive thrombus (or blood clot). There are other possible causes of AMI including but not limited to coronary artery spasm, coronary artery trauma or laceration, and arterial wall thickening due to non-atherosclerotic causes but these are a small minority of cases, limited to approximately 6% of patients (2).

The symptoms of AMI include severe prolonged chest pain, nausea and shortness of breath. Signs of AMI include, among other things anxiety, tachycardia (elevated heart rate) and elevated blood pressure. In the emergency room, electrocardiographic (ECG) recordings of the heart's electrical activity are used to help diagnose AMI. Characteristic changes in the ECG tracing can help to detect both the presence and location of myocardial infarction. In addition, serial blood samples to detect the release of cardiac enzymes such as creatine kinase MB (an isoform of creatine kinase characteristic to

cardiac muscle) from necrotic tissue into the blood can be used to confirm the diagnosis. These two procedures are routinely performed on all patients presenting to the emergency room with symptoms of AMI (2-4). In addition, angiography, an x-ray technique used to visualize coronary arteries by injecting x-ray-opaque dye directly into the coronary artery, may be performed to determine or verify the location, extent and severity of the blocked arteries. Since angiography is a fairly invasive procedure involving threading a catheter from the femoral artery through the aorta and into the coronary artery, its use in the acute phase is not routine (5).

1.3.1 Reperfusion

If blood flow is quickly restored to the heart little or no damage may occur; however, if flow is severely reduced for longer than 15-30 minutes, irreversible damage will arise (2,6,7). Up to approximately 6 hours of ischemia, some percentage of tissue can be salvaged by successful reperfusion (restoration of blood flow) but beyond this time no further tissue can be rescued (6,8-10). However, there is evidence that reperfusion, even late after the onset of ischemia when no more reversibly damaged tissue exists, may result in faster and more complete healing of the infarcted region (10,11) and possibly a reduction in the risk for development of ventricular wall aneurysm and rupture (8) as well as a reduction in mortality rates (2,12).

1.3.1.1 Tissue States; Stunned and Hibernating Myocardium

Although reperfusion can salvage reversibly damaged tissue, contractility does not always immediately normalize in this viable muscle. Two clinical scenarios of viable yet non-contracting myocardium have been recognized: stunned and hibernating myocardium (13-17). Stunned myocardium refers to non-contracting regions with essentially normal blood flow after reperfusion; these regions regain their contractility

spontaneously over a period of days to weeks. However, if reperfusion therapy is not completely successful, regions of myocardium with just enough blood flow to maintain viability may result. Despite partial recanalization of the occluded vessel, a critical coronary stenosis remains, with a chronic significant reduction in resting blood flow. This hibernating myocardium may regain its contractility if blood flow is returned to normal values through some interventional procedure (*ie*: angioplasty, coronary artery bypass surgery). Separation of tissue regions into viable/non-viable groups using classifications based solely on contractility will often be incorrect and may not indicate whether the above noted interventional procedures would be appropriate (18-20).

1.3.1.2 Methods of Reperfusion

Reperfusion can be accomplished by a variety of methods. Angioplasty, a procedure in which a balloon is threaded into the diseased coronary artery (similar to angiography[1]) and inflated to dilate the artery open, is used in both the acute situation and later if viable yet ischemic (hibernating) tissue is suspected to exist (2,21,22). Surgical reperfusion, *ie:* coronary artery bypass grafting where blood flow is routed around the blocked coronary artery by means of a transplanted vessel from elsewhere in the patient's body (*eg:* internal mammary artery), has been performed with variable success since the 1970's (2,23). Bypass surgery has been used to a limited degree in the acute setting although it remains as a standard therapy for those patients with symptoms related to chronic coronary artery obstruction. However, in the past decade the greatest impact on the treatment of AMI patients has been the use of thrombolytic therapy, with agents that

[1] Angiography and angioplasty are often done at the same time, with the results of the angiogram being used to guide angioplasty. Until recently, angiography was only used to determine whether angioplasty was feasible, to confirm the success of angioplasty or to administer thrombolytic therapy directly into the infarct-related artery. However, angiography is now being used as a diagnostic tool on its own to verify the extent of coronary obstruction and to help plan further therapy (22).

dissolve blood clots which are blocking coronary arteries (2,7,12). These thrombolytic agents can be administered intravenously (and therefore non-invasively) or directly into the coronary artery using techniques similar to angiography to deliver the agent. Unfortunately, thrombolytic therapy can not be administered in 50% or more of infarct cases due to concerns regarding serious complications such as intracranial haemorrhage and other internal bleeding (7). In these cases, angioplasty (if available) may be indicated as an alternative. Nonetheless, the importance of reperfusion for the survival of the patient is well recognized.

The non-invasive assessment of myocardial viability is obviously quite important, particularly with the widespread use of reperfusion therapy. Few patients present to the emergency room early enough to salvage all ischemic myocardium (*ie:* less than ½ hour) but patients who have potentially salvageable tissue may be treated differently than patients with no potential for salvage. If there is no potential for salvage, the patient may receive pharmaceutical therapy to prevent further infarction and may be put on a program of rehabilitation. However, even in cases where no residual viability is established, further interventional therapy may be beneficial as mentioned previously, but it may not need to be urgently performed and the patient can be allowed time to recuperate. In extreme cases where the extent of damage is very large, a heart transplant may be indicated. On the other hand, if there is potentially salvageable myocardium, further interventions may be indicated[2]. While these more invasive procedures are fairly successful in restoring blood flow, they result in increased short term medical costs (although in the long term, health care dollars will likely be saved by a reduced likelihood

[2] Up to 40% of patients treated with thrombolytics do not fully achieve reperfusion. In these patients, (rescue) angioplasty may be performed in an attempt to open the blocked arteries (5).

for further hospitalization in these patients). The best investment of these dollars for interventional procedures will be guided by accurate separation of patients into groups with salvageable and non-salvageable myocardium.

With the development of newer treatment techniques, greater demand for the accurate determination of tissue viability has arisen. Trans-myocardial laser revascularization (TMLR), where trans-luminal channels are made in the ventricular wall with a laser in order to reperfuse and possibly stimulate angiogenesis in ischemic regions has been shown to be highly effective (24, 25). This technique may be useful in patients with diffuse coronary artery disease (affecting both the major and minor coronary vessels rendering angioplasty or bypass surgery impossible) or in those who have had a previous. unsuccessful operation. For invasive techniques such as this to be used effectively, the clinician needs to be very confident that the benefits outweigh the potential risks and thus must be very sure that the tissue is viable. Of course, in addition to determining viability. regional blood flow must also be measured in order to separate hibernating and stunned myocardium since by definition, stunned myocardium will regain its contractility without further reperfusion. However, the determination of viability is a vital step in the patient's treatment and prognosis.

1.4 The Determination of Viability

Although it was previously mentioned that ECG recordings and enzyme levels are used to diagnose AMI, these techniques are of limited value in determining the region of infarction. ECG recordings can be used to locate the approximate area (posterior. anterior, etc ..) but not the exact extent (2). Thus, diagnostic imaging techniques are necessary if accurate identification of the extent of infarcted myocardial tissue is desired.

1.4.1 Nuclear Medicine Techniques

Currently used methods for the determination of myocardial viability are primarily nuclear medicine techniques. Single photon emission computed tomography (SPECT) using ^{201}Tl has been widely used for over a decade as an indicator of both viability and flow (26-29). ^{201}Tl is a potassium analog whose uptake is dependent on a functioning sodium-potassium pump in the cell membrane. Recently, other radiopharmaceuticals such as ^{99m}Tc-SestMIBI (methoxyisobutyl isonitrile) (30) and ^{123}I-labelled fatty acids (^{123}I-phenylpentadecanoic acid (IPPA) (31) or beta-methyl iodophenyl pentadecanoic acid (BMIPP)(32,33)) have been evaluated as indicators of viability as well; most of these tracers accumulate actively in viable muscle tissue but their delivery is dependent on both regional blood flow (for tracer delivery) and viability. Currently, the generally accepted gold standard for myocardial viability is positron emission tomography (PET) using ^{18}FDG (flourine-18 labelled deoxyglucose) which is a tracer of myocardial glucose metabolism (18,19,34-36). Preservation of glucose metabolism indicates viable tissue in ischemic zone. During ischemia glucose metabolism is increased preferentially in comparison to the usual myocardial energy substrate, free fatty acids. Thus, if flow is also determined using PET (generally with ^{13}N-labelled ammonia ($^{13}NH_3$)) regions with reduced blood flow but maintained or increased glucose metabolism (perfusion-metabolism mismatch regions) are viable and hibernating. ^{18}FDG PET has been quite successful in predicting the recovery of myocardial function after myocardial revascularization procedures (19,37). In addition, ^{201}Tl SPECT has shown good correlation with both the results of ^{18}FDG PET and recovery of function after revascularization (19,38,39).

These nuclear medicine techniques have been used extensively and are very valuable in the determination of myocardial viability. However, their major limitation is poor resolution. The typical spatial resolution of a ^{201}Tl SPECT image is approximately 1 cm; for PET it is a little bit better (~6 mm). However, these dimensions are large in relation to the thickness of the myocardial wall (~8-10 mm) and differences between the inner and outer wall can not be seen. Following occlusion of a coronary artery, tissue death occurs in a wavefront pattern starting from the inner myocardial wall (subendocardium) and extending towards the outer wall (subepicardium) as the duration of ischemia increases (6-10,40). In addition, the potential for restoration of contractility is dependent on the degree of transmural extent of the infarct (41-43). Thus, transmural differences in viability, if known, may be very important in deciding the course of treatment or prognosis of a patient but can not be assessed presently with the low resolution of nuclear medicine imaging.

1.4.2 Echocardiography

Another widely used imaging modality for cardiac imaging is ultrasound or echocardiography. Echocardiography can be used to measure contractility but, as stated above, this can not be used to differentiate between infarcted and viable yet non-contracting tissue (stunned, hibernating) (18,19,20). Furthermore, attempts at tissue characterization using echocardiography have shown limited success to date (44). Recently, dobutamine (a synthetic catecholamine) has been combined with echocardiography to differentiate infarcted from viable tissue (45-50). When administered at high doses (20-40 μg/kg/min) the contractility of normally perfused tissue increases while in ischemic tissue a redistribution of coronary flow away from areas supplied by stenotic coronary arteries (coronary steal) results in a decrease in

contractility. This biphasic response (an initial increase followed by a decrease in contractility as infusion rate increases) in ischemic tissue can be used to diagnose regional ischemia (51). At low doses (5-15 μg/kg/min) an increase in contractility in a region that has reduced contractility at baseline is considered indicative of viable tissue. Dobutamine echocardiography has been shown to be quite reliable in predicting recovery when compared to ^{18}FDG PET (45) and the eventual outcome of the patient (46-48,50,52). Although the transmural extent of infarction can not be directly assessed, the technique can detect whether the non-contractile yet viable myocardium has the potential to contract which may be equally as valuable. However, this technique requires the comparison of contractility with and without dobutamine. While a qualitative analysis of contractility is most often used, a quantitative analysis is difficult due to the difficulty in accurately delineating the endocardial surface with echocardiography (53).

1.4.3 *In vivo* NMR Spectroscopy

In vivo nuclear magnetic resonance (NMR) spectroscopy has been used extensively to study AMI. Surface coils, single voxel techniques such as ISIS and 1,2 or 3D chemical shift imaging (CSI) can be used to localize signal from a specific volume or volumes (54). ^{31}P NMR can be used to detect changes in the intracellular concentrations of certain metabolites in cardiac tissue, measurements that previously could only be determined using invasive procedures such as tissue biopsies (54). During ischemia, the intracellular levels of phosphocreatine (PCr), which is used to produce ATP, are depleted and ATP and ADP stores also slowly decline. There is a large increase in inorganic phosphate (P_I) and intracellular pH (estimated from the chemical shift between P_i and PCr) decreases as increasing amounts of lactic acid are produced by anaerobic glycolysis. With reperfusion, PCr and ATP stores are restored and P_i returns to normal levels in

normal tissue (55). Although *in vivo* spectroscopy can provide a wealth of useful information, the low sensitivity and low abundance of ^{31}P results in voxel sizes on the order of 3×3×3 cm or 27 cc for CSI at 1.5T. Even at higher fields (3-4 T), it is likely that voxel sizes will still be larger than those achieved with PET (54) which can not accurately delineate the extent of infarcted tissue. At the present time ^{31}P NMR is mainly used in animal studies and some limited trials in humans.

1.5 Cardiac MRI

MRI is an accepted technique for high resolution anatomical imaging of the heart (56). Sub-millimetre resolution is possible although in practice most images have in-plane resolution on the order of 1-2 mm. This is because there is a trade-off between image resolution and imaging time *ie*: increasing image resolution requires an increase in the imaging time if signal-to-noise ratio is to be maintained (57). Ultrafast imaging sequences (50-100ms acquisition time) may have pixel sizes in the range of 3 mm or more as a trade-off for speed of image acquisition. High resolution images can take anywhere from 1 second to 15 minutes or more to acquire. A great number of pathological states can be differentiated on the basis of tissue T_1 and T_2 relaxation times (58) and many MR imaging sequences have been developed to exploit these differences.

1.5.1 Non-Contrast Enhanced MRI in the Determination of Myocardial Viability

Many studies have examined the ability of non-contrast-enhanced MRI to distinguish between infarcted and viable tissue. In 1980 Williams *et al* (59) showed that proton T_1 in infarcted myocardial tissue was greater was than in normal tissue (Frank *et al* (60) presented an abstract in 1976 with similar results but a published paper could not

be found). Since then, many groups have shown that contrast in T_1 and T_2 exists between damaged and normal myocardium, primarily due to changes in water compartmentalization and tissue edema; however, T_1 contrast is weak (61-64) and T_2 contrast, while greater than T_1, tends to overestimate infarct size (64-69). Differences in T_2*, another MR tissue parameter sensitive to differences in blood oxygenation, has been suggested as a way to separate stunned from infarcted myocardium (70,71). However, T_2* contrast is dependent on a variable combination of tissue viability and blood flow and these techniques need to be explored further before entering clinical practice. Other MR techniques such as magnetization transfer (72,73), arterial spin tagging (74) and diffusion imaging (75) have been used with limited success.

The use of cine MRI, where images are taken throughout the cardiac cycle to make a movie loop of the beating heart has been combined with dobutamine stress testing (76-81). The use of MRI allows easier identification of the endocardial surface of the heart making a quantitative analysis of contractility more accurate than ultrasound imaging. Recently, MRI imaging techniques which place a grid of magnetization (tag lines) on the heart at end diastole have been developed; as the heart contracts the grid deforms and this deformation can be used to quantitate regional function (82).

Imaging of other nuclei such as ^{23}Na or ^{87}Rb has been attempted with some success (83-85). Since these agents are directly involved in cellular functioning they may provide valuable measures of cell viability. At the present time however, the resolution of these images is considerably less than current ^{1}H techniques (on the order of ½ cm or more), being similar to nuclear medicine methods. At present they remain important research tools but lack the needed resolution to be important for patient management.

1.5.2 Contrast-enhanced MRI in the Determination of Myocardial Viability

Contrast agents have been used extensively in cardiac MRI to monitor perfusion and assess viability. Susceptibility agents which greatly decrease T_2 or T_2* have recently shown some promise; however, these agents act to decrease signal intensity and hence signal-to-noise ratio (SNR) on most MR images (51,86-89). Paramagnetic ions strongly shorten T_1 due to magnetic interactions of their unpaired electrons with water protons. In 1978 Lauterbur *et al* (90) showed that the injection of manganese increased T_1 contrast (over the non-contrast-enhanced situation) between ischemic and normal myocardial tissue in a canine model of left anterior descending coronary artery (LAD) occlusion. Many other paramagnetic contrast agents have been developed and studied, particularly Gd-DTPA which has been available since the early 1980's (91). These contrast agents reduce absolute T_1 values and hence increase SNR and contrast-to-noise ratios in T_1-weighted cardiac images. Evidence from other groups, including our own, has suggested that the administration of Gd-DTPA may result in T_1 contrast between viable and infarcted myocardium (62,92-95).

1.6 Gd-DTPA and the Determination of Myocardial Viability

Gd-DTPA is a diffusible contrast agent that was developed in the early 1980's. It consists of gadolinium (Gd^{3+}) chelated to diethylenetriaminepentaacetic acid (DTPA) and has a molecular weight of 500 daltons. The toxicity of free Gd is reduced through chelation but it stills maintains some of its effectiveness in reducing T_1 ((relaxivity, β); β is reduced by a factor of approximately 2 due to the interference of access to Gd by DTPA) (91). The chelator DTPA determines the tissue distribution of the agent; it is excluded by a healthy cell membrane, and thus its distribution volume is limited to the

vascular and interstitial space (extracellular) in normal tissue. Gd-DTPA is eliminated from the body by glomerular filtration.

1.6.1 Theory of Increased Signal Enhancement in Infarcted Tissue after Administration of Gd-DTPA

Loss of cell membrane viability is the ultimate indicator of irreversible myocyte injury since the membrane is responsible for functions such as cell membrane regulation and the maintenance of ionic gradients (6,96-98). Although cell membranes in irreversibly damaged tissue begin to show signs of abnormally increased permeability during the period of coronary occlusion (96,97,99), reperfusion of these myocytes results in explosive cell swelling and bursting (6,100). Thus, in this tissue the membranes become very permeable to Gd-DTPA and the distribution volume of Gd-DTPA increases to include the space once occupied by the cytoplasm (95,101,102). The increased Gd in these regions results in increased signal intensity on MR images which are sensitive to changes in T_1. We believe that viable myocytes within stunned and hibernating myocardium, having maintained cell membrane integrity, remain impermeable to Gd-DTPA.

1.6.2 Measurement of the Distribution Volume of Gd-DTPA

In order to measure the distribution volume of Gd-DTPA a constant infusion of Gd-DTPA was used. Based on the modified Kety equation for diffusible tracers (62,101,103,104), when blood and tissue concentrations have reached an equilibrium the tissue concentration of Gd-DTPA is related to the partition coefficient λ as follows[3]:

$$\lambda = \frac{[Gd-DTPA]_{tissue}(\infty)}{[Gd-DTPA]_{blood}(\infty)}$$

[3] The partition coefficient λ differs from distribution volume only by a factor of blood hematocrit (*ie*: distribution volume = $\lambda \cdot (1-hct)$ where hct is hematocrit.

where ∞ indicates that the constant infusion has been on for an infinite amount of time and hence, the calculation of λ is not dependent on regional perfusion. However, the approach to equilibrium depends on regional blood flow and distribution volume (Figure 1-1). Normal tissue with normal blood flow reaches equilibrium more quickly than infarcted tissue with a larger distribution volume. Further, in viable tissue with low blood flow (ischemic or hibernating) equilibrium is reached more slowly due to reduced

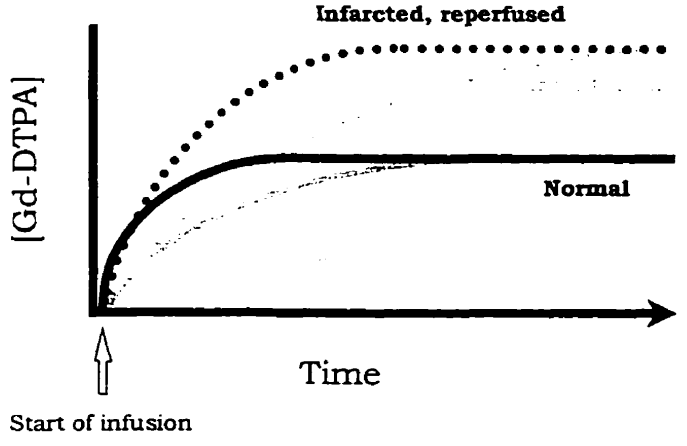

Figure 1-1 Schematic of enhancement patterns in various tissue regions during a constant infusion of Gd-DTPA

In normal, well perfused tissue, [Gd-DTPA] reaches an equilibrium with blood fairly quickly but in infarcted tissue with an increased distriubution volume, equilibrium is reached more slowly. Regional ischemia lengthens the time to reach equilibrium since tracer delivery to tissue is impaired. This schematic uses a constant infusion.

delivery of tracer. Our infusion protocol consisted of a bolus followed by a prolonged constant infusion. Although in theory λ needs to be calculated at an infinite time after the start of the infusion, previous studies have shown that if blood flow is at least 10% of normal, equilibrium will be reached within 15-20 using this infusion protocol (104). Since Gd-DTPA is cleared by the kidneys (91) this infusion protocol results in a steady

state or constant extracellular concentration as the amount being infused equals the amount being cleared. This allows longer imaging times to be used (at centres with slower MR scanners) or more imaging procedures to be accomplished (functional studies, higher resolution imaging).

Most previous studies with Gd-DTPA or similar extracellular agents have utilized a bolus injection of contrast agent. After such an injection the enhancement patterns are dependent on both regional blood flow and distribution volume; signal in the tissue is thus dependent on the time after injection (92,94,105,106). With a constant infusion protocol this dependence is reduced. Figure 1-2 shows an *in vivo* example in a canine

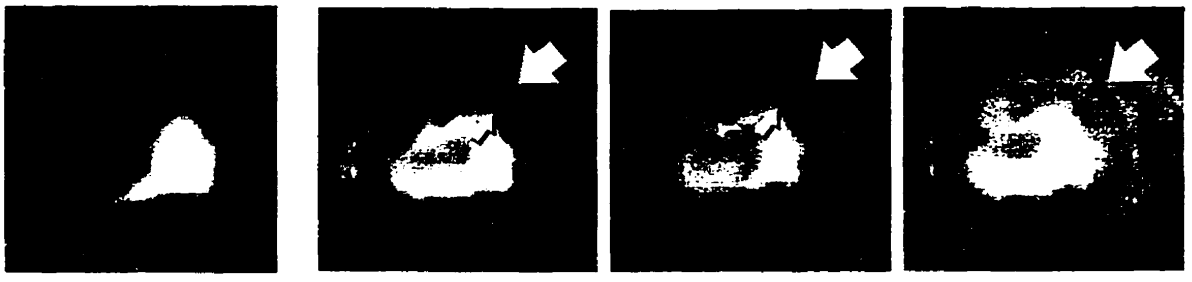

a) Pre-contrast b) 2 minutes c) 12 minutes d) 40 minutes

Figure 1-2 *In vivo* changes in T_1-wighted MR image signal intensity during a constant infusion of Gd-DTPA

Pre infusion (a) relatively constant signal enhancement is seen. At 2 minutes after the start of the infusion signal enhancement in the periphery of the infarct is seen (big arrow) but there is a subendocardial signal void (b, small arrow). By 40 minutes after the start of the infusion the signal void filled in (c,d).

model 1 week after reperfusion of a 2 hour occlusion of a coronary artery. Before Gd-DTPA infusion (Fig. 1-2a) tissue signal intensity is homogeneous on a T_1-weighted MR image. Two minutes after the start of the infusion (Fig. 1-2b) there is a region of increased signal intensity but along the subendocardial wall of the heart there is a signal

void due to reduced blood flow limiting the delivery of tracer to this region. As the infusion continues this subendocardial signal void fills in (Fig. 1-2c,d; 12 and 40 minutes after the start of the infusion respectively) allowing a high-resolution non-invasive determination of myocardial viability without the confounding factor of regional tissue perfusion (signal intensity is minimally dependent on perfusion).

1.7 Hypothesis

This work sought to answer the question of whether magnetic resonance imaging with Gd-DTPA could be used to determine myocardial viability after acute myocardial infarction. *The central hypothesis was that the loss of cell membrane integrity in infarcted tissue would result in a greater distribution volume (λ) for Gd-DTPA.* Thus, during a constant infusion of Gd-DTPA when tissue concentration of Gd is related to λ, regions of increased signal intensity on MR images would represent infarcted tissue. By using a constant infusion protocol, the dependence on regional blood flow would be reduced. Previous studies of myocardial viability using Gd-DTPA have not addressed the causes of signal enhancement in damaged tissue nor have they characterized changes in the cause of enhancement with time. By directly measuring the distribution volume of Gd-DTPA this thesis hoped to address some of these issues.

1.8 Objectives and Organization of Thesis

To address the hypothesis, the objectives of this work were to:

i) validate that λ was related to myocardial viability in a canine model of ischemia and reperfusion (Chapters 2 and 3).

ii) examine the time course of changes in λ after reperfusion in this model, *ie*: how soon did λ increase and did it increase or decrease with time (Chapters 2 and 3).

iii) investigate whether λ would be increased in the absence of reperfusion and whether this increased λ could be detected using our technique. This would be important in the clinical situation when the true success of reperfusion may not be known (Chapter 4).

iv) validate the results of the canine studies in a limited clinical trial of patients with acute myocardial infarction (Chapter 5).

The thesis was organized as follows:

Chapter 2 λ was measured after reperfusion periods of 2 hours to 3 weeks following a 2 hour occlusion of a coronary artery in the canine model. This represented a reasonable range of times over which the clinical determination of myocardial viability was needed. λ was found to be indicative of myocardial viability, as measured with ^{201}Tl at all of these reperfusion time periods. *The contents of this chapter were published in Magnetic Resonance in Medicine (Magn. Res. Med. **36**, 684-693 (1996)); the authors were Raoul S. Pereira, Frank S. Prato, Gerald Wisenberg and Jane Sykes. Minor changes were made to the text to improve the flow and clarity and a few references were added but the majority of the paper was left unchanged. I was responsible for designing and carrying out the experiments, Drs. Prato and Wisenberg supervised the project and also helped in the design of the studies and Jane Sykes provided technical support for the animal studies. Dr. Dick J. Drost also provided technical assistance when using the Siemens MR unit.*

Chapter 3 Expanding on the previous chapter, this chapter examined reperfusion times of less than 2 hours and greater than 3 weeks in order to more fully characterize λ

and its relationship to viability. We noted in chapter two that as early as two hours post-reperfusion λ in infarcted tissue was markedly increased and beyond 1 day of reperfusion a trend towards decreasing λ was noted (although λ was always greater in infarcted than in normal tissue). The results of this chapter showed that as early as 1 minute post reperfusion to as late as 8 weeks increases of λ in damaged tissue were noted. The results also suggested that immediately following reperfusion, λ in infarcted tissue increased gradually over a period of 2 hours or more and did not immediately increase to its final value. In addition, this chapter validated a technique to measure λ *in vivo* using image signal intensities rather than the *ex vivo* method we previously used involving radioactive counting of ^{111}In-DTPA in tissue sections. The results of these first two chapters also showed that even if reperfusion was not very successful (and blood flow was as low as 10% of normal) increases in λ could still be seen in infarcted tissue. *The contents of this chapter were accepted with revisions in June 1998 by Magnetic Resonance in Medicine; the authors were Raoul S. Pereira, Frank S. Prato, Jane Sykes and Gerald Wisenberg. Once again, only minor changes were made to the text. I was responsible for designing and performing the experiments and Drs. Prato and Wisenberg supervised the research and helped in the experimental design. Jane Sykes provided technical support and also provided assistance and advice in the development of the animal model.*

Chapter 4 Chapters 2 and 3 dealt with the situation where blood flow was restored at least in part to the coronary artery. This chapter presented some limited results where the ligature was not removed from the coronary artery so the artery was

permanently occluded. Animals were sacrificed at 4 hours, 2 days and 1 week post occlusion and marked increases in λ were seen at 2 days and longer. At 4 hours although λ appeared to increase in some sections, the increases were not very large and in the extremely low flow regions no increases were seen. While this work is by no means complete, it gave us confidence that after at least 2 days we would see increases in λ in damaged tissue regardless of whether or not reperfusion was attempted and allowed us to begin the clinical trial described in Chapter 5. *The studies contained in this chapter were developed and analyzed by me with the aid of Drs. Frank Prato and Gerald Wisenberg. Jane Sykes provided technical support as well as assistance and advice with the animal model.*

Chapter 5 Finally, based on the results of Chapters 2 to 4 the technique was tested in humans in a limited clinical trial. This trial is ongoing: to date 7 patients have been studied and the available results are presented here. These results indicated that the constant infusion procedure is feasible in humans and accurate when compared to accepted measures of viability such as ^{201}Tl SPECT and dobutamine stress testing. *The contents of this chapter will be submitted for publication when more patients have been studied. The results presented here are those obtained to date and have confirmed our hypothesis that damaged human tissue has increased values of λ as was seen in dogs. The protocol was developed by myself with the aid of Drs. Prato, Wisenberg and Ken Yvorchuk. The ^{201}Tl SPECT studies were carried out by the Department of Nuclear Medicine at St. Joseph's Health Centre and I have been performing the MRI studies.*

1.9 References

1. Heart Disease in Canada, *Heart and Stroke Foundation of Canada internet site*. Ottawa, Ontario, Canada, 1997.
2. R.C. Pasternak, E. Braunwald, B.E. Sobel, Acute Myocardial Infarction. *in* "Heart Disease, A Textbook of Cardiovascular Medicine" (E. Braunwald, Ed). p. 1200 W.B. Saunders, Toronto, 1992.
3. T.M. Guest, A.S. Jaffe, Rapid diagnosis of acute myocardial infarction. *in* "The Treatment of Myocardial Infarction" (N.S. Kleiman, Ed), *Cardiology Clinics* **13(3)**. 283-294 (1995).
4. J.E. Adams, D.R. Abendschein, A.S. Jaffe, Biochemical markers of myocardial injury. Is MB creatine kinase the choice for the 1990s?. *Circulation* **88**. 750-763 (1992).
5. H.V. Anderson, Role of angiography. *in* "The Treatment of Myocardial Infarction" (N.S. Kleiman, Ed), *Cardiology Clinics* **13(3),** 407-419 (1995).
6. K.A. Reimer, R.B. Jennings, A.H. Tatum, Pathobiology of acute myocardial ischemia, metabolic, functional and ultrastructural studies. *Am. J. Cardiol.* **52**. 72A-81A (1983).
7. M.L. Simoons, Risk-benefit of thrombolysis. *in* "The Treatment of Myocardial Infarction" (N.S. Kleiman, Ed), *Cardiology Clinics* **13(3)**, 339-345 (1995).
8. K.A. Reimer, J.E. Lowe, M.M. Rasmussen, R.B. Jennings, The wavefront phenomenon of ischemic cell death. 1. Myocardial infarct size *vs* duration of coronary occlusion in dogs. *Circulation* **56,** 786-794 (1977).
9. K.A. Reimer, R.B Jennings, The "wavefront phenomenon" of myocardial ischemic cell death. II Transmural progression of necrosis within the framework of ischemic bed size (myocardium at risk) and collateral flow. *Lab. Invest.* **40,** 633-644 (1979).
10. V. Richard, C.E. Murray, K.A. Reimer, Healing of myocardial infarcts in dogs. Effects of late reperfusion. *Circulation* **92,** 1891-1901 (1995).
11. J.S. Hochman, H. Choo, Limitation of myocardial infarct expansion by reperfusion independent of myocardial salvage. *Circulation* **75,** 299-306 (1987).
12. H.D. White, Selecting a thrombolytic agent. *in* "The Treatment of Myocardial Infarction" (N.S. Kleiman, Ed), *Cardiology Clinics* **13(3),** 347-354 (1995).
13. E. Braunwald, R.A. Kloner, The stunned myocardium: Prolonged, post-ischaemic ventricular dysfunction. *Circulation* **66,** 1146-1149 (1982).
14. E. Braunwald, J.D. Rutherford, Reversible ischemic left ventricular dysfunction: Evidence for the "hibernating myocardium". *JACC*, **8**, 1467-1470 (1986).
15. H. Kusoda, E. Marban, Cellular mechanisms of myocardial stunning. *Ann. Rev. Physiol.*, **54,** 243-256 (1992).
16. M.L. Charlat, P.G. O'Neill, C.J. Hartley, R. Bolli, Prolonged abnormalities of left ventricular diastolic wall thinning in the "stunned" myocardium in conscious dogs: time course and relation to systolic function. *JACC*, **13,** 185-194 (1989).
17. S.G. Ellis, C.I. Henschke, T. Sandor, J. Wynne, E. Braunwald, R.A. Kloner, Time course of functional and biochemical recovery of myocardium salvaged by reperfusion. *JACC* **1,** 1047-1055 (1983).
18. R. Bolli, Myocardial "stunning" in man. *Circulation*, **6,** 1671-1691 (1992).

19. V. Dilsizian, R.O. Bonow, Current diagnostic techniques of assessing myocardial viability in patients with hibernating and stunned myocardium. *Circulation* **87**, 1-20 (1993).
20. P. Perone-Filardi, S.L. Bacharach, V. Dilsizian, S. Maruea, J.A. Marin-Neto, J.A. Arrighi, J.A. Frank, R.O. Bonow, Metabolic evidence of viable myocardium in regions with reduced wall thickness and absent wall thickening in patients with chronic left ventricular dysfunction. *JACC* **20**, 161-168 (1992).
21. M.R. Johnson, Principles and practice of coronary angiography. *in* "Cardiac Imaging" (D.J. Skorton, H.R. Schelbert, G.L. Wolf, .H. Brundage, Eds), p.220 W.B. Saunders, Toronto, 1996.
22. M.C.G. Horrigan, E.J. Topol, Direct angioplasty in acute myocardial infarction. State of the art and current controversies, *in* "The Treatment of Myocardial Infarction" (N.S. Kleiman, Ed), *Cardiology Clinics* **13(3)**, 321-328 (1995).
23. M.E. Seleka, Cardiac surgical procedures following myocardial infarction. *in* "The Treatment of Myocardial Infarction" (N.S. Kleiman, Ed), *Cardiology Clinics* **13(3)**, 321-328 (1995).
24. M. Mirhoseini, S. Shelgikar, M.M. Cayton, New concepts in revascularization of the myocardium. *Ann. Thorac. Surg.* **45**, 415-420 (1988).
25. B.J. DeGuzman, D.B. Lautz, F.Y. Chen, R.G. Laurence, R.M. Ahmad, K.A. Horvath, L.H. Cohn, Thoracoscopic transmyocardial laser revascularization. *Ann. Thorac. Surg.* **64**, 171-174 (1997).
26. G.M. Pohost, L.M. Zir, R.H. Moore, K.A. McKusick, T.E. Guiney, G.A. Beller, Differentiation of transiently ischemic from infarcted myocardium by serial imaging after a single dose of thallium-201. *Circulation* **55**, 294-302 (1977).
27. G.A. Beller, D.D. Watson, P. Ackel, G.M. Pohost, Time course of thallium-201 redistribution after transient myocardial ischemia. *Circulation* **61**, 791-797 (1980).
28. C.A. Moore, J. Cannon, D.D. Watson, S. Kaul, G.A. Beller, Thallium-201 kinetics in stunned myocardium characterised by severe post-ischaemic systolic dysfunction. *Circulation* **81**, 1622-1632 (1990).
29. A. Elhendy, G. Trocino, A. Salustri, J.H. Cornel, J.R.T.C. Roelandt, E. Boersma, R.T. van Domburg, E.P. Krenning, G.M. El-Said, P.M. Fioretti, Low-dose dobutamine echocardiography and rest-redistribution thallium-201 tomography in the assessment of spontaneous recovery of left ventricular function after recent myocardial infarction. *Am. Heart J.* **131**, 1088-1096 (1996).
30. P. Rigo, T. Benoit, S. Braat, The role of technitium-99m-sestamibi in the evaluation of myocardial viability. *in* "Myocardial Viability: Detection and Clinical Relevance" (A.S. Iskandrian, E.E.van der Wall, Eds), p.39, Kluwer, Dordrecht, 1994.
31. C.L. Hansen, J. Heo, C. Oliner, W. Van Decker, A.S. Iskandrian, Prediction of improvement in left ventricular function with iodine-123-IPPA after coronary revascularization. *J. Nucl. Med.* **36**, 1987-1993 (1995).
32. F.F. Knapp, P. Franken, J. Propp, Cardiac SPECT with iodine-123-labelled fatty acids: Evaluation of myocardial viability with BMIPP. *JNM* **35**, 1022-1030 (1995).

33. P.R. Franken, P. Dendale, F. De Geeter, D. Demoor, A. Bossuyt, P. Block. Prediction of functional outcome after myocardial infarction using BMIP and sestamibi scintigraphy. *J. Nucl. Med.* **37**, 718-722 (1996).
34. M.E. Phelps, E.J. Hoffman, C. Selin, S.C. Huang, G. Robinson, N. MacDonald, H.R.. Schelbert, D.E. Kuhl, Investigation of ^{18}F-2-deoxyglucose for the measurement of myocardial glucose metabolism. *JNM* **19**, 1311-1319 (1978).
35. Y. Choi, R.C. Brunken, R.A. Hawkins, S.C. Huang, D.B. Buxton, C.K. Hoh, M.E. Phelps, H.R. Schelbert, Factors affecting myocardial 2-[F-18]fluoro-2-deoxy-D-glucose uptake in positron emission tomography studies of normal humans. *Eur. J. Nucl. Med.* **20**, 308-318 (1993).
36. R.O. Bonow, V. Dislizian, A. Cuoloco, S.L. Bacharach, Identification of viable myocardium in patients with chronic coronary artery disease and left ventricular dysfunction: Comparison of thallium scintigraphy with reinjection and PET imaging with ^{18}F-fluorodeoxyglucose. *Circulation* **83**, 26-37 (1991).
37. N. Tamaki, Y. Yonekura, K. Yamashita, H. Saji, Y. Magata, M. Senda, Y. Konishi, K. Hirata, T. Ban, J. Konishi, Positron emission tomography using fluorine-18 deoxyglucose in evaluation of coronary artery bypass grafting. *Am. J. Cardiol.* **64**, 860-865 (1989).
38. A.S. Iskandrian, A.-H. Hakki, S.A. Kane, I.P. Goel, E.D. Mundth, A.-H. Hakki, B.L. Segal, Rest and redistribution thallium-201 myocardial scintigraphy to predict improvement in left ventricular function after coronary arterial bypass grafting. *Am. J. Cardio.* **51**, 1312-1316 (1983).
39. V. Dilsizian, P. Perrone-Filardi, J.A. Arrighi, S.L. Bacharach, A.A. Quyyumi, N.M.T. Freedman, R.O. Bonow, Concordance and discordance between stress-redistribution-reinjection and rest-redistribution thallium imaging for assessing viable myocardium. Comparison with metabolic activity by positron emission tomography. *Circulation* **88**, 941-952 (1993).
40. K.A. Reimer, R.S. VanderHeide, V.J. Richard, Reperfusion in acute myocardial infarction: Effect of timing and modulating factors in experimental models. *Am. J. Cardiol.* **72**, 13G-21G (1993).
41. B.L. Karolle, R.E. Carlson, A.M. Aisen, A.J. Buda, Transmural distribution of myocardial oedema by NMR relaxometry following myocardial ischaemia and reperfusion. *Am. Heart. J.* **122**, 655-664 (1991).
42. A.N. Lieberman, J.L. Weiss, B.I. Jugdutt, L.C. Becker, B.H. Bulkley, J.H. Garrison, G.M. Hutchins, C.A. Kallman, M.L. Weisfeldt, Two-dimensional echocardiography and infarct size: Relationship of regional wall motion and thickening to the extent of myocardial infarction in the dog. *Circulation* **63**, 739-745 (1981).
43. M.J. Hurley, M.C. Sterling, M. Choy, A.J. Buda, K.P. Gallagher, Direct measurement of inner and outer wall thickening dynamics with epicardial echocardiography. *Circulation* **74**, 164-172 (1986).
44. J.E. Pérez, M.R. Holland, B. Barzilai, S.M. Handley, B.F. Vandenberg, J.G. Miller, D.J. Skorton, Ultrasonic tissue characterization of cardiovascular tissue. *in* "Cardiac Imaging" (D.J. Skorton, H.R. Schelbert, G.L. Wolf, .H. Brundage, Eds), p.606..B. Saunders, Toronto, 1996.

45. L.A. Piĕrard, M. DeLandsheere, C. Berthe, P. Rigo, H.E. Kulbertus, Identification of viable myocardium by echocardiography during dobutamine infusion in patients with myocardial infarction after thrombolytic therapy: Comparison with positron emission tomography. *JACC* **15**, 1021-1031 (1990).
46. G. Barilla, M. Gheorghiade, M. Alam, F. Khaja, S. Goldstein, Low-dose dobutamine in patients with acute myocardial infarction identifies viable but not contractile myocardium and predicts the magnitude of improvement in wall motion abnormalities in response to coronary revascularisation. *Am. Heart J.* **122**, 1522-1531 (1991).
47. S.C. Smart, S. Sawada, T. Ryan, D. Segar, L. Atherton, K. Berkovitz, P.D.V. Bourdilon, H. Feigenbaum, Low-dose dobutamine echocardiography detects reversible dysfunction after thrombolytic therapy of acute myocardial infarction. *Circulation* **88**, 405-415 (1993).
48. M. Previtali, A. Poli, L. Lanzarini, R. Fetiveau, A. Mussini, M. Ferrario, Dobutamine stress echocardiography for assessment of myocardial viability and ischaemia in acute myocardial infarction treated with thrombolysis. *Am. J. Cardiol.* **72**, 124G-130G (1993).
49. C.G. Cigarroa, C. deFilippi, E. Brickner, L.G. Alvarez, M.A. Wait, P.A. Grayburn, Dobutamine stress echocardiography identifies hibernating myocardium and predicts recovery of left ventricular function after coronary revascularization. *Circulation* **88**, 430-436 (1993).
50. P.A. Marcovitz, V. Shayna, R.A. Horn, A. Hepner, W.F. Armstrong, Value of dobutamine stress echocardiography in determining the prognosis of patients with known or suspected coronary artery disease. *Am. J. Cardiol.* **78**, 404-408 (1996).
51. T. Ryan, Stress Echocardiography *in* "Cardiac Imaging D.J. Skorton, H.R. Schelbert, G.L. Wolf, .H. Brundage, Eds), p.503, W.B. Saunders, Toronto, 1996.
52. I. Afridi, N.S. Kleiman, A.E. Raizner, W.A. Zoghbi, Dobutamine echocardiography in myocardial hibernation: Optimal dose and accuracy in predicting recovery of ventricular function after coronary angioplasty. *Circulation* **91**, 663-670 (1995).
53. J.-F. Reng, M.N. Kotler, A.-H. Hakki, I.P. Panidis, G.S. Mintz, J. Ross, Quantitation of regional left ventricular function by two-dimensional echocardiography in normals and patients with coronary artery disease. *Am. Heart J.* **110**, 552-559 (1985).
54. R.G. Weiss, P.A. Bottomley, Cardiac magnetic resonance spectroscopy: Principles and applications. *in* "Cardiac Imaging" (D.J. Skorton, H.R. Schelbert, G.L. Wolf, .H. Brundage, Eds), p.784, W.B. Saunders, Toronto, 1996.
55. A.J. Farrall, R.T. Thompson, G. Wisenberg, C.M. Campbell, D.J. Drost, Myocardial infarction in a canine model monitored by two dimensional ^{31}P chemical shift spectroscopic imaging. *Magn. Reson. Med.* **38**, 577-584 (1997).
56. E.T. Martin, A.R. Fuisz, G.M. Pohost, Imaging cardiac structure and pump function. *in* "Cardiac Magnetic Resonance Imaging" (N. Reichek, Ed), *Cardiology Clinics* **16(2)**, 135-160 (1998).
57. E. McVeigh, E. Atlar, Balancing contrast, resolution, and signal-to-noise ratio in magnetic resonance imaging. *In* " The Physics of MRI. 1992 AAPM Summer

School Proceedings" (M.J. Bronskill, P. Sprawls, Eds.). American Institute of Physics, Woodbury, NY., p.234 (1993).

58. P.A. Bottomley, C.J. Hardy, R.E. Argersinger, G. Allen-Moore, A review of ^{1}H nuclear magnetic resonance relaxation in pathology: Are T_1 and T_2 diagnostic? *Med. Phys.* **14**, 1-37 (1987)
59. E.S. Williams, J.L. Kaplan, F. Thatcher, G. Zimmerman, S.B. Knoebel, Prolongation of proton spin lattice relaxation times in regionally ischemic tissue from dog hearts. *JNM* **21**, 449-453 (1980).
60. J.A. Frank, M.A. Feiler, M.V. House, P.C. Lauterbur, M.J. Jacobson, Measurement of proton nuclear magnetic resonance longitudinal relaxation times and water content in infarcted canine myocardium and induced pulmonary injury (abst.). *Clin. Res.* **24**, 217A (1976).
61. G. Wisenberg, F.S. Prato, S.E. Carroll, K.L. Turner, T.P. Marshall, Serial NMR imaging of acute myocardial infarction with and without reperfusion. *Am. Heart J.* **115**, 510-518 (1988).
62. L.D. Diesbourg, F.S. Prato, G. Wisenberg, D.J. Drost, T.P. Marshall, S.E. Carroll, B. O'Neill, Quantitation of myocardial blood flow and extracellular volumes using a bolus injection of Gd-DTPA: Kinetic modelling in canine ischaemic disease. *Magn. Reson. Med.* **23**, 239-253 (1992).
63. C.B. Higgins, R. Herfkens, M.J. Lipton, R. Sievers, P. Sheldon, L. Kaufman, L.E. Crooks, Nuclear magnetic resonance imaging of acute myocardial infarction in dogs: Alterations in magnetic relaxation times. *Am. J. Cardiol.* **42**, 184-188 (1983).
64. D.L. Johnston, S. Homma, P. Liu, D.G. Weilbaecher, R. Rokey, T.J. Brady, R.D. Okada, Serial changes in nuclear magnetic resonance times after myocardial infarction in the rabbit: Relationship to water content, severity of ischaemia, and histopathology over a six-month period. *Magn. Reson., Med.* **8**, 363-379 (1988).
65. T. Ryan, R.D. Tarver, J.L. Duerk, S.G. Sawada, N.C. Hollenkamp, J. Johnson, A. Hobson, J. Sims, Distinguishing viable from infarcted myocardium after experimental ischaemia and reperfusion by using nuclear magnetic resonance imaging. *JACC* **15**, 1355-1364 (1990).
66. D.L. Johnston, T.J. Brady, A.V. Ratner, B.R. Rosen, J.B. Newell, G.M. Pohost, R.D. Okada, Assessment of myocardial ischaemia with proton magnetic resonance effects of a three hour coronary occlusion with and without reperfusion. *Circulation* **71**, 591-601 (1985).
67. D.L. Johnston, P. Liu, B.R. Rosen, R.A. Levine, P.A. Beaulieu, T.J. Brady, R.D. Okada, *In vivo* detection of reperfused myocardium by nuclear magnetic resonance imaging. *JACC* **9**, 127-135 (1987).
68. A. Bouchard, R.C. Reeves, G. Cranney, S.P. Bishop, G.M. Pohost, Assessment of myocardial infarct size by means of T_2-weighted ^{1}H nuclear magnetic resonance imaging. *Am. Heart. J.* **117**, 281-289 (1989).
69. X.H. Krauss, E.E. van der Wall, A. van der Laarse, J. Doornbox, N.A.A. Matheijssen, A. de Roos, J.A.K. Blokland, A.E. van Voorthuisen, A.V.G. Bruschke, Magnetic resonance imaging of myocardial infarction: Correlation with enzymatic, angiographic, and radionuclide findings. *Am. Heart J.* **122**, 1274-1283 (1991).

70. D. Li, P. Dhawale, P.J. Rubin, E.M. Haacke, R.J. Gropler, Myocardial signal response to dipyridamole and dobutamine: Demonstration of the BOLD effect using a double-echo gradient echo sequence. *Magn. Reson. Med.* **36**, 16-20 (1996).
71. P. Niemi, B.P. Poncelet, K.K. Kwong, R.M. Weiskoff, B.R. Rosen, T.J. Brady, H.L. Kantor, Myocardial intensity changes associated with flow stimulation in blood oxygenation sensitive magnetic resonance imaging. *Magn. Reson. Med.* **36**, 78-82 (1996).
72. O. Haraldseth, R.A. Jones, J. Schjøtt, P.A. Rinck, P. Jynge, A.N. Øskendal, Early detection of regional myocardial ischemia in *ex vivo* piglet hearts: MR imaging with magnetization transfer. *JMRI* **4**, 603-608 (1994).
73. T.D. Scholz, R.F. Hoyt, J.R. DeLeonardis, T.L. Ceckler, R.S. Balaban, Water-macromolecular proton magnetization transfer in infarcted myocardium: A method to enhance magnetic resonance image contrast. *Magn. Reson. Med.* **33**, 178-184 (1995).
74. K. Young, S. Francis, J. Hykin, R.W. Bowtell, P.A. Gowland, Perfusion-weighted images of human myocardium *in vivo* ISMRM 5th Scientific Meeting, Vancouver, B.C., p.842 (April 1997).
75. R.R. Edelman, J. Gaa, V.J. Wedeen, E. Loh, J.M. Hare, P. Prasad, W. Li, *In vivo* measurement of water diffusion in the human heart. *Magn. Reson. Med.* **32**, 423-428 (1994).
76. D.J. Pennell, S.R. Underwood, C.C. Manzara, H. Swanton, J.M. Walker, P.J. Ell, D.B. Longmore, Magnetic resonance imaging during dobutamine stress in coronary artery disease. *Am. J. Cardiol.* **70**, 34-40 (1992).
77. F.P. van Rugge, E.E. van der Wall, A. de Roos, A.V.G. Bruschke, Dobutamine stress magnetic resonance imaging for detection of coronary artery disease. *JACC* **22**, 431-439 (1993).
78. F.P. van Rugge, E.E. van der Wall, S.J. Spanjersberg, A. de Roos, N.A.A. Matheijssen, A.H. Zwinderman, P.R.M. Dijkman, J.H.C. Reiber, A.V.G. Bruschke, Magnetic resonance imaging during dobutamine stress for detection and localization of coronary artery disease. Quantitative wall motion analysis using a modification of the centerline method. *Circulation* **90**, 127-138 (1994).
79. P.A.C. Dendale, P.R. Franken, G.-J. Waldman, D.G.E. De Moor, D.A.M. Tombeur, P.F.C. Block, A. De Roos, Low-dosage dobutamine magnetic resonance imaging as an alternative to echocardiography in the detection of viable myocardium after acute infarction. *Am. Heart J.* **130**, 134-140 (1995).
80. F.M. Baer, E. Voth, C.A. Schneider, P. Theissen, H. Schicha, U. Sechtem, Comparison of low-dose dobutamine-gradient-echo magnetic resonance imaging and positron emission tomography with [^{18}F]fluorodeoxyglucose in patients with chronic coronary artery disease. A functional and morphological approach to the detection of residual myocardial viability. *Circulation* **91**, 1006-1015 (1995).
81. F.M. Baer, E. Voth, E. LaRosée, C.A. Schneider, P. Theissen, H.J. Deutsch, H., Schicha, E. Erdmann, U. Sechtem, Comparison of dobutamine transesophageal echocardiography and dobutamine magnetic resonance imaging for detection of residual myocardial viability. *Am. J. Cardiol.* **78**, 415-419 (1996).

82. E. McVeigh, Regional myocardial function. *in* "Cardiac Magnetic Resonance Imaging" (Reichek, N., Ed), *Cardiology Clinics* **16(2)**, 189-206 (1998).
83. R.J. Kim, J.A.C. Lima, E.L. Chen, S.B. Reeder, F.J. Klocke, E.A., Zerhouni, R.M. Judd. Fast ^{23}Na magnetic resonance imaging of acute reperfused myocardial infarction. *Circulation* **95**, 1877-1885 (1997).
84. V.V. Kupriyanov, L.C. Stewart, B. Xiang, J. Kwat, R. Deslauriers, Pathways of Rb^+ influx and their relation to intracellular [Na^+] in the perfused rat heart: A ^{87}Rb and ^{23}Na NMR study. *Circ. Res.* **76**, 839-851 (1995).
85. J.L. Allis, C.D. Smith, A.M.L. Seymour, G.K. Radda, ^{87}Rb NMR studies of the perfused rat heart. *FEBS Lett.* **242**, 215-217 (1989).
86. M.F. Wendland, M. Saeed, T. Masui, N. Derugin, C.B. Higgins, First pass of an MR susceptibility contrast agent through normal and ischemic heart: Gradient-recalled echo-planar imaging. *JMRI* **3**, 755-760 (1993).
87. Y. Rozenman, X. Zou, H.L. Kantor, Cardiovascular MR imaging with iron oxide particles: Utility of a superparamagnetic contrast agent and the role of diffusion in signal loss. *Radiology* **175**, 655-659 (1990).
88. S. Nilsson, G. Wikström, A. Ericsson, M. Wikström, A. Øksendal, A. Waldenström, A. Hemmingsson, A., Double-contrast MR imaging of reperfused porcine myocardial infarction. An experimental study using Gd-DTPA-BMA and Dy-DTPA-BMA. *Acta Radiol.* **37**, 27-35 (1996).
89. S. Nillson, G. Wikström, A. Ericsson, M. Wikström, A. Øksendal, A. Waldenström, A. Hemmingson, Myocardial cell death in reperfused and nonreperfused myocardial infarctions. MR imaging with dysprosium-DTPA-BMA in the pig. *Acta Radiol.* **37**, 18-26 (1996).
90. P.C. Lauterbur, M.H. Mendonça, Dias, A.M. Rudin, Augmentation of tissue water proton spin-lattice relaxation rates by *in vivo* addition of paramagnetic ion. *In* "Frontiers of Biological Energetics, Volume 1" (P.L. Dutton, J.S. Leigh, A. Scarpa, A., Eds.) p.752 Academic Press, New York, 1978.
91. H.-J.Weinmann, R.C. Brasch, W.-R.Press., G.E. Wesbey, G.E., Characteristics of gadolinium-DTPA complex: A potential NMR contrast agent. *AJR* **142**, 619-624 (1984).
92. G.E. Wesbey, C.B. Higgins, M.T. McNamara, B.L. Engelstad, M.J. Lipton, R. Sievers, R.L. Ehman, J. Lovin, R.C. Brasch, Effect of gadolinium-DTPA on the magnetic resonance relaxation times of normal and infarcted myocardium. *Radiology* **153**, 165-169 (1984).
93. M.T. MacNamara, D. Tscholakoff, D. Revel, R. Soulen, H. Schechtmann, E. Botvinick, C.B. Higgins, Differentiation of reversible and irreversible myocardial injury by MR imaging with and without Gd-DTPA. *Radiology* **158**, 765-769 (1986).
94. A. de Roos, J. Doornbos, E.E. van der Wall, A.E. van Voorthuisen, MR imaging of acute myocardial infarction: Value of Gd-DTPA. *AJR* **150**, 531-534 (1988).
95. R.S. Pereira, F.S. Prato, G. Wisenberg, J. Sykes, J., The determination of myocardial viability using Gd-DTPA in a canine model of acute myocardial ischemia and reperfusion. *Magn. Reson. Med.* **36**, 684-693 (1996).

96. K.A. Reimer, R.B. Jennings, M.L. Hill, Total ischemia in dog heart *in vitro*: 2: High energy phosphate depletion and associated defects in energy metabolism, cell volume regulation, and sarcolemmal integrity. *Circ. Res.* **49**, 901-911 (1981).
97. R.B.Jennings, K.A. Reimer, Lethal myocardial ischaemic injury. *Am. J. Pathol.* **102**, 241-255 (1991).
98. J.L. Farber, K.R. Chien, S., Mittnacht, S., The pathogenesis of irreversible cell injury in ischemia. *Am. J. Pathol.* **102**, 271-281 (1991).
99. R.A. Kloner, R.E. Rude, N. Carlson, P.R. Maroko, L.W.V. DeBoer, E. Braunwald, Ultrastructural evidence of microvascular damage and myocardial cell injury after coronary artery occlusion: which comes first? *Circulation* **62(5)**, 945-952 (1980).
100. R.A. Kloner, C.E. Ganote, D.A. Whalen, R.B. Jennings, Effect of a transient period of ischemia on myocardial cells: II: Fine structure during the first few minutes of reflow. *Am. J. Pathol.* **74**, 399-422 (1974).
101. C.Y. Tong, F.S. Prato, G. Wisenberg, T.-Y. Lee, S.E. Carroll, D. Sandler, J. Wills, D.J. Drost, Measurement of the extraction efficiency and distribution volume for Gd-DTPA in normal and diseased canine myocardium. *Magn. Reson. Med.* **30**, 337-346 (1993).
102. R.J. Kim, J.A.C. Lima, E.L. Chen, R,M. Judd, R.M., Myocardial Gd-DTPA kinetics determine MRI contrast enhancement and reflect the extent and severity of myocardial injury after acute reperfused infarction. *Circulation* **94**, 3318-3326 (1996).
103. S.S. Kety, The theory and application of the exchange of inert gas at the lungs and tissues. *Pharm. Rev.* **3**, 1-41 (1951).
104. C.Y. Tong, F.S. Prato, G. Wisenberg, T.-Y. Lee, S.E. Carroll, D. Sandler, Wills, J., Techniques for the measurement of the local myocardial extraction efficiency for inert diffusible contrast agents such as gadopentate dimeglumine. *Magn. Reson. Med.* **30**, 332-336 (1993).
105. J.A.C. Lima, R.M. Judd, A. Bazille, S.P. Schulman, E. Atalar, E.A. Zerhouni, Regional heterogeneity of human myocardial infarcts demonstrated by contrast-enhanced MRI: Potential mechanisms. *Circulation* **92**, 1117-1125 (1995).
106. R.M. Judd, C.-H. Lugo-Olivieri, M. Arai, T. Kondo, P. Croisille, J.A.C. Lima, V. Mohan, L.C. Becker, E.A. Zerhouni, Physiological basis of myocardial contrast enhancement in fast magnetic resonance images of 2-day-old reperfused canine infarcts. *Circulation* **92**, 1902-1910 (1995).

2 The determination of myocardial viability using Gd-DTPA in a canine model of acute myocardial ischemia and reperfusion[1]

2.1 Introduction

Since reperfusion following acute myocardial infarction often results in regions of contractile dysfunction which may ultimately recover (1-5), a technique to discern reversibly and irreversibly damaged tissue in the early period after ischemia would aid greatly in patient management (6,7). As mentioned in the introductory chapter, the most common currently used techniques for the determination of myocardial viability are positron emission tomography (PET) with ^{18}F-deoxyglucose (8-10) and single photon emission computed tomography (SPECT) with ^{201}Tl (11-13) but these techniques suffer from low resolution, of the order of 1 cm, which makes it difficult to determine accurately the extent, and more specifically the transmural extent of the infarct which is an important indicator of the future function of the infarct zone (14,15).

Our hypothesis was that increased signal intensity when using magnetic resonance imaging (MRI) during a constant infusion of the paramagnetic contrast agent gadolinium triaminepentaacetic acid (Gd-DTPA) would be indicative of myocardial tissue death. Gd-DTPA is a contrast agent which distributes in normal tissue to the space outside the cell, *i.e.*: the extracellular space (16,17). In infarcted tissue, where the cell membrane loses its integrity, the space to which Gd-DTPA can distribute (distribution volume) increases. As the distribution volume (ml/g of tissue) increases, the tissue concentration

---

[1] The contents of this chapter were published in *Magnetic Resonance in Medicine* under the above title by Raoul S. Pereira, Frank S. Prato, Gerald Wisenberg and Jane Sykes (*Magn. Res. Med.* **36**, 684-693 (1996). Minor changes were made to the text to improve the flow and clarity and a few references were added but the majority of the paper was left unchanged. I was responsible for designing and carrying out the experiments, Drs. Prato and Wisenberg supervised the project and also helped in the design of the studies and Jane Sykes provided technical support for the animal studies Dr. Dick J. Drost also provided technical assistance when using the Siemens MR unit.

of Gd-DTPA in these regions increases which can result in greater signal enhancement than in normal tissue on MR images, especially T_1-weighted images.

Many studies have examined the role of MRI in detecting infarction after acute ischemia. Even without the use of contrast agents, differences between viable and necrotic tissue have been noted in MR images (18-22). MR imaging after a bolus of Gd-DTPA has been shown to result in signal decrease (23,24) or enhancement (25,26) in the region of infarct relative to normal regions. The results of these studies were encouraging but failed to clarify whether regions varied in signal intensity due to regional perfusion, altered capillary permeability or extracellular space. Fedele *et al* (27) examined patients using a bolus followed by a constant infusion of Gd-DTPA but did not optimize the infusion protocol as has been done by Tong *et al* (28) and this may explain their variable results. Our infusion scheme of a bolus followed by a constant infusion results in contrast differences between regions based solely on the distribution volume of Gd-DTPA (not perfusion) by establishing equilibrium in tissue, and also takes into account the rapid clearance of Gd-DTPA by the kidneys (16,29,30).

^{201}Tl is a potassium analog whose uptake in myocardial tissue is primarily dependent on the Na^+-K^+ ATPase pump in the cell membrane (31). The initial uptake of this tracer is dependent on flow but if flow is relatively uniform, the distribution of the tracer 20 to 30 minutes after injection is related to viability (32-34). ^{201}Tl has been the favoured tracer of myocardial viability in nuclear medicine for over a decade and its distribution characteristics have been extensively studied (35-40).

This study compared the uptake of ^{201}Tl (taken as the indicator of viability) to the distribution volume of Gd-DTPA in canine hearts in which two hours of myocardial

ischemia was followed by a variable period of reperfusion (29,41). It was expected that an inverse relationship would exist between the myocardial tissue concentration of ^{201}Tl and Gd-DTPA *ie*: ^{201}Tl uptake would drop as the fraction of infarcted tissue increased while the distribution volume of Gd-DTPA would rise as the myocytes lost cell membrane integrity.

2.2 Theory and Methods

The kinetics of Gd-DTPA uptake can be modelled by the Modified Kety model (41):

$$[Gd-DTPA]_i(t) = FE\int_0^t [Gd-DTPA]_a(\tau)\cdot e^{\frac{-FE}{\lambda}(t-\tau)}\,d\tau \qquad [1]$$

where F is regional perfusion, E is the extraction fraction of Gd-DTPA, [Gd-DTPA] is the arterial (a) and tissue (i) concentration of Gd-DTPA, and λ is the partition coefficient of Gd-DTPA.

If the input arterial function $[Gd\text{-}DTPA]_a$ is a constant infusion, the tissue and blood concentrations of Gd-DTPA will eventually reach an equilibrium. At this time λ simplifies to the ratio of the tissue and arterial concentrations of Gd-DTPA (41):

$$\lambda = \frac{[Gd-DTPA]_i(\infty)}{[Gd-DTPA]_a(\infty)}. \qquad [2]$$

Tong *et al* (1993) (28) have previously shown that a bolus followed immediately by a constant infusion ensures 90% equilibrium between the myocardium and blood concentrations will be reached in much less than an hour for most flow conditions if the ratio of the bolus to constant infusion concentration is 50:1 and normal renal clearance is assumed. Therefore for our experiments where myocardial flow is relatively normal at

the time of the infusion (*i.e.:* after reperfusion), a one hour constant infusion is sufficient for equilibrium to be reached in all tissue sections (if very low flow regions, *ie:* less than 0.05 ml/min/g, are suspected, a longer constant infusion might be needed)[2].

In order to test our hypothesis, a canine model of reperfused acute myocardial infarction was used. Acute myocardial infarction was simulated by ligating the left anterior descending coronary artery for two hours. After this time period, the coronary artery was reperfused for periods of time ranging from 2 hours to 3 weeks. Blood flow was measured both during the occlusion and after reperfusion. One hour before sacrifice, Gd-DTPA was infused; ^{201}Tl was also injected before the time of sacrifice as a measure of myocardial viability and its concentration compared to that of Gd-DTPA.

Twenty beagles were used to study the relationship between ^{201}Tl uptake and the partition coefficient of Gd-DTPA with varying periods of reperfusion after a two hour ischemic event. These animals ranged in age from 6 months to 3 years and weighed between 8 and 12 kg. The reperfusion periods studied were: 2 hrs.(2 dogs)., 4 hrs.(2), 1 day (27 hrs.) (2), 1 week(8), 2 weeks(2) and 3 weeks(2). One dog was used as a sham where surgery was performed but the coronary artery was not ligated. This dog recovered for one week and underwent the same procedures for tracer administration as the other dogs. Another dog was used as a control to evaluate the effects of one week of chronic occlusion and the LAD occlusion was not released. Again, this dog underwent similar procedures for tracer administration as the other dogs. The first 27 hour dog was

---

[2] Note that Eq. [2] correctly defines λ and although it is related to the distribution volume the two differ by a constant for an extracellular agent such as Gd-DTPA. Distribution volumes could actually be calculated from λ if the peripheral hematocrit was known; however, since it is λ that is important in Eq. [1] and since the peripheral hematocrit is not known we have decided to quote that which is measured *ie*: λ. In fact, given that the hematocrit is approximately 40% the distribution volume would be approximately $(1\text{-hct})\cdot\lambda \approx 0.6\cdot\lambda$ (which explains why λ can take on values greater than 1).

planned as one day (24 hr) but due to unforeseen circumstances the reperfusion period had to be extended to 27 hours. For consistency, the second dog at this time period was also studied at 27 hours but for simplicity herein after the reperfusion period is called 1 day.

The beagles were anaesthetized with thiopental sodium intravenously, and general anaesthesia was maintained with 1-2% isoflurane after endotracheal intubation. For reperfusion periods exceeding 4 hours sterile procedure during surgery was followed. A left thoracotomy was performed, the pericardium incised and the heart exposed and suspended in a pericardial cradle. The left anterior descending coronary artery (LAD) was dissected free and a silk ligature was placed around it, usually just distal to the first major diagonal branch. A femoral artery was catheterized in order to allow an arterial blood reference sample to be taken for the microsphere blood flow measurement. Occlusion of the LAD was produced by tightening the ligature using a snare: this occlusion was sustained for two hours. One hour after occlusion, a blood flow measurement was made using radiolabelled microspheres (Dupont Pharma, 15 μm) injected directly into the left atrium with a 25 gauge needle. At the end of two hours, the ligature was released. For dogs undergoing 2 hours and 4 hours of reperfusion, the chest was not closed and the dog was not recovered but maintained on the surgical table for the duration of the study. For all other dogs, the chest wall was closed and the dog was allowed to recover until the time of the final experiment.

At the time of the final experiment , the dog was anaesthetized and the heart exposed by reopening the thoracotomy wound. The final experiment was timed to end by animal sacrifice at the end of the specified reperfusion period. The alternate femoral

artery (for microsphere blood samples) and a femoral vein (for the Gd-DTPA administration) were catheterized. A second microsphere injection, again directly into the left atrium, was performed one hour and 15 minutes prior to sacrifice using a differently labelled radioactive microsphere. Different labels were used for the two blood flow measurements: two of Sc^{46}, Cr^{51}, Sc^{85}, Nb^{95}, Ce^{141}, or Gd^{153}. Following this microsphere injection, a bolus (approx. 0.3 mmol/kg) followed by a one hour constant infusion (approx. 0.006 mmol/kg·min) of Gd-DTPA (Magnevist, Berlex, Berlin, Germany; 0.5mmol/ml) was administered through the femoral vein cannula. The Gd-DTPA bolus and infusion included trace quantities of radioactive In^{111}-DTPA (200μCi bolus, 4μCi/min constant infusion; Frosst Radiopharmaceuticals, Kirkland, Quebec, Canada) which distributes to the same space as Gd-DTPA and allowed us to determine λ using ^{111}In radioactivity as previously demonstrated by Tong *et al* (28). Thirty minutes before the end of the constant infusion, a 150μCi bolus of $^{201}TlCl$ (Dupont Pharma) was injected into the peripheral intravenous line. For the dog undergoing 1 week of chronic occlusion, Gd-DTPA was infused for 90 minutes prior to sacrifice and ^{201}Tl was injected 2.5 hours prior to sacrifice in order to allow enough time for these agents to wash into the ischemic regions. In the 10 minutes preceding the end of the constant infusion, arterial blood samples were taken in order to calculate the partition coefficient (Eq. [2]). At the end of the constant infusion, the dog was sacrificed with a bolus intravenous injection of KCl and the heart immediately excised and placed in a resealable plastic bag to prevent desiccation.

The excised heart was imaged at 1.5T on a Siemens Helicon unit within 12 hours of sacrifice using a T1-weighted 3D FLASH sequence (TR/TE 23/10ms, 40°,

256×256×128) in order to map the distribution of Gd-DTPA. Using these images as a guide, the left ventricle was sectioned into 60 to 130 segments with weights ranging from 0.2g to 1.2g. In the areas of myocardium with increased concentration of Gd-DTPA (defined as the bright areas on the MR images) and seen on gross anatomy as discoloured visibly infarcted myocardial tissue, the tissue was separated transmurally into three sections: subendocardium, middle and subepicardium (Fig. 2-1). These sections were themselves split into 2 to 4 pieces in order to increase the number of pieces of jeopardized myocardium available for study and to decrease possible partial volume effects. Directly across from these regions of myocardium, normal tissue was similarly cut into subendocardial, middle and subepicardial sections in order to obtain normal controls. The remainder of the left ventricle was sectioned transmurally. All the tissue sections and blood samples were counted for radioactivity using a multichannel NaI(Tl) gamma ray spectrometer (LKB Wallac 1282 Compugamma, Turku, Finland). After correcting for background activity and spectrum spillover the counts were used to calculate blood flow, ^{201}Tl uptake and the partition coefficient of Gd-DTPA.

^{201}Tl uptake in each dog was normalized to the average of the upper 50% of ^{201}Tl values in that dog in order to allow comparisons between animals. This was possible since at least half of the samples were in regions unaffected by the LAD occlusion and therefore represented normal myocardium.

To examine the *in vivo* time course of λ, two dogs underwent the same procedures for LAD occlusion and reperfusion but were imaged at 1.5T (Siemens Helicon) at approximately one week intervals after reperfusion. Cardiac images were taken during a constant infusion of Gd-DTPA and after equilibrium between blood and tissue had been

reached. ECG-triggered and respiratory gated flow compensated FLASH (spoiled gradient echo) sequences were used with TE=12ms and flip angle 40°.

In order to address the question of partial volume effect associated with sectioning the myocardium into relatively large segments (compared to the MR image voxel size of 0.5×0.5×0.6mm), partition coefficients for all the dogs at one week were separated into three groups according to the flow in each section during occlusion. The low flow group included sections with flow during the occlusion below 0.4 ml/min/g while the normal flow group included tissue sections with flow during the occlusion above 0.7 ml/min/g. Finally, an intermediate flow region was defined with flow between 0.4 and 0.7 ml/min/g. The partition coefficients of the tissue sections in each group were plotted on a histogram in order to examine their distribution.

To evaluate the relationship between different measures, correlation coefficients were calculated and their significance determined as suggested by Zar using the Student's t-test (42). To determine whether a pooled correlation coefficient could be calculated at each reperfusion time point, all the correlation coefficients were compared using a multiple comparison test followed by a Tukey-type procedure to determine which correlation coefficients were different from each other. The alpha value for all tests was 0.05.

A two way ANOVA with *post hoc* Student-Newman-Keuls test was used to compare the transmural variation of λ and ^{201}Tl uptake. In the ANOVA, factor one had three levels corresponding to transmural location (subendocardium, middle, subepicardium) and factor two had two levels corresponding to tissue type (jeopardized or normal). Separate tests were performed to compare transmural λ and ^{201}Tl uptake.

2.3 Results

The LAD occlusion resulted in a reduction in blood flow, as measured by microspheres, in the region supplied by this artery. The relationship between blood flow during occlusion and ^{201}Tl uptake was strong in all animals except for the sham occlusion where no relationship was seen; a representative graph of one dog is shown in Fig. 2-2. The linear correlation coefficient between occlusion blood flow and ^{201}Tl uptake ranged from 0.55 to 0.9 ($p<0.05$ in all cases). In most dogs, blood flow returned to near normal values in the occluded region after release of the ligature. In some dogs, blood flow did not normalize after the reperfusion period and in the 2 and 4 hour reperfusion animals, hyperemia was still evident in the previously ischemic regions. In all cases, the correlation between ^{201}Tl uptake and blood flow measured at the time of ^{201}Tl injection was weaker than the relationship between ^{201}Tl uptake and blood flow measured at the time of occlusion. Similar results were noted for the relationship between blood flow and λ with the difference that the correlation was negative *ie:* for λ to be increased it was necessary, but not sufficient, for the tissue in question to have reduced blood flow at the time of the LAD occlusion.

In dogs at one week of reperfusion which showed a transmural variation in MR signal intensity (n=3), ^{201}Tl uptake and partition coefficient were examined in jeopardized and normal myocardium. The average values of ^{201}Tl uptake for each transmural section (subendocardium, middle, subepicardium) for jeopardized myocardium and normal myocardium are shown in Fig. 2- 3a) and for λ in Fig. 2- 3b). In the jeopardized tissue, the two-way ANOVA indicated a significant difference between both λ and ^{201}Tl uptake in the subepicardial and subendocardial regions (*ie:* a significant

increase in λ and a significant decrease in ^{201}Tl uptake from subepicardium to subendocardium). The normal tissue showed no difference in λ with transmural location; however, the ^{201}Tl uptake was significantly increased in the middle section. While the data in Fig. 2- 3 corresponds to dogs in the one week reperfusion group, similar results were found in dogs which underwent shorter and longer reperfusion periods.

The MR images of the excised hearts showed regions of increased signal intensity in the anterior wall of the left ventricle. Representative images from one dog (1 day reperfusion) are shown in Fig. 2- 4. The size of this region varied from animal to animal but always started in the apex and extended a variable distance toward the base of the heart. In some animals the region extended the full thickness of the wall (transmurally) but in most cases it was confined to the subendocardial and middle regions. In the sham operated animal, the MR image showed uniform signal intensity throughout the left ventricle.

A strong significant negative correlation ($p<0.05$ for all time periods) was seen between ^{201}Tl uptake and λ in all dogs with the exception of the dog with the sham occlusion. A plot of all the dogs from each group is shown in Figs. 2-5a-f, showing that similar relationships were found regardless of time of reperfusion. Data for each time point could be pooled since the correlation coefficients for dogs with the same reperfusion time were not significantly different.

In order to examine how λ changed with time of reperfusion we divided the myocardial tissue sections into 2 regions based on ^{201}Tl uptake and blood flow during the occlusion. Normal tissue was defined as sections with ^{201}Tl uptake above 0.7 and flow during occlusion above 0.7 ml/min/g while infarcted or damaged tissue included sections

with both ^{201}Tl uptake below 0.7 and occlusion flow below 0.4 ml/min/g. These thresholds were chosen to hopefully avoid any partial volume effect where sections would consist of a mixture of viable and infarcted tissue resulting in artificially intermediate values. At each time point data was pooled since λ vs ^{201}Tl uptake was not significantly different except at 1 day and 3 weeks. The normal and infarcted groups were averaged for each reperfusion time period and the results are shown in Fig. 2- 6. In one of the two dogs with 1 day of reperfusion, only 2 samples were contained in the infarcted group since the size of the infarct was very small. This resulted in a significant difference in the regression for this animal compared to the other at this time point; therefore, this dog was excluded from the analysis. At each reperfusion period, the average value of the partition coefficient in the infarcted sections was significantly different than the normal sections ($p<0.05$, Student's t-test). Fig. 2- 6 shows a trend towards decreasing partition coefficient as reperfusion time extended towards three weeks.

Fig. 2- 7 shows the distribution of partition coefficients from the dogs with one week of reperfusion divided into three groups as defined in the methods section addressing the question of the importance of partial volume in the tissue samples.

Fig. 2- 8 is a graph of the relationship between λ and ^{201}Tl uptake in the dog with a one week chronic occlusion which showed a strong negative correlation of -0.81 ($p<0.05$, $n=100$).

Fig. 2- 9 shows the progression with time after reperfusion of the ratios of the signal intensities in the jeopardized and normal regions in two animals imaged from 4 to

22 days after reperfusion. For both animals the ratios decreased monotonically with time of reperfusion while the ratio between normal tissue and blood stayed relatively constant.

The possibility that diffusion of tracers in the time interval between sacrifice and tissue sectioning could alter the correlation between λ and ^{201}Tl uptake was examined in the 8 dogs sacrificed after 1 week of reperfusion. There was no significant correlation of the individual correlation coefficients or regression slopes as a function of storage time (3 for 3 hours, 1 for 6 hours, 1 for 9 hours and 3 for 12 hours). Therefore there was no noticeable effect of diffusion of tracers associated with the time between sacrifice and imaging.

2.4 Figures

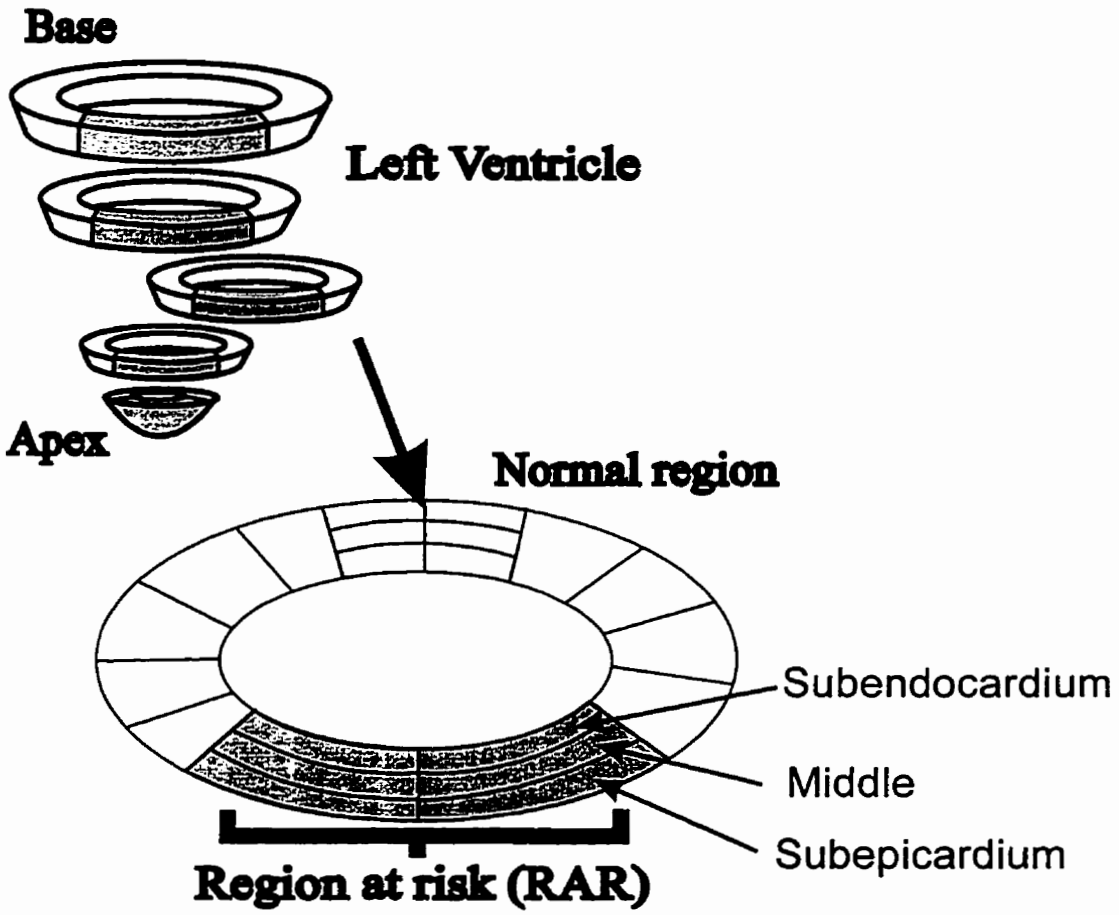

Figure 2-1 Sectioning of ventricular slices

Schematic showing sectioning of myocardium for radioactive gamma counting. The left ventricle was divided into transverse sections which were then divided into sections of 0.2-1.0 g. In the regions with increased Gd-DTPA concentration the sections were taken transmurally, and contralateral to this area, where tissue was unaffected by the occlusion, sections were also taken.

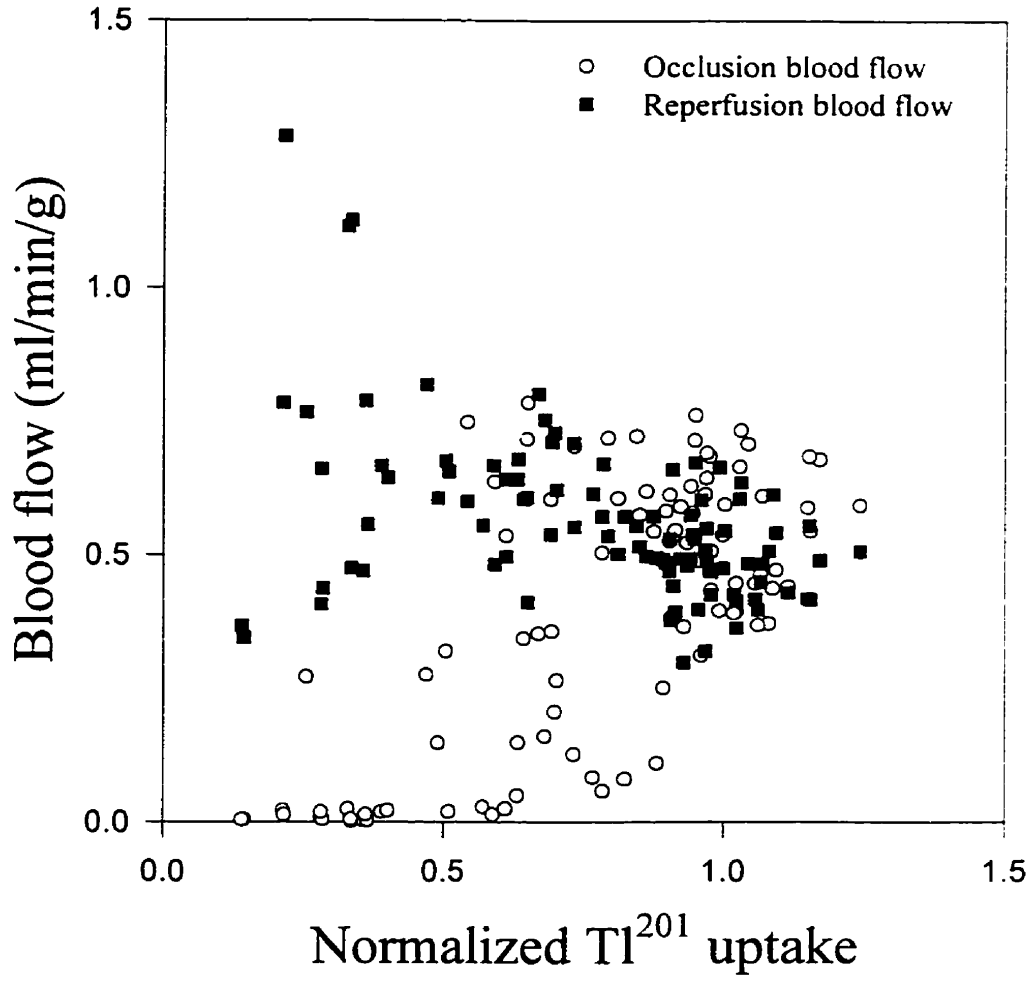

Figure 2-2 Occlusion and reperfusion blood flow *vs* ^{201}Tl uptake

Blood flow during and 3 hours after reperfusion of a two hour occlusion of the left anterior descending coronary artery *vs* ^{201}Tl uptake in one animal sacrificed after 4 hours of reperfusion. Hyperemia was evident in some regions with extremely low flow during occlusion. There was a significant positive correlation of ^{201}Tl uptake with blood flow during occlusion ($r=0.70$; $n=97$; $p<0.05$) whereas ^{201}Tl uptake correlated much less strongly with blood flow at the time of ^{201}Tl injection ($r=-0.46$).

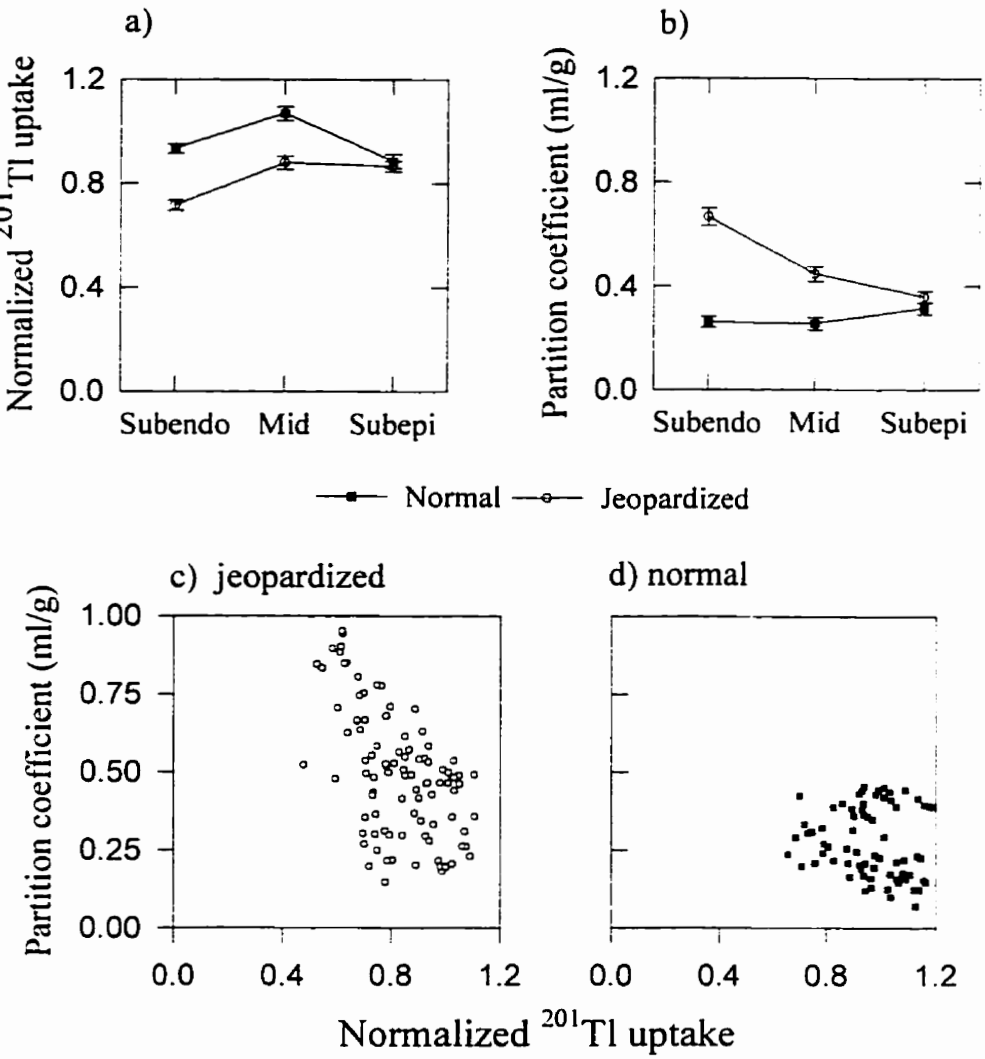

Figure 2-3 Transmural variation of partition coefficient and blood flow

Variation of a) normalized ^{201}Tl uptake and b) partition coefficient (λ) across the myocardial wall in jeopardized myocardium and normal myocardium from 3 dogs at one week. These dogs showed a transmural difference in MR signal intensity in a region of reduced flow during occlusion. In jeopardized myocardium as λ dropped significantly from subendocardium to subepicardium, ^{201}Tl uptake showed a significant increase. In normal myocardium λ stayed level while ^{201}Tl showed a curious increase in the middle section. Figs. c) and d) show the relationship between λ and ^{201}Tl for all the tissue sections in the jeopardized regions and normal regions respectively. For the jeopardized sections, $r=-0.56$ ($p<0.05, n=110$) and in the normal sections, $r=-0.25$ ($p>0.05$, $n=50$). Subendo = subendocardium, Mid = middle, Subepi = subepicardium. Error bars represent ± sem.

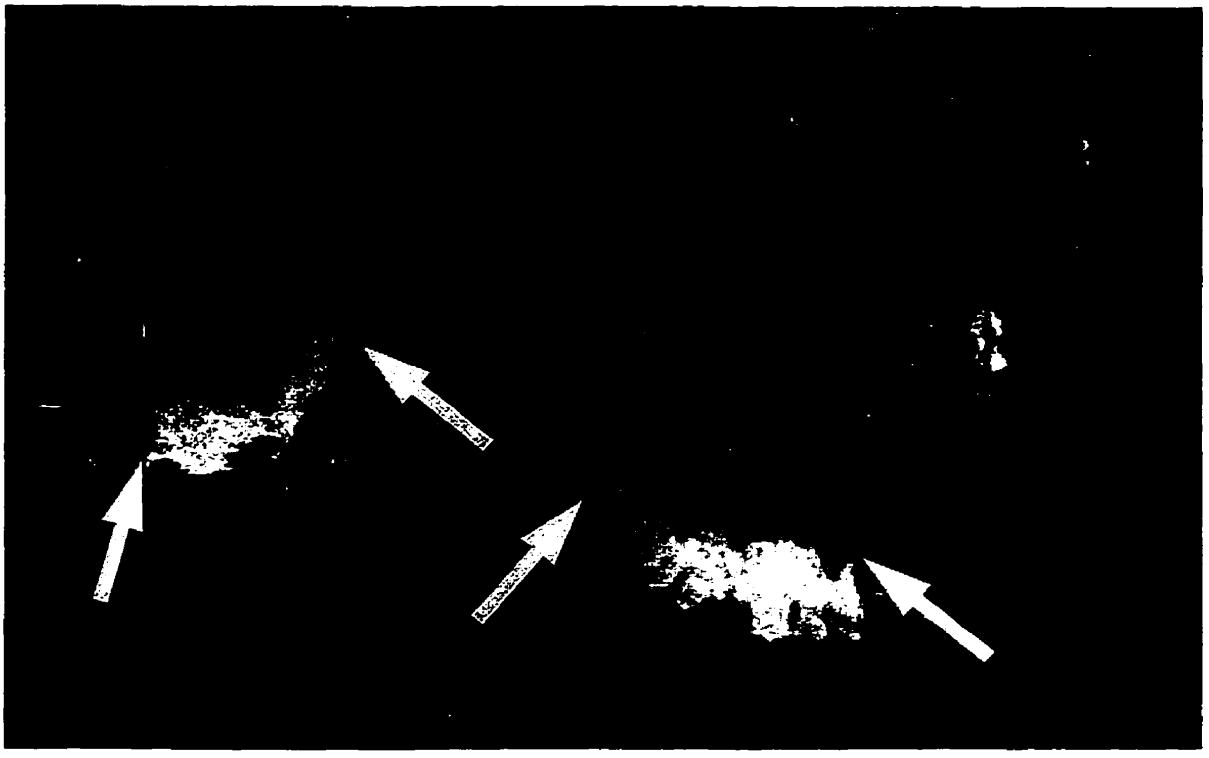

Figure 2-4 Representative images of excised heart

Representative images of an excised heart 1 day after the reperfusion of a 2 hour occlusion of the LAD. The animal was sacrificed after a bolus followed by a 1 hour constant infusion of Gd-DTPA. These images show the sharp delineation between elevated and normal partition coefficients that is possible using MRI. The contrast evident in the septum is due to a portion of the bicuspid valve (bright flap along the subendocardial wall of the left ventricle) and fat at the subepicardial junction of the left ventricle and atrium.

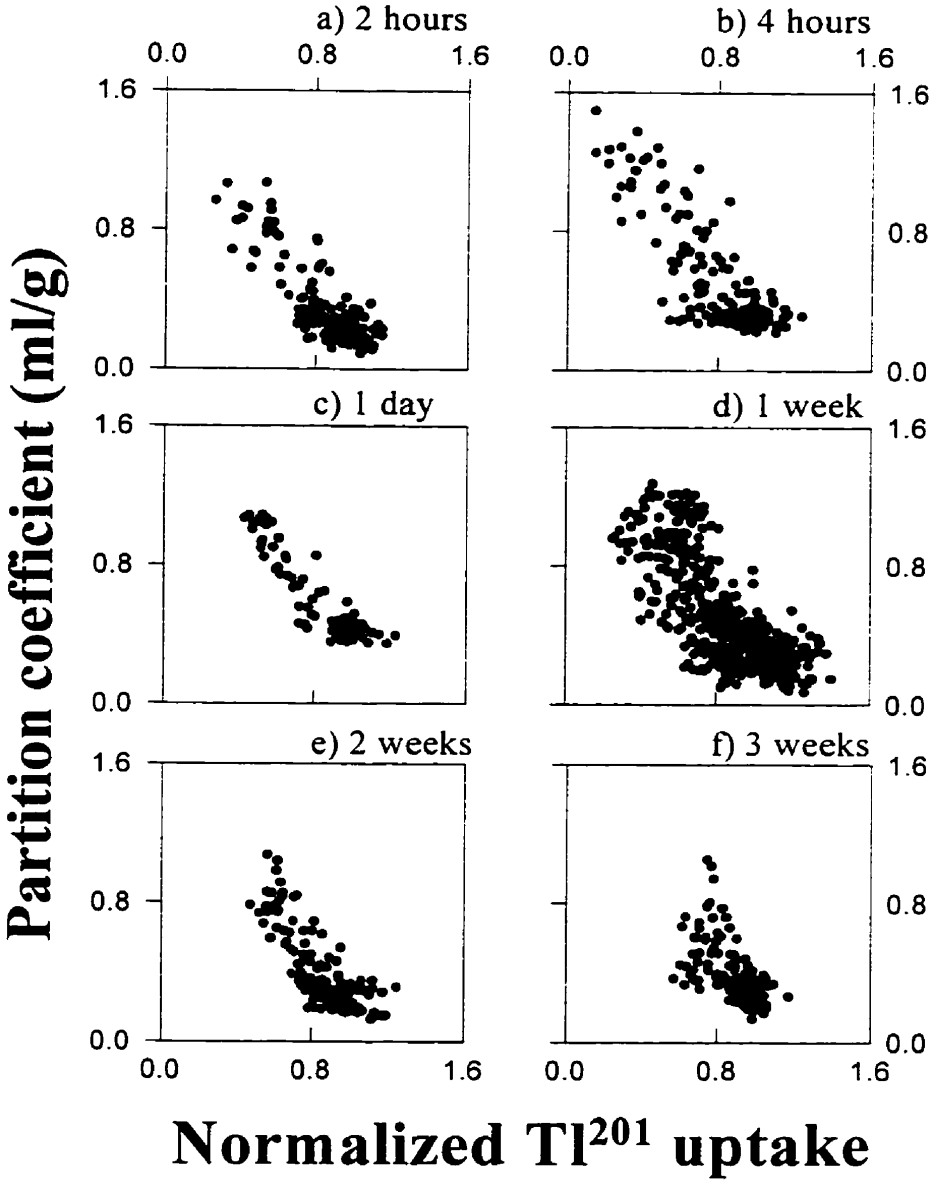

Figure 2-5 λ *vs* ^{201}Tl uptake

Relationship between partition coefficient (λ) and ^{201}Tl uptake from 2 hours to 3 weeks after reperfusion of a two hour occlusion of the left anterior descending coronary artery. For each reperfusion time point the data from different dogs at that time point can be pooled since analysis showed that correlation coefficients were not significantly different except at 3 weeks. The difference at 3 weeks may be related to the partial volume effect due to significant shrinkage in the area of the infarction.

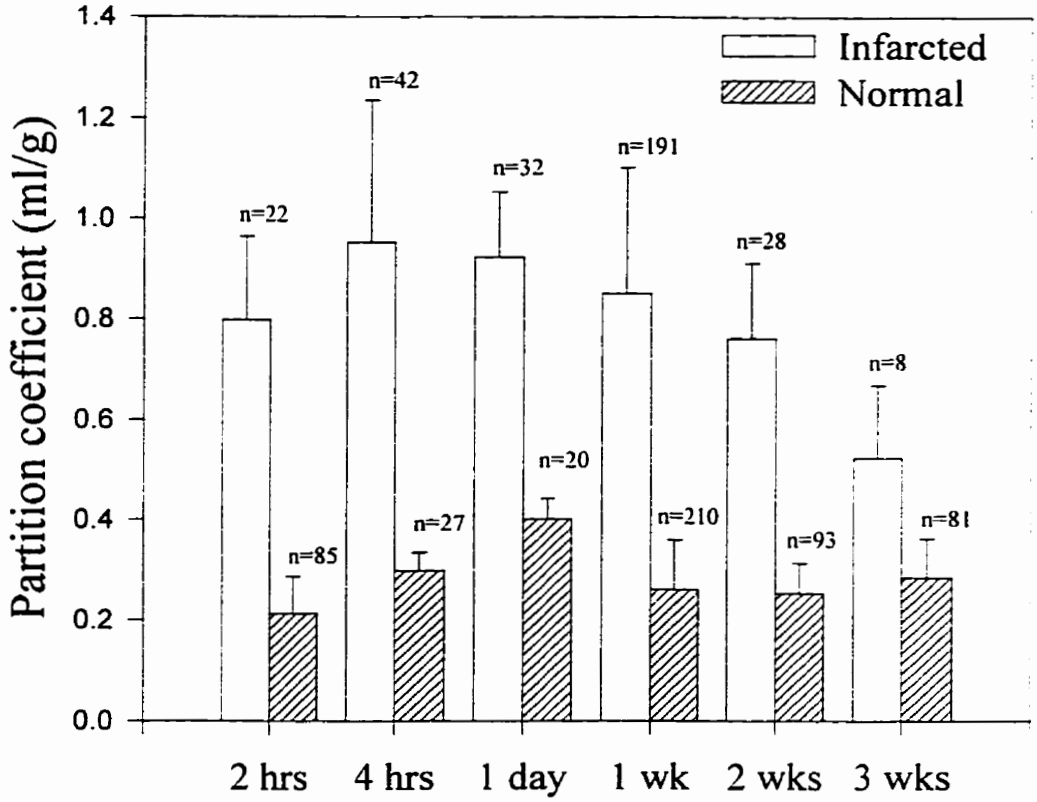

Figure 2-6 Variation of λ with time after reperfusion

Variation of partition coefficient (λ) in infarcted (flow during occlusion < 0.4ml/min/g, ^{201}Tl uptake <0.7) and normal (flow during occlusion >0.7ml/min/g, ^{201}Tl uptake >0.7) tissue groups from 2 hours to 3 weeks after reperfusion (Number of samples indicated above groups and error bars represent 1 s.d.).

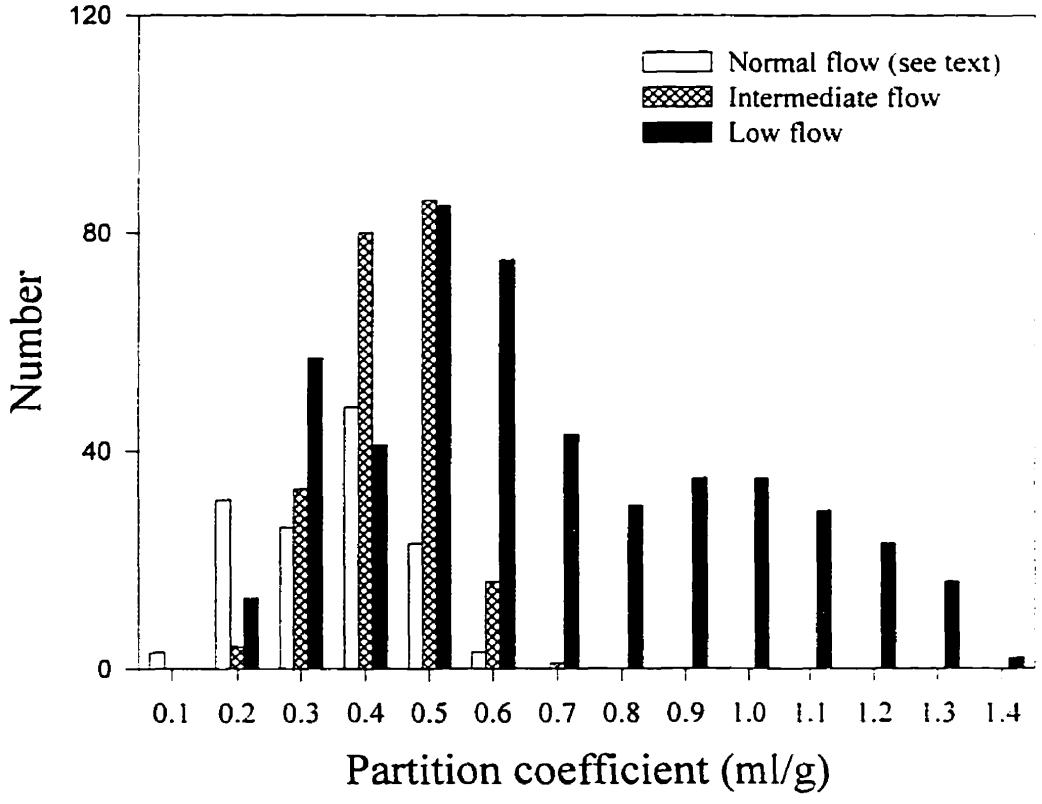

Figure 2-7 Histogram of λ with different flow during occlusion

Distribution of partition coefficients based on flow during occlusion in all dogs studied after 1 week of reperfusion. Partition coefficients in regions with normal flow during occlusion (> 0.7 ml/min/g) are normal, regions with low flow during occlusion (< 0.4 ml/min/g) are both normal and increased but regions with intermediate flow (0.4 - 0.7 ml/min/g) are mostly normal.

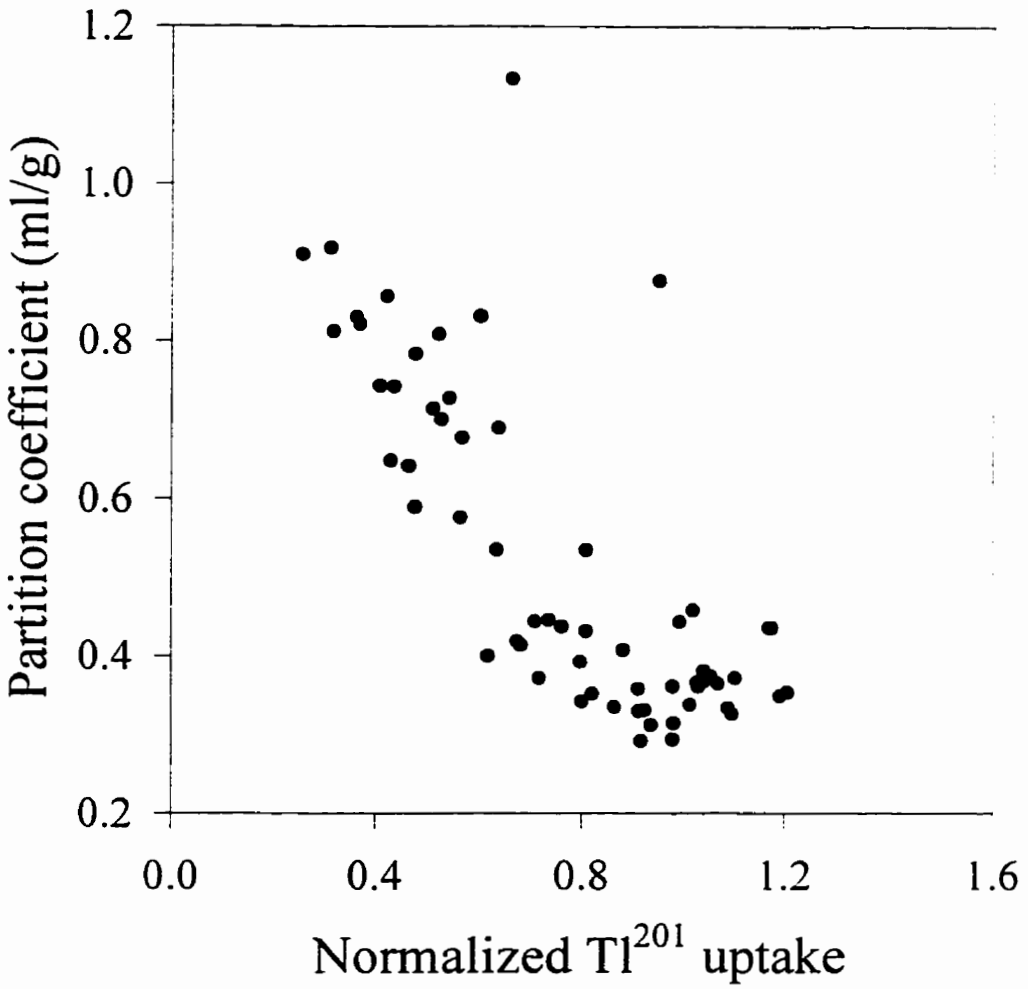

Figure 2-8 λ *vs* ^{201}Tl uptake in chronic myocardial ischemia

Relationship between partition coefficient (λ) and normalized ^{201}Tl uptake in one dog after a week of chronic ischemia. ^{201}Tl injected 2.5 hours before sacrifice in order to allow it to reach areas of low blood flow. The strong correlation ($r = -0.81$, $p<0.01$) suggests that Gd-DTPA can be used during chronic ischemia. The two outlying sections could suggest a minor overestimation of infarct size (relative to ^{201}Tl).

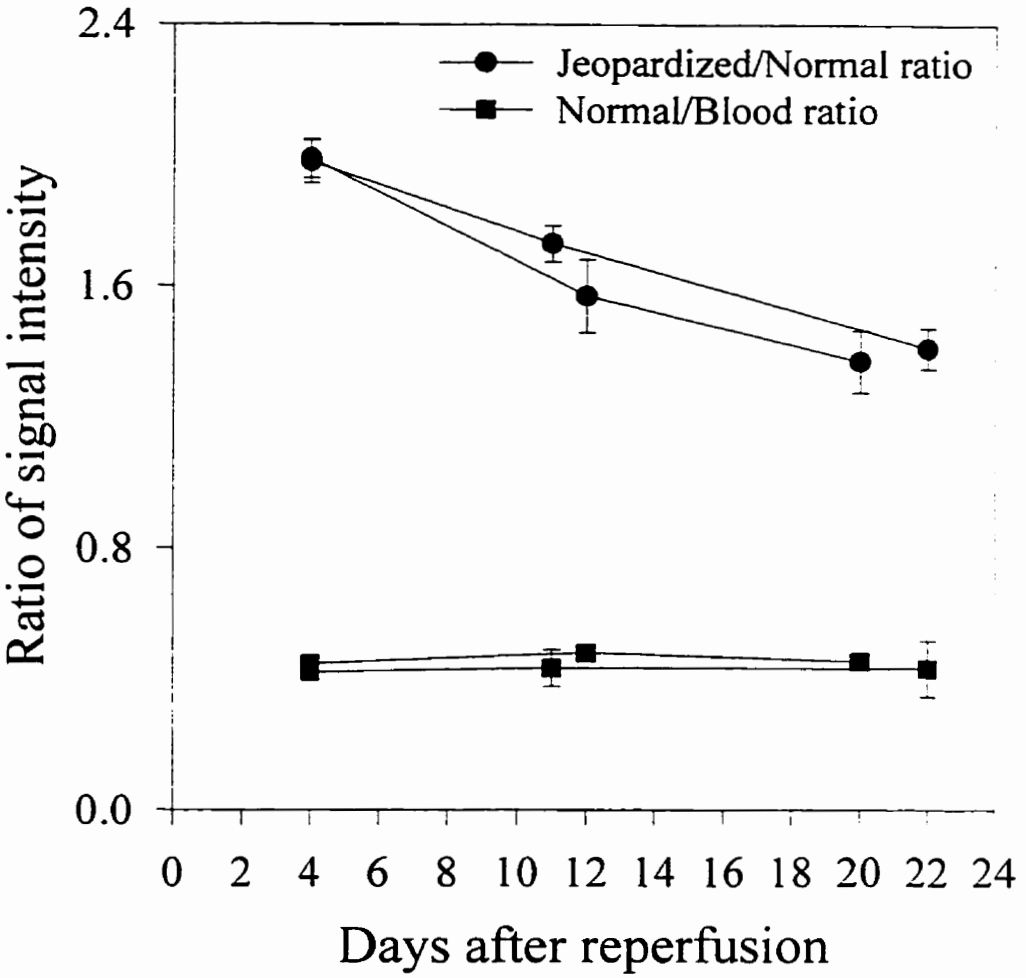

Figure 2-9 Signal intensity ratio *vs* time after reperfusion

Change in ratio of signal intensities in gradient echo sequences between jeopardized and normal tissue or normal tissue and blood with time following reperfusion. The ratio between jeopardized and normal tissue decreased from 4 days to 3 weeks while the ratio between normal tissue and blood stayed level as expected. This within subject variability follows the trends in λ seen in Fig. 2- 6. Error bars represent ± 1 sem in the regions of interest.

2.5 Discussion

Examination of Fig. 2- 7 suggests that partial volume effects did not significantly affect our results. As would be expected, when flow during the occlusion was normal (flow>0.7ml/min/g), partition coefficients had normal values. In regions of low blood flow during occlusion (flow < 0.4 ml/min/g), values of λ were centred about both low and high values (indicating infarcted tissue and tissue which survived despite low blood flow). This is consistent with the clinical case where low blood flow does not always result in infarcted tissue. Finally, in regions where blood flow was intermediate (0.4-0.7 ml/min/g) most tissue sections had normal partition coefficients indicating cell survival. This suggests the presence of an intermediate flow region during occlusion where tissue recovers and not simply a partial volume effect in these sections. However, close examination of Fig. 2- 7 indicates that, as expected, partial volume effects account for a small number of tissue sections which must have included both normal and infarcted tissue (*ie:* intermediate values of flow which correspond to intermediate values of the partition coefficient). This result is consistent with the MR images of the excised hearts which showed, at least out to two weeks, strong demarcation between high and low values of λ with little evidence of an intermediate zone of any significant size with intermediate λ values.

The fact that blood flow during occlusion correlated strongly with ^{201}Tl uptake 2 hours to 3 weeks later is consistent with reduced blood flow leading to infarction (43). ^{201}Tl uptake was weakly correlated with blood flow at the time of ^{201}Tl injection, further suggesting that ^{201}Tl distribution at this time was related to viability.

The signal enhancement on the MR images in the area of the occlusion was seen in all the dogs from 2 hours to 3 weeks after reperfusion . This suggested that Gd-DTPA

could be used very soon after an ischemia/reperfusion event to separate viable and infarcted tissue. This was supported by Figs. 2-5 and 2-6 which show that at least up to two weeks, not only is the relationship between ^{201}Tl uptake and λ very similar. but the actual values of λ in the infarcted region (λ_{inf}, defined by low flow during the occlusion and low ^{201}Tl uptake) are fairly constant with time. This suggests that changes seen after 2 hours of reperfusion are indicative of changes to be seen one week later in the absence of additional therapeutic intervention. Due to the low number of animals in some groups. ANOVA testing of possible differences in time could not be performed; however. Fig. 2-6 showed a trend that partition coefficient in the infarcted regions drops as reperfusion time increases. For statistical significance, it may be necessary to perform more experiments at each time point but this would involve killing many more animals. Instead the trend seen in these results was confirmed by imaging the same dogs after a constant infusion of Gd-DTPA at increasing times (1,2 and 3 weeks) of reperfusion. The ratio of signal intensities between the infarcted and normal regions dropped monotonically towards one with time after reperfusion (see Fig. 2- 9) implying that the T_1 values were getting closer to each other, and hence Gd-DTPA concentrations in these regions were equalizing.

Figures 2-3 and 2-4 clearly indicate that contrast-enhanced MRI has the potential to assess the transmural viability of myocardial tissue. Not only may it be superior to nuclear medicine imaging with ^{201}Tl because of superior spatial resolution but also because ^{201}Tl uptake in normal myocardium achieves higher concentration in the middle tissue sections as compared to the subendocardium and subepicardium; a result, to our knowledge, not previously reported.

Even up to three weeks post-reperfusion there was signal enhancement seen on the MR images and the values of λ_{inf}, although lower than at one week, were well separated from normal values. It was expected that the partition coefficient would fall as time post-reperfusion increased as infarcted cells were replaced with fibrous scar tissue (44-47). From previous MRI studies, we would expect that the signal intensity of a healed infarct will drop relative to normal tissue (assuming the same imaging parameters) due to the dense scar tissue replacing infarcted myocardium (23,24). We still need to do studies using longer reperfusion times (*ie*: greater than 3 weeks) to determine if viable and non-viable tissue can still be separated according to their values of λ.

Of course, often in the clinical situation a sustained occlusion occurs at the time of infarction. Therefore to fully characterize the role of Gd-DTPA distribution volume in the diagnosis of ischemic injury, we also need to know what happens to λ if a sustained occlusion occurs. Such tissue is often associated with a contrast void immediately following a bolus injection of Gd-DTPA (48,49). It is also known that when 4-8 days of chronic ischemia leads to infarction, a prolonged (90min) constant infusion shows increased values of λ similar to those reported here in ischemia/reperfusion (41); however, the actual relationship between increased values of λ and viability, as determined using a viability marker such as ^{201}Tl was unknown. We addressed this question directly and found that there was a relationship between λ and ^{201}Tl uptake after one week of chronic occlusion. Of course the precise evaluation of λ and its relationship to viability in chronic ischemia will require more extensive studies similar to those reported here for ischemia/reperfusion.

Despite these questions the evidence presented here and elsewhere (27,50) indicates that the detection of increased values of λ is indicative of myocardial infarction. Our work, and that of others, suggests that measurements in humans could be carried out successfully using a number of injection and MR imaging protocols. Two possibilities include i) imaging the myocardium during a bolus passage of Gd-DTPA after a single injection which, according to Eq. [1], would allow the measurement of the FE product as well as λ (41,51,52) and ii) imaging the myocardium during a constant infusion of Gd-DTPA when the myocardial concentration of Gd-DTPA has reached a steady-state.

The bolus tracking technique is attractive since patient imaging times are minimal and if both the tissue concentration curve and arterial concentration curve can be determined, absolute quantification of both λ and myocardial blood flow would be possible. However the technique will be difficult to properly implement since T_1 maps or T_1-like maps must be generated once every few heart beats and this may exceed the limits of even the fastest imaging gradients (53). Further assumptions regarding fast proton exchange during bolus transit may invalidate the technique and make the measurement of partition coefficient a near impossibility (54,55). In addition the assessment of the entire myocardium would require more than one bolus injection since MR imaging techniques to follow a single bolus passage in sufficient slices to evaluate the entire left myocardium seem an impossibility at this time. In contrast, imaging during a constant infusion surmounts all these problems with the drawbacks being increased patient preparation time and the inability to estimate regional blood flow.

If only the extent of infarct is to be determined, then this could be more easily achieved by MR imaging after a constant infusion of Gd-DTPA. Our technique is

attractive in that readily available T_1-weighted images can be used and reconstructed within seconds of acquisition for a physician to examine. Signal intensity on these images would be related to partition coefficient which , based on this work, is directly related to myocardial viability. Another attractive application of this technique would be the simultaneous determination of both pathology and function with the use of cine imaging (56). A cine loop of the heart taken during a constant infusion would show both the Gd-DTPA-determined infarct zone and its contractile function in relationship to the rest of the ventricle.

The technique of using a constant Gd-DTPA infusion with MRI promises to be a useful method of determining myocardial viability. The relationship to post-reperfusion blood flow is eliminated since all regions of the myocardium with blood flow greater than 5% of the normal tissue would reach equilibrium if the constant infusion is maintained for a least one hour (28). If very low flow regions are suspected, the constant infusion could be extended or serial MR images could be taken as the infusion is running until the signal intensity in all regions does not change (57).

One concern regarding the implementation of this technique would be the relatively high doses we have used in this canine model (bolus 0.3mmol/kg, constant infusion 0.006 mmol/kg/min) compared to the presently used typical clinical dose (0.1mmol/kg). This higher dose was part of our continuing research which was standardized when bolus injections of 0.3mmol/kg were typically used. On analysis of blood samples from the dogs reported here taken after the infusion of Gd-DTPA (0.3mmol/kg bolus, 0.006mmol/kg/min constant infusion) we found a concentration of 0.7μmol/ml. Extrapolation from these results suggests that, for patients with normal

renal clearance of Gd-DTPA, a bolus injection of 0.1mmol/kg followed by a constant infusion of 0.002 mmol/kg/min should give sufficient delineation of regions of increased λ on an MR image with an acceptable patient contrast burden. Assuming a 50% hematocrit, values of λ for normal tissue of 0.3ml/g, and infarcted tissue of 0.8ml/g, and a relaxivity constant of $5mmol^{-1}sec^{-1}$ at 1.5T we anticipate that differences in T_1 between normal and infarcted myocardium will be in the order of 250ms and therefore easily resolvable by MR imaging. With respect to toxicity the plasma concentration after a bolus injection of 0.1mmol/kg will be approximately 1 μmol/ml of blood 5 minutes after the injection whereas after tissue steady state has been achieved using a constant infusion of 0.002mmol/kg/min, the plasma concentration will only be 0.23 μmol/ml. This of course assumes normal renal clearance of Gd-DTPA. If clearance is compromised then the constant infusion should be proportionately reduced in concentration *ie*: if glomerular filtration is reduced by a factor of X then the concentration of the constant infusion should also be reduced by a factor of X.

2.5.1 Summary

In conclusion, our canine study strongly suggests that myocardial regions of increased distribution volume of Gd-DTPA are indicative of loss of viability following ischemia/reperfusion injury. In fact, increases which occur as early as 2 hours after the start of reperfusion may be predictive of changes which will be seen anywhere from 4 hours to 3 weeks later. It may now be appropriate to evaluate the use of this Gd-DTPA bolus/constant infusion technique in humans using a clinical trial in which the predictive value of the early changes in distribution volume are compared to currently available tests of myocardial viability (*eg*: ^{201}Tl SPECT) and functional recovery determined by radionuclide, MRI or ultrasound wall motion studies.

2.6 References

1. E. Braunwald, R.A. Kloner, The stunned myocardium: prolonged, postischemic ventricular dysfunction. *Circulation.* **66(6)**, 1146-1149 (1982).
2. H. Kusoda, E. Marban, Cellular mechanisms of myocardial stunning. *Annu. Rev. Physiol.* **54**, 243-256 (1992).
3. M.L. Charlat, P.G. O'Neill, C.J. Hartley, R. Roberts, R. Bolli, Prolonged abnormalities of left ventricular diastolic wall thinning in the 'stunned' myocardium in conscious dogs: time course and relation to systolic function. *J. Am. Coll. Cardiol.* **13(1)**, 185-194 (1989).
4. R. Bolli, Myocardial 'stunning' in man. *Circulation.* **86(6)**, 1671-1691 (1992).
5. S.G. Ellis, C.I. Henschke, T. Sandor, J. Wynne, E. Braunwald, R.A. Kloner, Time course of functional and biochemical recovery of myocardium salvaged by reperfusion. *J. Am. Coll. Cardiol.* **1(4)**, 1047-1055 (1983).
6. E.H.G. Venneker, B.L.F. van Eck-Smit, G.L. van Rijk-Zwikker, The cardiac surgeon's viewpoint of myocardial viability, *in* "Myocardial Viability: Detection and Clinical Relevance" (A.S. Iskandrian, E.E. van der Wall, Eds.), p. 163, Kluwer, Dordrecht, 1994.
7. A.S. Iskandrian, J. Heo, C. Stanberry, When is myocardial viability an important clinical issue? *J. Nucl. Med.* **35(Suppl)**, 4S-7S (1994).
8. M.E. Phelps, E.J. Hoffman, C. Selin, S.C. Huang, G. Robinson, N. MacDonald, H. Schelbert, D.E. Kuhl. Investigation of ^{18}F-2-deoxyglucose for the measurement of myocardial glucose metabolism. *J. Nucl. Med.* **19(12)**, 1311-1319 (1978).
9. H.R. Schelbert, Metabolic imaging to assess myocardial viability. *J. Nucl. Med.* **35(Suppl)**, 8S-14S (1994).
10. R.W. Burt, O.W. Perkins, B.E. Oppenheim, D.S. Schauwecker, L. Stein, H.N. Wellman, R.M. Witt, Direct comparison of flourine-18-FDG SPECT, flourine-18-FDG PET and rest thallium-201 SPECT for detection of myocardial viability. *J. Nucl. Med.* **36(2)**, 176-179 (1995).
11. A.S. Iskandrian, Thallium reinjection imaging: the search for an optimal protocol. *J. Nucl. Med.* **34(5)**, 743-746 (1993).
12. A.F.M. Kuijper, H.W. Vliegen, E.E. van der Wall, W.P. Oosterhuis, A.H. Zwinderman, B.L.F. van Eck-Smit, M.G. Niemeyer, E.K.J. Pauwels, The clinical impact of thallium-201 reinjection scintigraphy for detection of myocardial viability. *Eur. J. Nucl. Med.* **19**, 783-789 (1992).
13. R.C. Hendel, Single photon perfusion imaging for the assessment of myocardial viability. *J. Nucl. Med.* **35(Suppl)**, 23S-31S (1994).
14. A.N. Lieberman, J.L. Weiss, B.I. Jugdutt, L.C. Becker, B.H. Bulkley, J.H. Garrison, G.M. Hutchins, C.A. Kallman, M.L. Weisfeldt, Two-dimensional echocardiography and infarct size: Relationship of regional wall motion and thickening to the extent of myocardial infarction in the dog. *Circulation* **63**, 739-745 (1981).
15 Hurley, M.J., Sterling, M.C., Choy, M., Buda, A.J., Gallagher, K.P., Direct measurement of inner and outer wall thickening dynamics with epicardial echocardiography. *Circulation* **74**, 164-172 (1986).

16. H-J. Weinmann, R.C. Brasch, W-R. Press, G.E. Wesbey, Characteristics of Gadolinium-DTPA complex: a potential NMR contrast agent. *AJR.* **142**, 619-624 (1984).
17. A. Ericsson, T. Bach-Gansmo, F. Niklasson, A. Hemmingsson. Combination of gadolinium and dysprosium chelates as a cellular integrity marker in MR imaging. *Acta Radiologica* **36**, 41-46 (1995).
18. M.R. Goldman, T.J. Brady, I.L. Pykett, C.T. Burt, F.S. Buonanno, J.P. Kistler, J.H. Newhouse, W.S. Hinshaw, G..M. Pohost, Quantification of experimental myocardial infarction using nuclear magnetic resonance imaging and paramagnetic ion contrast enhancement in excised canine hearts. *Circulation* **66(5)**, 1012-1016 (1982).
19. X.H. Krauss, E.E. van der Wall, A. van der Laarse, J. Doornbos, N.A.A. Matheijssen, A. de Roos, J.A.K. Blokland, A.E. van Voorthuisen, A.V.G. Bruschke, Magnetic resonance imaging of myocardial infarction: correlation with enzymatic, angiographic and radionuclide findings. *Am. Heart. J.* **122**, 1274-1283 (1991).
20. T. Ryan, R.D. Tarver, J.L. Duerk, S.G. Sawada, N.C. Hollenkammp,J. Johnson, A. Hobson, J. Sims, Distinguishing viable from infarcted myocardium after experimental ischemia and reperfusion by using nuclear magnetic resonance imaging. *J. Am. Coll. Cardiol.* **15(6)**, 1355-1364 (1990).
21. P.W. Pflugfelder, G. Wisenberg, F.S. Prato, K.L. Turner, E. Carroll, Serial imaging of canine myocardial infarction by *in vivo* nuclear magnetic resonance. *J. Am. Coll. Cardiol.* **7(4)**, 843-849 (1986).
22. G. Wisenberg, K.J. Finnie, G. Jablonsky, W.J. Kostuk, T.P. Marshall, Nuclear magnetic resonance and radionucliide assessment of acute myocardial infarction in a randomized trial of intravenous streptokinase. *Am. J. Cardiol.* **62**, 1011-1016 (1988).
23. P.R.M. van Dijkman, E.E. van der Wall, A. de Roos, N.A.A. Matheijssen, A.C. van Rossum, J. Doornbos, A. van der Laarse, A.E. van Voorthuisen, A.V.G. Bruschke, Acute, subacute, and chronic myocardial infarction: quantitative analysis of gadolinium-enhanced MR images. *Radiology* **180(1)**, 147-151 (1991).
24. F.P. van Rugge, E.E. van der Wall, P.R.M. van Dijkman, H.W. Louwerenburg, A. de Roos, A.V.G. Bruschke, Usefulness of ultrafast magnetic resonance imaging in healed myocardial infarction. *Am. J. Cardiol.* **70(15)**, 1233-1237 (1992).
25. T. Nishimura, H. Kobayashi, Y. Ohara, N. Yamada, K. Haze, M. Takamiyz, K. Hiramori, Serial assessment of myocardial infarction by using gated MR imaging and Gd-DTPA. *AJR.* **152**, 715-720 (1989).
26. K. Lauerma, M. Saeed, M.F. Wendland, N. Derugin, K.K. Yu, C.B. Higgins, The use of contrast-enhance magnetic resonance imaging to define ischemic injury after reperfusion ; comparison in normal and hypertrophied hearts. *Investigative Radiology* **29(5)**, 527-535 (1994).
27. F. Fedele, T. Montesano, M. Ferro-Luzzi, E. Di Cesare, P. Di Renzi, F. Scopinaro, L. Agati, M. Penco, F. Serri, A. Vitarelli, A. Dagianti, Identification of viable myocardium in patients with chronic coronary artery disease and left ventricular dysfunction: role of magnetic resonance imaging. *Am. Heart. J.* **128**, 484-489 (1994).

28. C.Y. Tong, F.S. Prato, G. Wisenberg, T.Y. Lee, E. Carroll, D. Sandler, J. Wills. Techniques for the measurement of the local myocardial extraction efficiency for inert diffusible contrast agents such as gadopentate dimeglumine. *Magn. Res. Med.* **30**, 332-336 (1993).
29. C.Y. Tong, F.S. Prato, G. Wisenberg, T.Y. Lee, E. Carroll, D. Sandler, J. Wills, D. Drost. Measurement of the extraction efficiency and distribution volume for Gd-DTPA in normal and diseased canine myocardium. *Magn. Res. Med.* **30**, 337-346 (1993).
30. F.S Prato, G. Wisenberg, T.P. Marshall, P. Uksik, P. Zabel Comparison of the biodistribution of Gadolinium-153 DTPA and Technittium-99m DTPA in rats. *J. Nucl. Med.* **29(10)**, 1683-1687 (1988).
31. M.L. Delano, H. Sands, B.M. Gallagher, Transport of $^{42}K^{+}$, $^{201}Tl^{+}$ and [$^{99m}Tc(dpme)_2Cl_2$] by neonatal rat myocyte cultures. *Biochemical Pharmacology* **34(18)**, 3377-3380 (1985).o
32. G.M. Pohost, L.M. Zir, R.H. Moore, K.A. McKusick, T.E. Guiney, G.A. Beller. Differentiation of transiently ischemic from infarcted myocardium by serial imaging after a single dose of thallium-201. *Circulation* **55(2)**, 294-302 (1977).
33. F. Prigent, J. Maddahi, E.V. Garcia, Y. Satoh, K. van Train, D.S. Berman. Quantification of myocardial infarct size by thallium-201 single-photon emission computed tomography: experimental validation in the dog. *Circulation* **74(4)**, 852-861 (1986).
34. F. Prigent, J. Maddahi, E.V. Garcia, K. Resser, A.S. Lew, D.S. Berman. Comparative methods for quantifying myocardial infarct size. *J. Nucl. Med.* **28(3)**, 325-333 (1987).
35. H.F. Weich, H.W. Strauss, B. Pitt, The extraction of thallium-201 by the myocardium. *Circulation* **56(2)**, 188-191(1977).
36. G.A. Beller, D.D. Watson, P. Ackell, G.M. Pohost, Time course of thallium-201 redistribution after transient myocardial ischemia. *Circulation* **61(4)**, 791-797 (1980).
37. A.M. Grunwald, D.D. Watson, H.H. Holzgrefe, J.F. Irving, G.A. Beller, Myocardial thallium-201 kinetics in normal and ischemic myocardium. *Circulation* **64(3)**, 610-618 (1981).
38. R.D. Okada, Kinetics of thallium-201 in reperfused canine myocardium after coronary artery occlusion. *J. Am. Coll. Cardiol.* **3(5)**, 1245-1251 (1984).
39. R.D. Carlin, K-m Jan, Mechanism of thallium extraction in pump perfused canine hearts. *J. Nucl. Med.* **26(2)**, 165-169 (1985).
40. C.A. Moore, J. Cannon, D.D. Watson, S. Kaul, G.A. Beller, Thallium-201 kinetics in stunned myocardium characterized by severe postischemic systolic dysfunction. *Circulation* **81(5)**, 1622-1632 (1990).
41. L.D. Diesbourg, F.S. Prato, G. Wisenberg, D.J. Drost, T.P. Marshall, S.E. Carroll, B. O'Neill, Quantification of myocardial blood flow and extracellular volumes using a bolus injection of Gd-DTPA: kinetic modelling in canine ischemic disease. *Magn. Res. Med.* **23**, 239-253 (1992).
42. J.H. Zar, "Biostatistical Analysis," Prentice Hall, Englewood Cliffs, N.J., 1984.

43. R.A. Kloner, S.G. Ellis, R. Lange, E. Braunwald, Studies of experimental coronary artery reperfusion: effects on infarct size, myocardial function, biochemistry, ultrastructure and microvascular damage. *Circulation* **68(Suppl)**, I8-I15 (1983).
44. M.C. Fishbein, D. Maclean, P.R. Maroko, The histopathologic evolution of myocardial infarction. *Chest* **73(6)**, 843-849 (1978).
45. B.I. Jugdutt, R.W.M. Amy, Healing after myocardial infarction in the dog: changes in infarct hydroxyproline and topography. *J. Am. Coll. Cardiol.* **7(1)**, 91-102 (1986).
46. K.T. Weber, Cardiac interstitium in health and disease: the fibrillar collagen network, *in* "Basic Concepts in Cardiology" (A.M.Katz, ed), *J. Am. Coll. Cardiol.* **13(7)**, 1637-52 (1989).
47. R.C. Pasternak, E. Braunwald, B.E. Sobel, Acute myocardial infarction, *in* "Heart Disease: A Textbook of Cardiovascular Medicine" (E. Braunwald, ed), p.1200, W.B. Saunders Company, Toronto 1992.
48. W.J. Manning, D.J. Atkinson, W. Grossman, S. Paulin, R.R. Edelman, First-pass nuclear magnetic imaging studies using Gadolinium-DTPA in patients with coronary artery disease. *J. Am. Coll. Cardiol.* **18(4)**, 959-65 (1991).
49. N. Wilke, C. Simm, J. Zhang, J. Ellermann, X. Ya, H. Merkle, G. Path, H. Lüdemann, R.J. Bache, K. Uğurbil, Contrast-enhanced first pass myocardial perfusion imaging: correlation between myocardial blood flow in dogs at rest and during hyperemia. *Magn. Res. Med.* **29(4)**, 485-497 (1993).
50. M. Saeed, M.F. Wendland, T. Masui, C.B. Higgins, Reperfused myocardial infarctions on T_1- and susceptibility-enhanced MRI: evidence for loss of compartmentalization of contrast media. *Magn. Res. Med.* **31(1)**, 31-39 (1994).
51. J-P. Valleé, H.D. Sostman, J.R. MacFall, T. Wheeler, L.W. Hedlund, C.E. Spritzer, R.E. Coleman, Dipyridamole effect on MRI myocardial perfusion curves fitted by a two compartment model, in "Proc., SMR, Third Scientific Meeting, 1995", p 460.
52. T. Fritz-Hansen, H.B.W. Larsson, E. Rostrup, L. Søndergaard, P. Ring, O. Henriksen, Quantification of myocardial perfusion at rest and during dipyridamole infusion in humans, in "Proc. SMR, Third Scientific Meeting, 1995", p.460.
53. C.Y. Tong, F.S. Prato, A novel fast T_1-mapping method. *J. Magn. Res. Imag.* **4(5)**, 701-708 (1994).
54. K.M. Donahue, D. Burstein, W.J. Manning, M.L. Gray, Studies of Gd-DTPA relaxivity and proton exchange rates in tissue. *Magn. Res. Med.* **32(1)**, 66-76 (1994).
55. R.M. Judd, M.K. Atalay, G.A. Rottman, E.A. Zerhouni, Effects of myocardial water exchange on T_1 enhancement during bolus administration of MR contrast agents. *Magn. Res. Med.* **33(2)**, 215-223 (1995).
56. F.P. van Rugge, E.E. van der Wall, S.J. Spanjersberg, A. de Roos, N.A.A. Matheijssen, A.H. Zwinderman, P.R.M. van Dijkman, J.H.C. Reiber, A.V.G. Bruschke, Magnetic resonance imaging during dobutamine stress for detection and localization of coronary artery disease; quantitative wall motion analysis using a modification of the centreline method. *Circulation* **90(1)**, 127-138 (1994).
57. G. Wisenberg, Evaluation of Ischemic Heart Disease with Nuclear Magnetic Resonance, *in* "Cardiac Imaging; A companion to Braunwald's Heart Disease" (M.L.

Marcus, H.H. Schelbert, D.J. Skorton, G.L. Wolf, Eds.), p.911, W.B. Saunders Company, Toronto, 1991.

3 Assessment of myocardial viability using MRI during a constant infusion of Gd-DTPA; further studies at early and late periods of reperfusion[1]

3.1 Introduction

In chapter 2 I showed in a canine model that the myocardial tissue concentration (and hence signal intensity) of the MRI contrast agent Gd-DTPA after a prolonged constant infusion is related to viability as early as two hours and up to three weeks after reperfusion (1). At present, contrast-enhanced MRI studies are generally performed 2 or more days after the onset of acute myocardial infarction (AMI) and reperfusion therapy (2-4). MRI could prove valuable in directing further treatment if it could be applied very soon after reperfusion. However, studies need to be performed to determine how soon after reperfusion detectable increases in signal intensity can occur. Other groups have seen increases in signal intensity after contrast administration within 2 hours of reperfusion (5-9). In the present study, we used our constant infusion technique with a fast imaging sequence to examine enhancement patterns on a time scale of minutes after reperfusion of a two hour coronary artery occlusion.

In the previous study a trend towards decreasing distribution volume of Gd-DTPA in infarcted regions with time after reperfusion was noted (1, Chapter 2). This was most likely due to interstitial fibrosis which would have limited the volume of extracellular space available for Gd-DTPA distribution (10-13). In previous studies of healed human infarcts (6 or more weeks post AMI), enhancement in damaged tissue was not greater than that in normal tissue (14-16). These results in healed infarcts may have been due to

---

[1] The contents of this chapter were accepted with revisions in June 1998 by *Magnetic Resonance in Medicine* the authors were Raoul S. Pereira, Frank S. Prato, Jane Sykes and Gerald Wisenberg. Once again, only minor changes were made to the text. I was responsible for designing and performing the experiments and Drs. Prato and Wisenberg supervised the research and helped in the experimental design. Jane Sykes provided technical support and also assistance and advice in developing the animal model.

i) the use of a spin-echo pulse sequence where T_1 contrast can be weak if TR (which is dependent on the cardiac R-R interval) (17) is long ii) to the long acquisition times of the MR images which may have resulted in blurring of the thinned infarct regions due to respiratory motion (18) or iii) to the use of a bolus injection which may not have allowed adequate contrast agent delivery to infarcted regions in comparison to a constant infusion protocol (1,19). However, these possibilities could not be confirmed in those clinical studies.

The studies presented here aimed to further characterize contrast enhancement after Gd-DTPA administration, particularly in relation to our constant infusion technique. It was performed in two parts which complemented our earlier study: the first part (Procedure 1) examined changes from 3 days to 8 weeks after reperfusion of myocardial ischemia and the second part (Procedure 2) examined changes less than two hours after reperfusion.

3.2 Methods

Sixteen beagles were anaesthetized with thiopental sodium (Abbott, Canada) intravenously; general anaesthesia was maintained with 1-2% isoflurane after endotracheal intubation. The animals ranged in age from 1-3 years and weighed between 9 and 12 kg. A left thoracotomy was performed, the pericardium was incised and the heart was exposed and suspended in a pericardial cradle. The left anterior descending coronary artery (LAD) was dissected free. The rest of the experimental protocol was specific to Procedures 1 or 2.

3.2.1 Procedure 1: Study of reperfusion periods from 3 days to 8 weeks

In twelve dogs silk ligatures were placed around the LAD, just distal to the first major diagonal branch. A femoral artery was catheterized to allow an arterial blood reference sample to be taken for microsphere blood flow measurements. Occlusion of the LAD was produced by tightening the ligature using a snare. One hour after occlusion, a blood flow measurement was made using microspheres injected directly into the left atrium. After 2 hours of occlusion, reperfusion was established by releasing the ligature. The chest wall was closed and the dogs were sacrificed after 4 weeks (n=4), 6 weeks (n=4) or 8 weeks (n=4) of reperfusion.

Two animals in each of these three groups of four dogs underwent serial MR imaging during the recovery period to examine changes in distribution volume during the reperfusion period. Approximately 3 days after the first surgery the animals that were to undergo MR imaging were again anaesthetized as outlined above and taken to the MR suite. All imaging was performed on a whole-body Siemens Vision 1.5T MR scanner (Siemens, Erlangen, Germany). The animals were placed prone in a rigid radiofrequency transmit/receive coil the centre of which was positioned at the level of the heart. Images were acquired with the respirator switched to standby for the duration of the acquisition of each slice to eliminate possible breathing artefacts using a segmented cine FLASH sequence with 5 lines per heartbeat, TR/TE = 10 ms / 4.8 ms, $\alpha = 30°$, slice thickness 8 mm and a rectangular field of view. Based on animal shape the matrix was 130-165×256 corresponding to a 175-219×350 mm field of view (phase encoding dimension was adjusted to avoid aliasing artefacts while minimizing imaging time). Depending on heart rate, 8-10 cardiac phases were acquired. Since the final image in the cine sequence was preceded by 35-45 RF pulses from the preceding images the myocardial tissue signal

intensity would be driven close to steady state and thus related to T_1 (20). To examine this, we plotted signal intensity in damaged and normal tissue and apical blood for all the images in one cine loop; signal intensity was constant in each region by the last two images. The flip angle of 30° was chosen as a compromise between T_1-weighting and image quality since at higher flip angles, pulsatile flow artefacts became more prominent (21).

A transverse image plane was chosen and based on this image, long and short axis planes were located. After baseline images were acquired a bolus of Gd-DTPA (0.3 mmol/kg; Magnevist, Berlex Canada, Lachine, Quebec, Canada) was injected followed by a constant infusion (0.006 mmol/kg/min). The infusion was maintained until tissue signal intensity (determined from repeated MR imaging) did not change at which time images were again acquired. Imaging was continued at approximately one week intervals until the date of sacrifice (4 wks, 6 wks, 8 wks). Thus, all 6 animals were studied for 4 weeks, 4 animals were studied for 6 weeks and 2 animals were studied for 8 weeks. At each imaging session, the same slice locations were imaged.

During the final experiment the other femoral artery was catheterized for microsphere blood reference sampling and a differently labelled microsphere was injected to measure reperfusion flow. A bolus followed by a one hour constant infusion of Gd-DTPA (which we have previously shown to be long enough to achieve equilibrium in all but the most severely underperfused tissue(19)), with trace quantities of ^{111}In-DTPA (Frosst Radiopharmaceutical; Kirkland, Quebec, Canada), was started and ^{201}Tl was injected as an indicator of myocardial viability (22, 23) approximately 10 minutes after the start of the ^{111}In/Gd-DTPA infusion. In the dogs undergoing serial imaging, this

final procedure was performed in the magnet as outlined above. At the end of the one hour period, arterial blood samples were taken to calculate the partition coefficient. the animal was sacrificed with KCl and the heart excised.

3.2.2 Procedure 2: Study of the first two hours of reperfusion

In four dogs an inflatable balloon cuff (In Vivo Metric Systems vascular occluder. Healdsburg, California, USA) was guided around the LAD and sutured such that it surrounded the artery without obstructing it. When water was injected into the device. an inflatable bladder occluded the LAD. With the chest open, the system was tested and the success of occlusion was confirmed by cyanosis and akinesis of the LAD territory. A catheter was inserted into the left atrial appendage and sutured in place for microsphere injection and a femoral arterial catheter was inserted to allow reference blood samples to be taken for microsphere blood flow measurements. All lines were externalized. the chest was closed and the animal was taken to the MR suite.

During MR imaging, the animal was ventilated with 1-3% isoflurane and pancuronium bromide (Abbott, Canada) was used as necessary to suppress breathing movements during breath holding periods. In order to estimate partition coefficient. a saturation recovery turboFLASH (TFL) sequence was used (24). This sequence consisted of a non-selective 90° RF pulse followed by a recovery period of 20 ms and then a turboFLASH acquisition with TR/TE 2.4/1.2ms and a 15° flip angle. Signal intensity was linearly related to $1/T_1$ over the range of T_1 that we expected (25). Depending on animal shape the TFL matrix was 64-96×128 and corresponding to a 175-219×350 mm field of view (phase encoding dimension was adjusted to avoid aliasing artefacts while minimizing imaging time). A delay of 200 to 500 ms preceded image acquisition in order to acquire the images at end-diastole when flow effects in the

ventricle would be least prevalent. Since the size of the infarcted region was relatively large we could use the TFL for Procedure 2; in Procedure 1 the thinness of the healed infarcts was too small for the ~ 3mm resolution of the TFL.

A timeline of the protocol for this part of the study is shown in Fig. 3- 1. Blood flow was measured using radioactively labelled microspheres (one of ^{46}Sc, ^{85}Sr, ^{95}Nb or ^{141}Ce; 15 μm; Dupont Canada, Markham, Ontario, Canada) before and during occlusion and just before sacrifice. A bolus (0.2 mmol/kg) followed by a constant infusion of Gd-DTPA (0.004 mmol/kg/min) with trace quantities of ^{111}In-DTPA was started and continued for the rest of the study (19). This infusion was at a lower rate than that in Procedure 1 in order to ensure that the signal intensity of TFL sequence was linear over the range of concentrations we expected (25). Signal intensity was monitored using the TFL sequence until the blood and tissue reached a steady state which occurred within 5-10 minutes since all the tissue was well perfused. The balloon cuff was then inflated without removing the animal from the magnet; success of the occlusion was confirmed by the development of ECG changes. After two hours of occlusion, reperfusion was established by deflating the occluder, again without removing the animal from the bore of the magnet. Two to four short axis TFL image planes were chosen and acquired before Gd-DTPA infusion and throughout the rest of the study. Before and during the occlusion, images were taken at approximately 10 minute intervals. Following reperfusion, images were taken within 30 seconds of reperfusion and at approximately 1 minute intervals for the first 30 minutes and subsequently at 5-10 minute intervals until sacrifice. Cine images of the entire heart (4-5 short axis slices, 2 orthogonal long axis slices) using an ECG-gated segmented FLASH sequence (TR/TE 10/4.8 ms, 5 lines per heartbeat, 30°

flip angle) were taken prior to occlusion, 15 minutes after occlusion, 1 1/2 hours after occlusion and 1 hour after reperfusion to locate regions of abnormal wall motion. The dogs were sacrificed approximately 2 hours following reperfusion; this time was chosen based on our previous results showing that at 2 hours we expected to see an increase in signal intensity (1). ^{201}Tl was injected one hour before sacrifice as an independent indicator of myocardial viability and arterial blood samples were taken for the calculation of partition coefficient just before sacrifice with KCl. The heart was then immediately excised and placed in a re-sealable plastic bag to prevent desiccation.

3.2.3 Tissue Analysis

The excised hearts were imaged on the Siemens Vision MR scanner using a T_1-weighted 3D FLASH sequence (TR/TE 22/10 ms, α = 40°, 256 ×256 ×128, FOV 100 mm) to map the distribution of Gd-DTPA. Using these images as a guide the left ventricle was sliced into 4-6 sections of 8 mm thickness (the MR image slice thickness) and divided into 60-100 pieces of 0.2g - 1.0 g each. In the areas of myocardium with increased signal intensity on the T_1-weighted images the tissue was separated into three transmural sections: subepicardium, myocardium and subendocardium. These sections were themselves split into two to three pieces circumferentially to minimize possible partial volume effects (1, Fig. 2-1). The remainder of the tissue was sectioned transmurally. All the tissue sections and the blood samples were counted for radioactivity using a multichannel NaI(Tl) gamma ray spectrometer (LKB Wallac 1282 Compugamma; Turku, Finland). After correcting for background activity and spectrum spillover the counts were used to calculate blood flow, ^{201}Tl uptake and the partition coefficient of Gd-DTPA (λ) with the use of the following equation:

$$\lambda = \frac{[Gd-DTPA]_{tissue}}{[Gd-DTPA]_{blood}} = \frac{[^{111}In-DTPA]_{tissue}}{[^{111}In-DTPA]_{blood}}. \quad [1]$$

(We have previously shown that Gd-DTPA and ^{111}In-DTPA distribute to the same space in canine myocardium (19)) Excised tissue sections were matched with *in vivo* regions of interest. Regional blood flow, ^{201}Tl uptake and partition coefficient determined *ex vivo* could then be compared to the corresponding MR regions of interest.

^{201}Tl uptake in each dog was normalized to the average of the upper 50% of ^{201}Tl values in that dog to allow comparisons between animals. Similarly, flow was also normalized. This was possible because at least half of the tissue samples were in regions unaffected by the LAD occlusion and therefore represented normal myocardium.

3.2.4 Image Analysis

3.2.4.1 Procedure 1

At each imaging session, the last image in a cine loop containing the damaged region was selected. In each animal, images of the same orientation were used for analysis at each imaging session. Regions of interest were defined in damaged and normal tissue and also in the blood near the apex since this blood would be relatively stationary for most of diastole. The ratio of damaged (infarcted) to normal tissue signal intensity (I/N ratio) and normal tissue to blood signal intensity (N/B ratio) was calculated at each time point.

3.2.4.2 Procedure 2

Regions of interest (ROI) were defined in normal tissue, damaged tissue and blood in each TFL image and signal intensity in each ROI was determined (AnalyzeAVW, Biomedical Imaging Resource, Mayo Foundation, Rochester, MN (26)). Sample ROIs in damaged and normal tissue are shown in Fig. 3- 2. In each image, the signal increase (ΔS) from baseline was determined and the ratio between tissue and blood

was calculated. At equilibrium the ΔS ratio is equal to the partition coefficient of Gd-DTPA (9,27):

$$\Delta S\ ratio\ = \frac{\Delta S_{tissue}}{\Delta S_{blood}} = \lambda \qquad [2]$$

If signal intensity is linearly related to R_1 (=$1/T_1$) by a constant k such that

$$S = k \cdot R_1 \qquad [3]$$

then following contrast administration the difference in signal from baseline is

$$\Delta S = k \cdot R_{1c} - k \cdot R_{1_o} = k(R_{1c} - R_{1_o}) = k \cdot \Delta R_1 \qquad [4]$$

where R_{1c} and R_{1o} are post- and pre- contrast R_1 respectively. Assuming fast exchange of water protons (which will be dealt with later), the change in R_1 is equal to the product of relaxivity (β) and concentration of Gd-DTPA (28):

$$k \cdot \Delta R_1 = k \cdot \beta \cdot [Gd - DTPA]. \qquad [5]$$

Thus, the ratio of ΔS in tissue to blood is equal to:

$$\frac{\Delta S_{tissue}}{\Delta S_{blood}} = \frac{k \cdot \beta_{tissue} \cdot [Gd - DTPA]_{tissue}}{k \cdot \beta_{blood} \cdot [Gd - DTPA]_{blood}} = \frac{\beta_{tissue}}{\beta_{blood}} \cdot \lambda \qquad [6]$$

assuming [Gd-DTPA] in tissue and blood are at equilibrium. Eq.[6] reduces to Eq.[2] if β_{tissue} and β_{blood} are equivalent.

The assumptions inherent in this derivation were that:

1. signal intensity was linearly related to R_1 over the range of R_1 we expected;
2. fast exchange existed between the intra- and extra- vascular spaces in tissue and blood such that a single R_1 value characterized the entire voxel;
3. the relaxivity (β) of Gd-DTPA in tissue and blood was equal.

Jerosch-Herold *et al* (1998) (25) have tested the first assumption using Gd-DTPA-doped phantoms with concentrations ranging from 0 to 3 mmol/L. They found that signal intensity was linearly related to concentration up to 0.7 mmol/L and underestimated concentration minimally at 2 mmol/L. These results were confirmed by our laboratory in a similar study (unpublished data). Exchange between plasma and red blood cells is fast at standard contrast agent concentrations (29). In tissue, intracellular-interstitial exchange is considered to be intermediate to fast (29). Intravascular-extravascular exchange may not be fast in general, but at the concentrations that we expected during the constant infusion of Gd-DTPA fast exchange between these compartments may be a valid assumption (28, 30). Finally, Donahue *et al* (28) have shown that the relaxivity of Gd-DTPA in myocardial tissue and whole blood is almost identical, justifying assumption 3.

To test the hypothesis that the increase in the concentration of Gd-DTPA in damaged tissue was flow limited the ΔS ratio *vs* time curves were fit to the modified Kety model for diffusible tracers (31,32) in order to aid in discerning trends (Matlab. The Mathworks Inc., Natwick, Mass., USA).

$$c_{tissue}(t) = FE\int_0^t c_a(\tau)\cdot e^{\frac{FE}{\lambda}(t-\tau)}d\tau \qquad [7]$$

where c_a was the arterial blood concentration, FE was the flow extraction fraction product, and τ was a dummy variable of integration. Using this model the flow·extraction fraction product (FE product) can be determined; although flow can not be determined exactly without knowledge of E, E was expected to be on the order of 0.6 to 1 at the flow rates we expected in tissue and thus the FE product would be representative of flow (32). A unit step function was assumed as the arterial input in the modeling since the relative signal ratio of blood was one; the start of the step function relative to the onset of

reperfusion was allowed to vary in order to obtain the best fit. To facilitate comparisons between animals the data was grouped into time points centred at -135, -105, -45, -15, 1, 3, 5, 7, 9, 12.5, 17.5, 22.5, 27, 35, 45, 55, 75, and 105 minutes.

3.2.5 Statistical Analysis

The partition coefficients for the study after reperfusion periods of 3 days to 8 weeks (procedure 1) were analyzed using a Kruskal-Wallis one way analysis of variance on ranks since the data was not normally distributed; Dunn's method was used to test for individual differences between groups. The results of the study of the first 2 hours of reperfusion (procedure 2) were analyzed using a one way repeated measures ANOVA on the damaged and normal signal intensity ratio vs time curves separately; *post hoc* testing was performed using a Student-Newman-Keuls test. The significance of correlation coefficients was determined using a Student's t-test (33). All tests were performed at an α of 0.05.

3.3 Results

3.3.1 Procedure 1; Studies of reperfusion periods from 3 days to 8 weeks

Fig. 3- 3 shows the results of the long term serial imaging study. Since the exact timing of the imaging sessions varied slightly due to scheduling and technical reasons, the time points were grouped as follows: 3 days, 4-11 days, 12-18 days, etc up to 56 days. Since the animals were sacrificed at varying times after reperfusion (4, 6 and 8 weeks) the first five points contained results from 6 animals, the next two contained 4 animals and the last two contained 2 animals. The time listed on the abscissa is the middle point of the time interval. The ratio of normal tissue to blood (N/B ratio) stayed constant with time after reperfusion. The ratio between damaged and normal tissue (I/N ratio) was elevated until 11 days of reperfusion when it began to slowly decline. Even

after 54 days of reperfusion the I/N ratio was elevated above one indicating that signal intensity in the damaged region was greater than in normal tissue.

Partition coefficient and ^{201}Tl uptake were strongly inversely correlated at 4 weeks and 6 weeks ($r = -0.75$ to -0.90, all $p<0.05$). At 8 weeks the correlation was less strong ($r = -0.57$ to -0.69, all $p<0.05$) and the range of both λ and ^{201}Tl uptake values decreased.

3.3.2 Procedure 2; The first two hours of reperfusion

Fig. 3- 4 shows the comparison between λ (ΔS ratio) determined *in vivo* just before sacrifice to λ determined *ex vivo* from radioactive counting of ^{111}In-DTPA in excised tissue and blood samples. The correlation coefficient was 0.99 ($p<0.0001$) and the slope was 0.97, implying that the assumptions stated above were correct and λ could be accurately quantified *in vivo*.

Fig. 3-5 shows the ΔS ratio *vs.* time curves in damaged tissue for all dogs: the occlusion began at –120 minutes and the onset of reperfusion (deflation of the occluding cuff) was at 0 minutes. No changes in ΔS ratios were seen in normal tissue throughout the course of the study and in damaged tissue, no changes were seen during occlusion. In three of the dogs, increases were noted as early as 10 minutes after the onset of reperfusion. In two of these animals, blood flow was successfully restored as measured by microspheres (Table 3-1); in the other two animals, blood flow was not completely restored and the signal intensity in the fourth dog rose much more slowly. Table 3-2 shows the results of the fits to the modified Kety model; the average start time when signal intensity in the damaged tissue began to rise was 2.5 ± 2.05 minutes. The FE product determined in all animals was at least one order of magnitude lower than the

blood flow measured by microspheres. By 22.5 minutes post reperfusion significant increases in λ were noted in all animals (0.72 ± 0.22 vs 0.32 ± 0.04 ml/g, t-test, $p = 0.008$). In the first 3 animals, signal intensity ratio had reached a plateau by 2 hours post reperfusion while in the fourth it was still increasing at that time. For the 3 animals where signal intensity ratio reached a plateau, the average value was 1.02 ± 0.10 ml/g at 2 hours of reperfusion.

The partition coefficient and ^{201}Tl uptake were strongly inversely correlated in all 4 animals ($r = -0.75$ to -0.95, $p < 0.05$).

To examine how λ changed with time after reperfusion, we assigned the myocardial tissue sections into two groups based on ^{201}Tl uptake and blood flow during the occlusion, similar to our previous study (1, Chapter 2). Normal tissue was defined as sections with both ^{201}Tl uptake and occlusion blood flow above 0.7 and damaged tissue included sections with ^{201}Tl uptake below 0.7 and occlusion blood flow below 0.4. These thresholds were chosen to avoid any partial volume effect where sections would consist of a mixture of viable and infarcted tissue resulting in artificially intermediate values.

The results shown in Fig. 3-6 are combined with the results from our previous study (1, Chapter 2) to better display the trends with time. The *in vivo* results from procedure 2 were included as the first bar at 30 minutes and, since the animals were sacrificed at 2 hours, the final partition coefficients (calculated from excised tissue sections) were combined with our previous results from 2 hours. At 4 and 6 weeks 4 animals are included in each group (2 of which underwent imaging). Thus, the number of animals included at each time point was as follows: 30 minutes (n=4), 2 hrs (6), 4 hrs (2), 1 day (3), 1 wk (8), 2 wks (2), 3 wks (2), 4 wks (4), 6 wks (4), 8 wks (4). Partition

coefficient in the damaged regions was always significantly higher ($p < 0.05$) than that in normal regions but there was a trend towards decreased partition coefficients in the damaged regions that did not achieve statistical significance.

After 8 weeks of reperfusion, no excised tissue sections that met our criteria for infarction could be found and thus these results could not be included in Fig. 3- 6. However, increased signal intensity could still be seen in the damaged regions. Fig. 3- 7 shows a comparison between an *ex vivo* image (one slice from the 3D FLASH acquisition) and the corresponding *in vivo* slice taken just before sacrifice; both images show closely corresponding regions of increased signal intensity.

3.4 Figures and Tables

Table 3-1 Regional blood flow (ml/min/g ± s.d.) in damaged and normal tissue for Procedure 2.

	Dog 1		Dog 2		Dog 3		Dog 4	
	Damaged	Normal	Damaged	Normal	Damaged	Normal	Damaged	Normal
Baseline	0.68	0.67	0.82	0.99	0.78	1.04	0.85	1.14
	±0.09	±0.09	±0.02	±0.06	±0.06	±0.20	±0.06	±0.08
Occlusion	0.16	0.73	0.00	1.04	0.04	1.10	0.03	1.15
	±0.22	±0.03	±0.003	±0.10	±0.03	±0.10	±0.02	±0.18
Reperfusion	0.73	0.67	0.18	0.74	0.85	0.98	0.12	1.03
	±0.06	±0.06	±0.06	±0.17	±0.13	±0.07	±0.12	±0.27

Table 3-2 Results of modified Kety model fits to ΔSI ratio *vs* time curves shown in Fig. 3- 5

Dog	Start time (minutes)	FE (ml/min/g)	Microsphere flow (ml/min/g)[†]
1	0.77	0.0334	0.75 ± 0.06
2	0.69	0.0176	0.18 ± 0.06
3	4.63	0.0485	0.85 ± 0.13
4	3.84	0.0088	0.12 ± 0.12

[†] Data from Table 1 (mean ± s.d.)

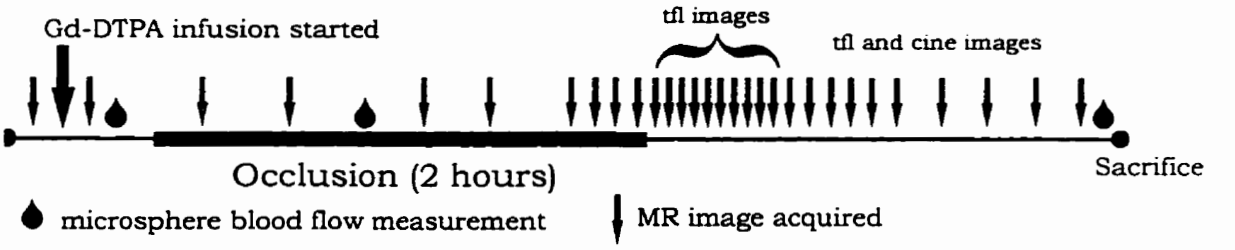

Figure 3-1 Timeline of experimental protocol for the procedure 2 (studies of the first two hours of reperfusion).

The entire study took place in the magnet and reperfusion was established without removing the animal from the bore of the MR scanner. The arrows represent the approximate timing of saturation recovery turboFLASH images (TFL); cine images were acquired in between the TFL images. Only TFL images were acquired for the first 30 minutes following reperfusion after which the frequency of TFL acquisitions decreased and higher resolution cine images were acquired.

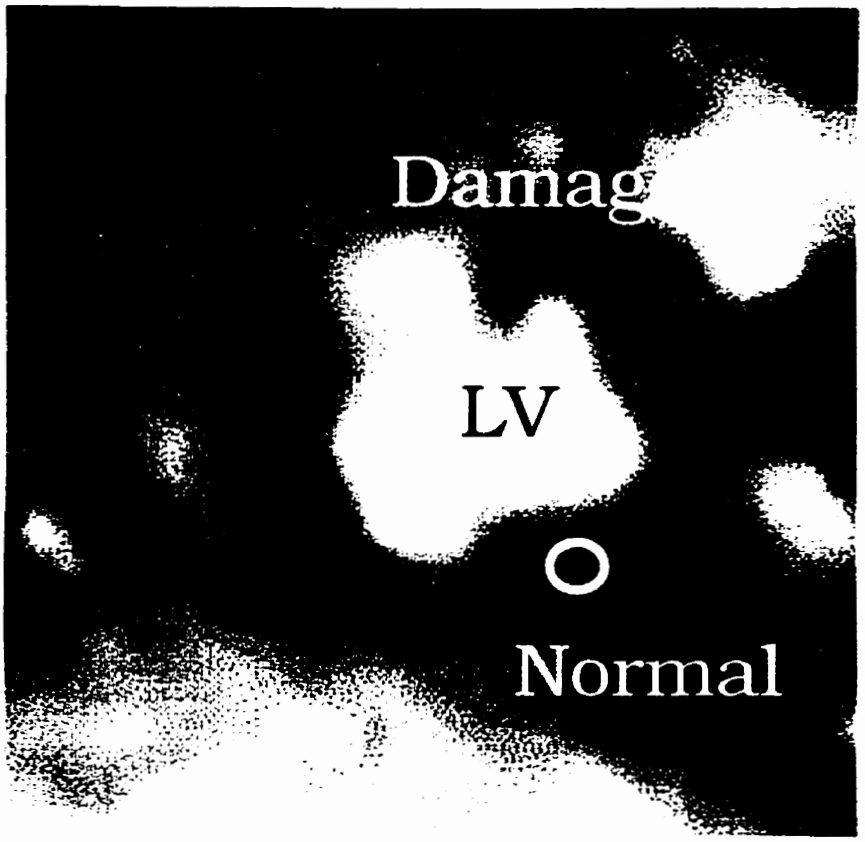

Figure 3-2 Short axis saturation recovery turboFLASH image showing sample regions of interest in damaged and normal tissue for dog 1 in procedure 2

This image was taken during a constant infusion of Gd-DTPA 45 minutes after reperfusion of a 2 hour LAD occlusion. RV, right ventricle; LV left ventricle.

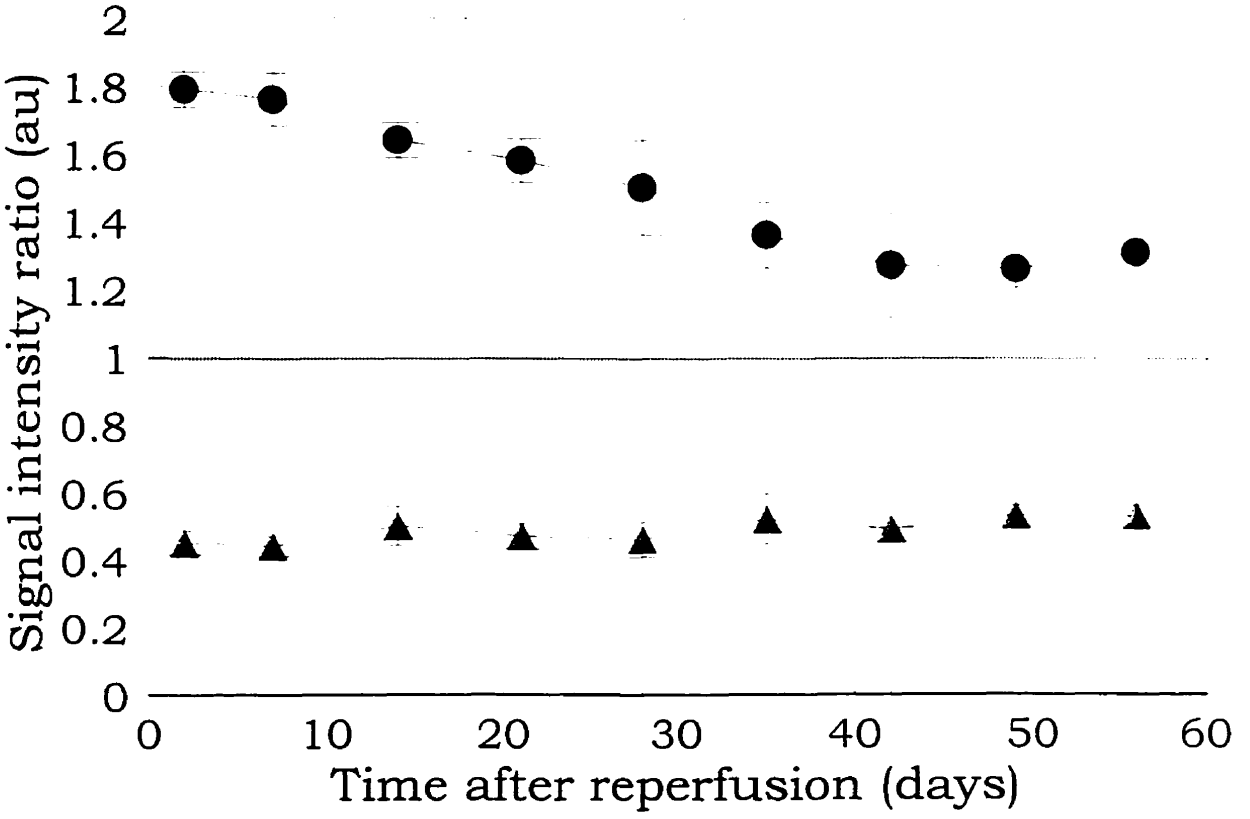

Figure 3-3 MRI Signal intensity ratios after reperfusion of coronary artery reperfusion

Ratio of infarcted to normal tissue signal intensity (●) and normal to blood signal intensity (▲) during a constant infusion of Gd-DTPA at various times after reperfusion (procedure 1). The ratio of infarcted to normal decreased with time but never reached 1. The ratio of normal to blood intensity did not change with time after reperfusion (mean ±s.d.).

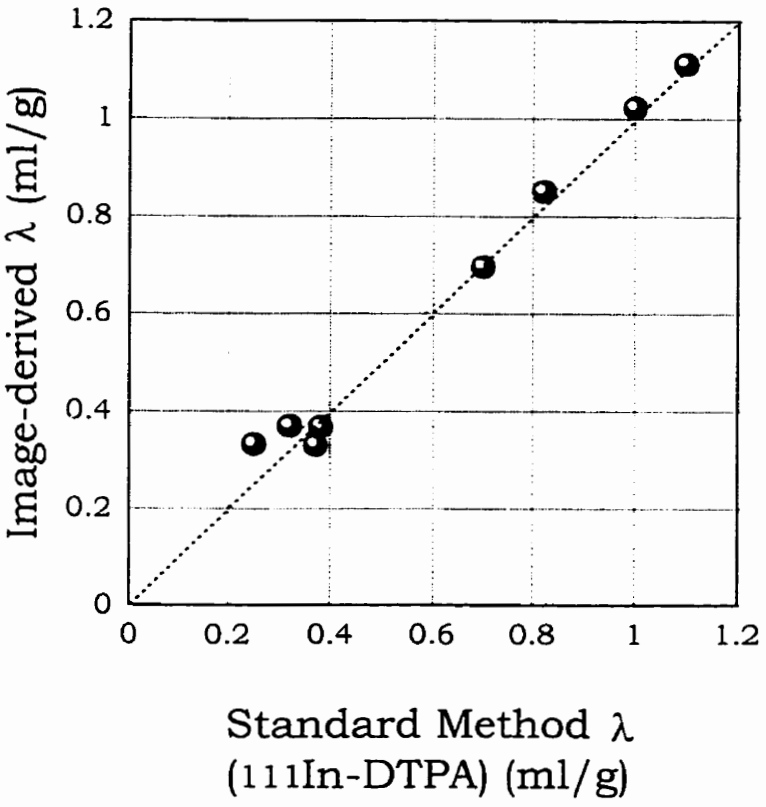

Figure 3-4 Validation of λ determined from *in vivo* signal intensities

Comparison of *in vivo* image-derived λ and that calculated from tissue samples using our standard method with ^{111}In-DTPA for all four dogs in procedure 2. The dotted line is the line of identity and the solid line is the best fit line to the data. The slope of the best fit line was 0.97 and the correlation coefficient was 0.99 ($p<0.0001$) implying that the image-derived λ was accurate.

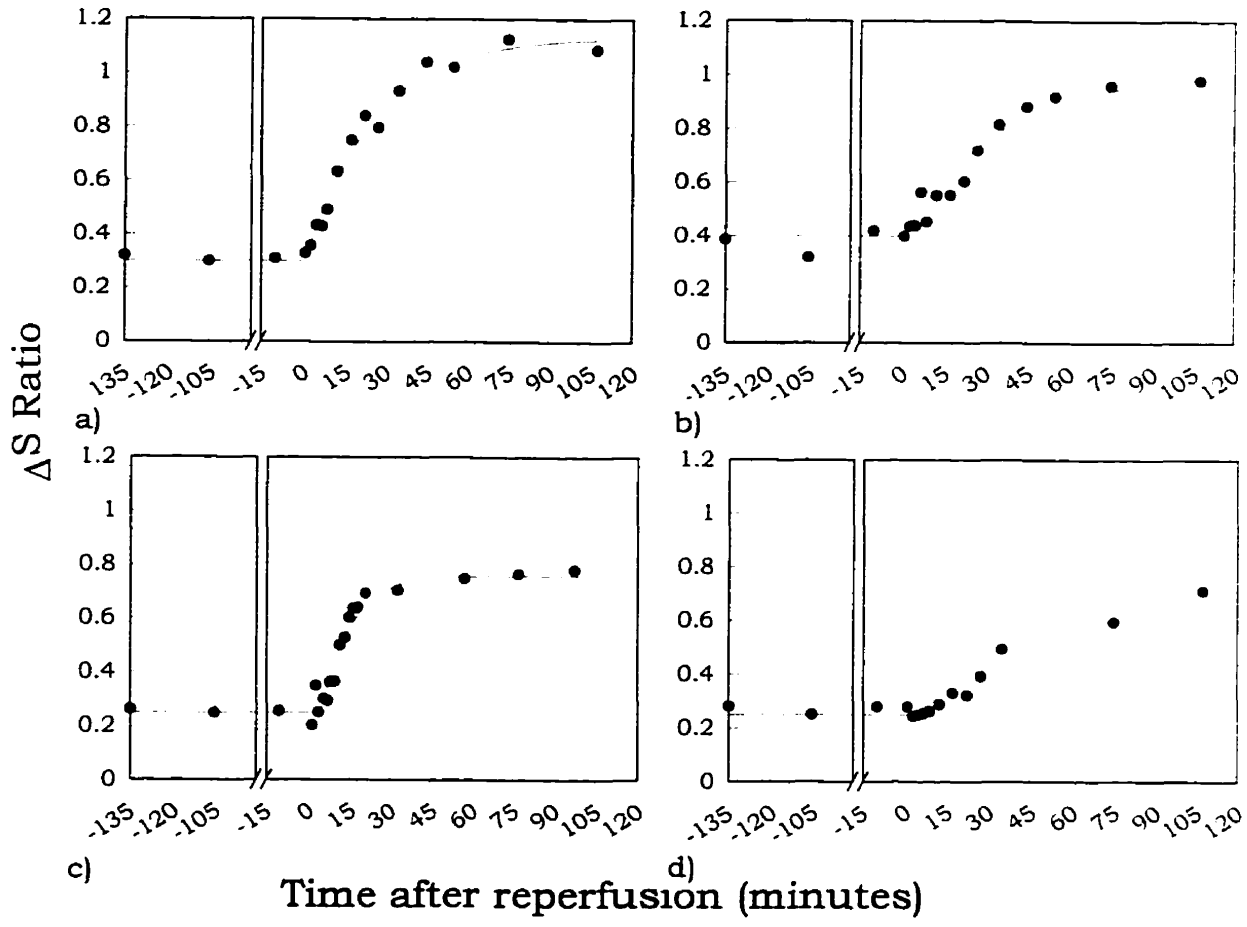

Figure 3-5 ΔS ratio *vs* time data from damaged tissue for all animals in procedure 2

The onset of reperfusion (deflation of the balloon cuff) was at time 0 and the occlusion began at −120 minutes. The lines are fits to the modified Kety model. In dogs 1-3 (a-c) the curves rose fairly quickly to a plateau but in dog 4 (d) the curve rose more slowly. The length of time to reach equilibrium was much longer than we expected for tracer equilibrium and the FE product determined from kinetic modeling was 1 order of magnitude smaller than blood flow determined using microspheres (Table 3-2), suggesting that the shape of the curves was primarily due to an increasing value of λ.

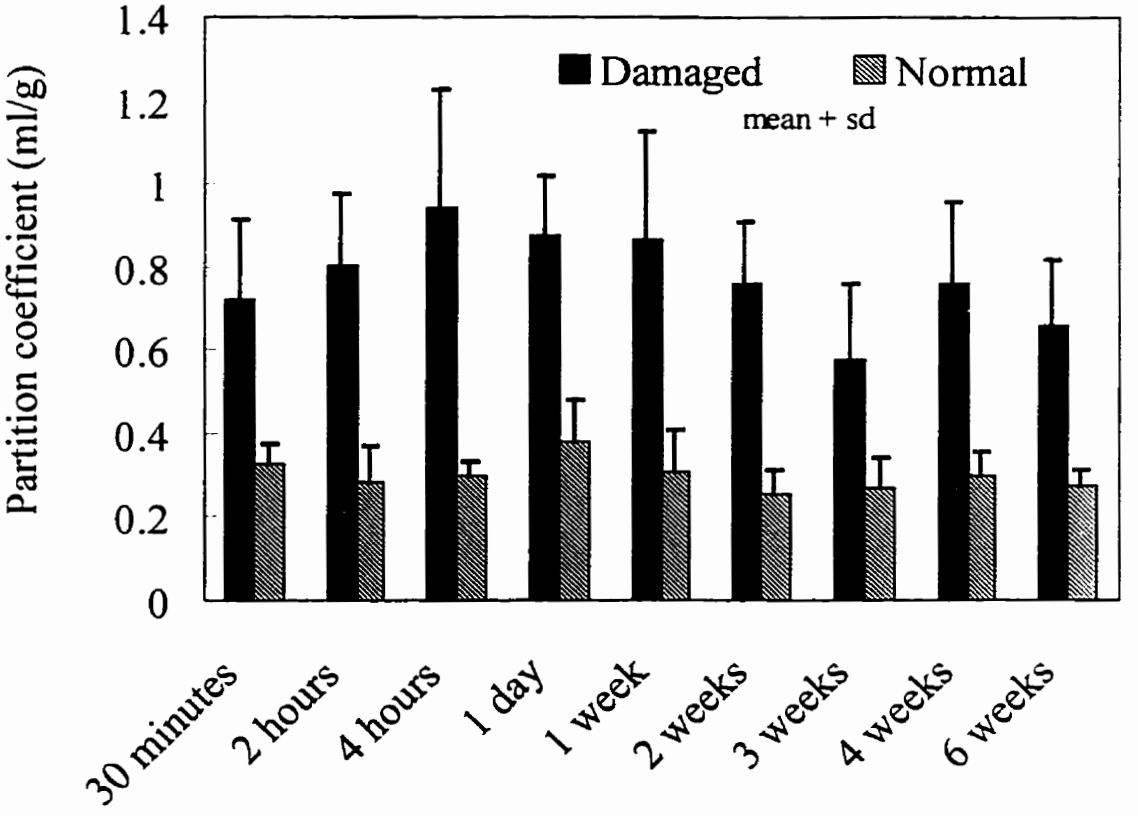

Figure 3-6 Variation of partition coefficient in normal and damaged tissue groups with time after reperfusion

λ from 2 hours to 6 weeks was measured after a constant infusion of ^{111} In-DTPA . Data at 30 minutes was calculated from signal intensities *in vivo* in procedure 2. Partition coefficient in damaged tissue was increased over that in normal tissue at 30 minutes post reperfusion and stayed increased up to 6 weeks. The data in this graph are a combination of data from ref. (1) and the data from this study (mean + sd). The number of animals included at each time point was: 30 minutes (n=4), 2 hrs (6), 4 hrs (2), 1 day (3), 1 wk (8), 2 wks (2), 3 wks (2), 4 wks (4), 6 wks (4), 8 wks (4).

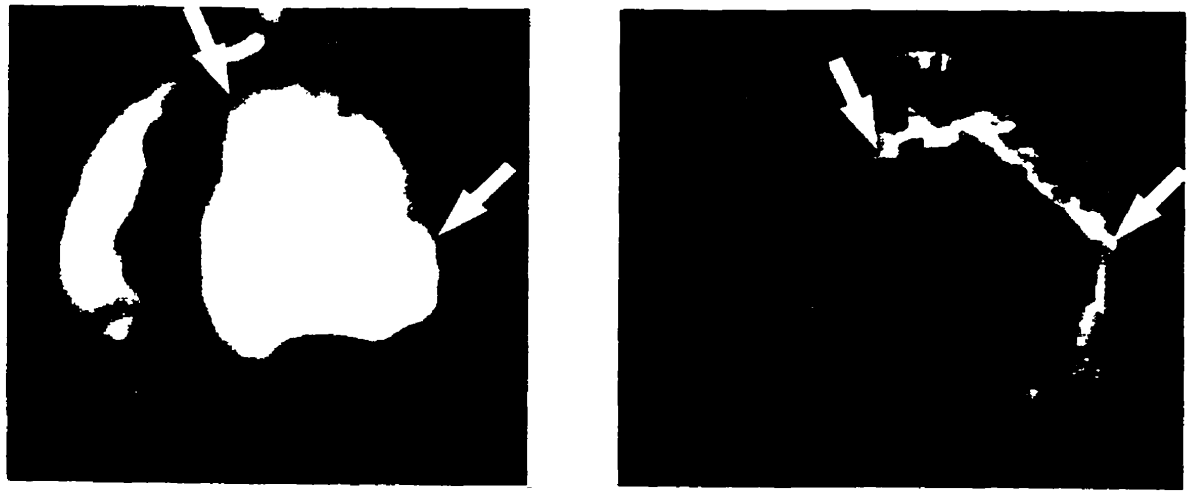

Figure 3-7 Images taken after 8 weeks of reperfusion

On the right is an ex vivo image beside the corresponding in vivo image taken immediately before sacrifice. Infarct shrinkage prevented the separation of infarcted and peri-infarcted tissue sections and thus no partition coefficient could be determined for purely damaged tissue; however, increased signal intensity could be seen in the infarcted region on both in vivo and ex vivo images (between arrows).

3.5 Discussion

The *in vivo* imaging results of procedure 1 (Fig. 3-3) confirmed our *ex vivo* results (Fig. 3-6) in that λ in damaged tissue decreased with time after reperfusion but was still elevated over that in normal tissue. Previous studies of reperfused infarctions have been unclear on the appearance of healed myocardial infarctions following Gd-DTPA administration (14-16). It is possible that some of this confusion may have been due to the use of a bolus injection of Gd-DTPA; the tissue concentration of Gd-DTPA may not have had time to reach observable levels before blood concentrations started to decrease. With a constant infusion procedure, even regions with low perfusion but elevated λ can reach equilibrium and thus show greater signal intensity in images. However, even in our study at later time points the damaged region was difficult to see *in vivo*. This was most likely due to both the thinness of the damaged region and also possibly to the decrease in partition coefficient that we observed at later time points. At 8 weeks of reperfusion, signal intensity in the damaged region was elevated over that in normal tissue by approximately 25% and the images of the excised hearts showed that there was still increased signal intensity and therefore increased partition coefficient in the damaged region. We used a cine gradient echo sequence for these *in vivo* studies in procedure 1, since the increased resolution and SNR allowed us to better detect the thinned infarct region. In procedure 2 the TFL sequence was used since the size of the infarct region was fairly large in relation to the resolution of TFL images (~2.7 mm). However, a partition coefficient for the damaged region could not be determined from excised tissue sections in this 8 week group presumably since the infarct was too small and partial volume effects were unavoidable. This thinning may make the detection of a bright

region difficult in the clinical situation. Nevertheless, clinical interpretation of these images, even with reduced enhancement, would be possible by examining wall thickness and contractility on cine images.

Loss of cell membrane integrity is the ultimate indicator of irreversible myocyte injury since the membrane is responsible for functions such as cell volume regulation and the maintenance of ionic gradients (34-36). Previous studies have shown that irreversible damage to myocytes occurs with occlusion periods of 15 minutes or more (37). Although cell membranes in irreversibly damaged tissue may begin to show signs of abnormally increased permeability during longer periods of coronary occlusion (34-38), reperfusion of these myocytes results in explosive cell swelling and bursting (39). Thus, in this reperfused infarcted tissue, the membranes become very permeable to the MR contrast agent Gd-DTPA, increasing its distribution volume (and hence concentration) (1,6,19,27). In our model, cell membrane integrity may have been compromised at the end of two hours of occlusion; however, we did not see any increases in partition coefficient during the occlusion period in procedure 2. This may have been partly due to impaired tracer delivery to these regions. Lim *et al* (1993), who injected the intravascular agent Gd-DTPA-Polylysine during a 90 minute occlusion also did not see enhancement until the onset of reperfusion when rapid enhancement was seen (7). However, other groups including our own have seen enhancement in non-reperfused infarcts at later times (4 hours to 3 weeks) (1,31,40,32). Studies of patients who have not undergone reperfusion therapy have shown similar results, although enhancement was not always consistent (2,14,27,41). Future work using the constant infusion method is needed to determine changes of partition coefficient in a chronic occlusion model.

The data in procedure 2 (Fig. 3- 5) showed a slight time lag between the onset of reperfusion and the beginning of ΔS ratio increase based on the modified Kety model fits. This time lag was seen in all four animals studied (Table 3-2) with an average value of 2.5 ± 2.05 minutes. In a canine model of reversible injury (15 minutes of occlusion followed by reperfusion) Jennings *et al* (1985) (42) found ultrastructural changes after 3 minutes but not after 20-30 seconds of reperfusion. Thus, it is possible that the time lag we observed was the time required for severe damage to develop in the cell membranes upon reperfusion.

Table 3-2 showed that the FE product determined using the modified Kety model was much lower than microsphere-determined flow in the infarcted regions. At the flow rates present in this infarcted tissue FE product should be fairly representative of flow if λ is constant (since E will approach 0.6 to 1) (32). Since the calculated FE was so low, the curves in Fig. 3- 5 likely represented the evolution of increased λ in these regions: tracer equilibration would be expected to be much quicker if flow was the only factor. Hence, the concentration of Gd-DTPA in the tissue and blood would have been at or very close to equilibrium and the ΔSI ratio in Figs. 4 and 5 would equal λ or lag very closely behind it since tracer equilibration would be rapid for small changes in λ as increasing amounts of cell membrane damage occurred. In Dog 4 (Fig. 3- 5d), flow after deflation of the balloon cuff was the most severely reduced of all the animals (Table 3-1) and some tissue sections had microsphere flows of nearly zero; in this animal reduced flow to the region may have played a role in either tracer delivery or the development of cell membrane damage. Nonetheless, partition coefficient was significantly increased in all dogs by 30 minutes after reperfusion including dogs 2 and 4 where reperfusion was poor.

Thus, increases of signal intensity in infarcted tissue using MRI and Gd-DTPA could be used very soon after reperfusion to identify infarcted tissue and direct further treatment.

The results of procedure 2 also showed that λ can be accurately and precisely quantified *in vivo* using MR image signal intensities. This could benefit tracer kinetic modeling studies seeking to determine blood flow with extracellular tracers if, following the bolus injection a constant infusion was started; then λ could be quantified and used to simplify the model and fitting procedures. In addition to simply the separation of damaged and normal tissue, the quantification of λ *in vivo* may also have other clinical benefits such as the determination of the severity of damage following an ischemic episode (43).

We have shown that the tissue concentration of Gd-DPTA during an infusion is related to myocardial viability within 10 minutes of the onset of reperfusion and at least as late as 8 weeks after reperfusion. The results of the present study, when combined with those of Chapter 2 indicate that MRI during a constant infusion of Gd-DTPA shows great promise as a non-invasive diagnostic test for myocardial viability in acute reperfused myocardial infarction.

3.6 References

1. R.S. Pereira, F.S. Prato, G. Wisenberg, J. Sykes, The determination of myocardial viability using Gd-DTPA in a canine model of acute myocardial ischemia and reperfusion. *Magn. Res. Med.* **36**, 684-693 (1996).
2. A. de Roos, A.C. van Rossum, E.E. van der Wall, S. Postema, J. Doornbos, N. Matheijssen, R.R.M. van Dijkman, F.C. Visser, A.E. van Voorthuisen. Reperfused and nonreperfused myocardial infarction: diagnostic potential of Gd-DTPA-enhanced MR imaging. *Radiology* **172**, 717-720 (1989).
3. A. de Roos, N.A.A. Matheijssen, J. Doornbos, P.R.M. van Dijkman, A.E. van Voorthuisen, E.E. van der Wall, Myocardial infarct size after reperfusion therapy: assessment with Gd-DTPA-enhanced MR imaging. *Radiology* **172**, 517-521 (1990).
4. E.R. Holman, A.C. van Rossum, T. Doesburg, E.E. van der Wall, A. de Roos. C.A. Visser, Assessment of acute myocardial infarction in man with magnetic resonance imaging and the use of a new paramagnetic contrast agent gadolinium-BOPTA. *Magn. Res. Imag.* **14**, 21-29 (1996).
5. S. Schaefer, C.R. Malloy, J. Katz, R.W. Parkey, L.M. Buja, J.T. Willerson, R.M. Peshock, Gadolinium-DTPA-enhanced nuclear magnetic resonance imaging of reperfused myocardium: identification of the myocardial bed at risk. *JACC* **12**. 1064-1072 (1988).
6. R.J. Kim, J.A.C. Lima, E.L. Chen, R.M. Judd, Myocardial Gd-DTPA kinetics determine MRI contrast enhancement and reflect the extent and severity of myocardial injury after acute reperfused infarction. *Circulation* **94**, 3318-3326 (1996).
7. T.-H. Lim, J.H. Lee, G. Gong, S.-J. Park, I. Lee, Significance of magnetic resonance signal enhancement in evaluation of myocardial infarction in cats. *Invest. Radiol.* **30**. 306-314 (1995).
8. M. Saeed, M.F. Wendland, Y. Takehara, T. Masui, C.B. Higgins, Reperfusion and irreversible myocardial injury: identification with a nonionic MR imaging contrast medium. *Radiology* **182**, 675-683 (1992).
9. M.F. Wendland, M. Saeed, K. Lauerman, N. Derugin, J. Mintorovich, F.M. Cavagna, C.B. Higgins, Alterations in T_1 of normal and reperfused infarcted myocardium after Gd-BOPTA versus Gd-DTPA on inversion recovery EPI. *Magn. Res. Med* **37**. 448-456 (1997).
10. M.C. Fishbein, D. Maclean, P.R. Maroko, The histopathologic evolution of myocardial infarction. *Chest* **73**, 843-849(1978).
11. K.T. Weber, Cardiac interstitium in health and disease: the fibrillar collagen network, in "Basic Concepts in Cardiology" (A.M. Katz, Ed.), *JACC* **13**, 1637-1652 (1989).
12. B.I. Jugdutt, R.W.M. Amy, Healing after myocardial infarction in the dog: changes in infarct hydroxyproline and topography. *JACC* **7**, 91-102 (1986).
13. R.C. Pasternak, E. Braunwald, B.E. Sobel, Acute myocardial infarction, in "Heart Disease: A Textbook of Cardiovascular Medicine" (E. Braunwald, Ed.), p.1200, W.B. Saunders, Toronto, 1992.
14. P.R.M. Dijkman, E.E. van der Wall, A. de Roos, N.A.A. Matheijssen, A.C. van Rossum, J. Doornbos, A. van der Laarse, A.E. van Voorthuisen, A.V.G. Bruschke,

Acute, subacute, and chronic myocardial infarction: quantitative analysis of gadolinium-enhanced MR images. *Radiology* **180**, 147-151 (1991).

15. H.W. Eichstaedt, R. Felix, F.C. Dougherty, M. Langer, W. Rutsch, H. Schmutzler. Magnetic resonance imaging (MRI) in different stages of myocardial infarction using the contrast agent gadolinium-DTPA. *Clin. Cardiol.* **9**, 527-535 (1986).
16. T. Nishimura, H. Kobayashi, Y. Ohara, N. Yamada, K. Haze, M. Takamiya, K. Hiramori, Serial assessment of myocardial infarction by using gated MR imaging and Gd-DTPA. *AJR* **153**, 715-620 (1989).
17. P.L. Davis, D.L. Parker, J.A. Nelson, J.S. Gillen, V.M. Runge, Interactions of paramagnetic contrast agents and the spin echo pulse sequence. *Invest. Radiol.* **23**. 381-388 (1988).
18. D.J. Atkinson, R.R. Edelman, Cineangiography of the heart in a single breath hold with a segmented turboFLASH sequence. *Radiology* **178**, 357-360 (1991).
19. C.Y. Tong, F.S. Prato, G. Wisenberg, T.Y. Lee, E. Carroll, D. Sandler, J. Sykes. Techniques for the measurement of the local extraction efficiency for inert diffusible contrast agents such as gadopentate dimeglumine. *Magn. Res. Med.* **30**, 332-336 (1993).
20. R.M. Judd, S.B. Reeder, E. Atalar, E.R. McVeigh, E.A. Zerhouni, A magnetization-driven gradient echo pulse sequence for the study of myocardial perfusion. *Magn. Res. Med.* **34**, 276-282 (1995).
21. T.A. Tasciyan, D.G. Mitchell, Pulsatile flow artifacts in fast magnetization-prepared sequences. *JMRI* **4**, 217-22 (1994).
22. V. Dilsizian, R.O.Bonow, Current diagnostic techniques of assessing myocardial viability in patients with hibernating and stunned myocardium. *Circulation* **87**. 1-20 (1993).
23. G.M. Pohost, L.M. Zir, R.H. Moore, K.A. McKusick, T.E. Guiney, G.A. Beller. Differentiation of transiently ischemic from infarcted myocardium by serial imaging after a single dose of thallium-201. *Circulation* **55**, 294-302 (1977).
24. N.V. Tsekos, Y. Zhang, H. Merkle, N. Wilke, M. Jerosch-Herold, A. Stillman, K. Uğurbil, Fast anatomical imaging of the heart and assessment of myocardial perfusion with arrhythmia insensitive magnetization preparation. *Magn. Res. Med.* **34**, 530-536 (1995).
25. M. Jerosch-Herold, N. Wilke, A.E. Stillman, Magnetic resonance quantification of the myocardial perfusion reserve with a Fermi function model for constained deconvolution. *Med. Phys.* **25**, 73-84 (1998).
26 R.A. Robb, D. P. Hanson, The ANALYZE software system for visualization and analysis in surgery simulation. *in*: "Computer Integrated Surgery". (S. Lavalle, R. Taylor, G. Burdea, R. Mosges, Eds.) (1993)
27. J.A.C. Lima, R.M. Judd, A. Bazille, S.P. Schulman, E. Atalar, E.A. Zerhouni. Regional heterogeneity of human myocardial infarcts demonstrated by contrast-enhanced MRI. Potential mechanisms. *Circulation* **92**, 1117-1125 (1995).
28. K.M. Donahue, D. Burstein, W.J. Manning, M.L. Gray, Studies of Gd-DTPA relaxivity and proton exchange rates in tissue. *Magn. Res. Med.* **32**, 66-76 (1994).

29. K.M. Donahue, R.M. Weiskoff, D. Burstein, Water diffusion and exchange as they influence contrast enhancement. *JMRI*, **7**, 102-110 (1997).
30 P. Wedeking, C.H. Sotak, J. Tesler, K.Kumar, C.A. Chang, M.F. Tweedle. Quantitative dependence of MR signal intensity on tissue concentration of Gd(HP-DO3A) in the nephrectomized rat. *MRI* **10**, 97-108 (1992).
31. L.D. Diesbourg, F.S. Prato, G. Wisenberg, D.J. Drost, T.P. Marshall, S.E. Carroll, B. O'Neill, Quantification of myocardial blood flow and extracellular volumes using a bolus injection of Gd-DTPA: kinetic modelling in canine ischemic disease. *Magn. Res. Med.* **23**, 239-253 (1992).
32. C.Y. Tong, F.S. Prato, G. Wisenberg, T.Y. Lee, E. Carroll, D. Sandler, J. Wills, D. Drost, Measurement of the extraction efficiency and distribution volume for Gd-DTPA in normal and diseased canine myocardium. *Magn. Res. Med.* **30**, 337-346 (1993).
33. J.H. Zar, "Biostatistical Analysis," Prentice Hall, Englewood Cliffs, NH, 1984.
34. R.B. Jennings, K.A. Reimer, Lethal myocardial ischemic injury. *Am. J. Pathol.* **102**, 241-255 (1981).
35. J.L. Farber, K.R. Chien, S. Mittnacht Jr, The pahogenesis of irreversible cell injury in ischemia. *Am. J. Pathol.* **102**, 271-281 (1981).
36. K.A. Reimer, R.B. Jennings, M.L. Hill, Total ischemia in dog hearts *in vitro*: 2: High energy phosphate depletion and associated defects in energy metabolism, cell volume regulation, and sarcolemmal integrity. *Circ. Res.* **49**, 901-911 (1981).
37. K.A. Reimer, R.S. VanderHeide, V.J. Richard, Reperfusion in acute myocardial infarction: Effect of timing and modulating factors in experimental models. *Am. J. Cardiol.* **72**, 13G-21G (1993).
38. R.A. Kloner, R.E. Rude, N. Carlson, P.R. Maroko, L.W.V. DeBoer, E. Braunwald, Ultrastructural evidence of microvascular damage and myocardial cell injury after coronary artery occlusion: which comes first? *Circulation* **5**, 945-952 (1980).
39. R.A. Kloner, C.E. Ganote, D.A. Whalen, R.B. Jennings, Effect of a transient period of ischemia on myocardial cells: II: Fine structure during the first few minutes of reflow. *Am. J. Pathol.* **74**, 399-422 (1974).
40. G.E. Wesbey, C.B. Higgins, M.T. McNamara, B.L. Engelstad, M.J. Lipton, R. Sievers, R.L. Ehman, J. Lovin, R.C. Brasch, Effect of gadolinium-DTPA on the magnetic relaxation times of normal and infarcted myocardium. *Radiology* **153**, 165-169 (1984).
41 A.C. van Rossum, F.C. Visser, M.J. van Eenige, M. Sprenger, J. Valk, F.W.A. Verheugt, J.P. Roos, Value of gadolinium-diethylene-triamine pentaacetic acid dynamics in magnetic resonance imaging of acute myocardial infarction with occluded and reperfused coronary arteries after thrombolysis. *Am. J. Cardiol.* **65**, 845-851 (1990).
42. R.B. Jennings, J. Schaper, M.L. Hill, C. Steenbergen Jr, K.A. Reimer, Effect of reperfusion late in the phase of reversible ischemic injury. Changes in cell volume, electrolytes, metabolites, and ultrastructure. *Circ. Res.* **56**, 262-278 (1985).
43. J.S. Schwitter, M. Saeed, M.F. Wendland, N. Derugin, E. Canet, R.C. Brasch, C.B. Higgins, Influence of severity of myocardial injury on distribution of

macromolecules: Extravascular versus intravascular gadolinium-based magnetic resonance contrast agents. *JACC* **30**:1086-1094 (1997).

4 Studies of Chronic Coronary Occlusion[1]

4.1 Introduction

Chapters 2 and 3 dealt with reperfused myocardial infarction, which due to the known importance and prevalence of reperfusion therapy, is an important clinical situation. However, 35% or more of AMI patients are not candidates for thrombolytic therapy (1), and of those who do receive some form of reperfusion therapy failure to restore blood flow may occur in up to 40% of these patients (2). As mentioned in the introduction, viable tissue with greatly reduced blood flow (hibernating myocardium) is frequently encountered and needs to be separated from infarcted tissue with greatly reduced blood flow. This would prove very important clinically since the decision to perform an interventional revascularization procedure may depend upon the state of the tissue in question. Thus, determination of λ in the setting of a chronic coronary artery occlusion was necessary to determine the full potential of our test.

As mentioned earlier, pathological studies have shown that after more than 15-30 minutes of coronary artery occlusion, irreversible damage to myocytes occurs (3). In addition, as early as 60-90 minutes increases in cell membrane permeability in damaged tissue have been detected (4,5). Beyond 24 hours of ischemia few major ultrastructural changes occur in irreversibly damaged tissue (6). These studies suggest that an indicator of cell membrane permeability such as Gd-DTPA may allow viability to be determined fairly early after the onset of chronic occlusion.

The major problem encountered in diagnosing myocardial viability in ischemic myocardium with any technique involving tracers or contrast agents is delivery of the

---

[1] The studies contained in this chapter were developed and analyzed by me with the aid of Drs. Frank Prato and Gerald Wisenberg. Jane Sykes provided technical support as well as assistance and advice with the animal model.

material into a region with persistently reduced flow. Although the primary coronary artery feeding a region of myocardium is occluded, blood may still reach a region using a pathway of collateral circulation, pre-existing or newly formed vessels from one coronary perfusion territory that overlap into another territory (7-9). In the case of stenosis or blockage of the major coronary artery supplying a perfusion territory, collateral circulation can supply blood to the ischemic territory. The degree of collateralization varies between species; in the absence of coronary artery disease it is more extensive in normal dogs than in normal humans (10). However, collateral growth and recruitment can be stimulated by gradual narrowing of the coronary arteries, intermittent periods of ischemia or by total occlusion although the former two are more effective (8,11). Since most AMI occurs in the setting of atherosclerotic narrowed coronary arteries (12), intermittent episodes of ischemia, although often non-symptomatic (silent ischemia (13)), often stimulate the growth and proliferation of collateral circulation. Thus, many patients already have some degree of collateral circulation at the time of a major infarction which reduces the damage that may occur (9,14) by providing a pathway for perfusion into the occluded territory. In this situation, the canine model is fairly representative of the diseased human case (10) and a tracer such as Gd-DTPA may be able to enter the region of reduced flow and diffuse into the extracellular space. In this respect a constant infusion procedure, where blood concentration of Gd-DTPA is maintained for a long time, would allow Gd-DTPA concentration in ischemic tissue (whether viable or not) to reach equilibrium and be representative of λ. Following a bolus injection, tissue concentration in ischemic tissue may never reach equilibrium due to the limited time for contrast agent delivery due to the fairly rapid blood clearance of Gd-DTPA.

Contrast-enhanced studies with MRI have focussed on both reperfused and permanent occlusions. In a study of 90 minutes of permanent occlusion (by which time irreversible damage is expected to occur (3)) decreased signal intensity was seen in infarcted tissue after bolus administration of $MnCl_2$ due to prolonged T_1 values in regions of decreased flow where $MnCl_2$ delivery was compromised (15). As early as 3½ to 5 hours post occlusion, signal enhancement or increases of λ in infarcted tissue have been seen after the administration of contrast agents but the changes have either been non-homogeneous (enhancement at the periphery of the infarct) or increases have not been substantial (16-19). Wesbey *et al* (1982) (20) found hyperenhancement after Gd-DTPA administration in a canine model of 24 hours of occlusion as did Diesbourg *et al* (1992) (21) after 1- 4 days of occlusion but Goldman *et al* (1982) (22) detected hypoenhancement in a similar 24 hour occlusion model. These studies serve to indicate the difficulties in assessing myocardial viability in the setting of chronic occlusion.

In this chapter we used a model of chronic occlusion in which the left anterior descending coronary artery (LAD) was permanently ligated. In the first two chapters, even though the artery was re-opened after two hours, blood flow in some segments was still greatly reduced, in some cases as low as 0.10 ml/min/g (on the order of 10% of normal flow) without a reduction in Gd-DTPA uptake. This led us to believe that very little residual flow was necessary for the procedure to successfully detect infarcted tissue. The results presented in this chapter are limited. One dog was studied per occlusion period, ranging from 4 hours to 1 week, and the results are in no way meant to constitute a comprehensive study. They were undertaken to examine when we could expect to see

increases in λ in the setting of chronic occlusion in order to help determine when our human studies should be performed.

4.2 Methods

Three female beagles were studied. The initial surgical preparation was identical to chapters two and three: anaesthesia with thiopental sodium followed by isoflurane ventilation and then a left thoracotomy to expose the heart, allowing a small section of the proximal LAD to be dissected free of the heart wall. A femoral arterial catheter was inserted to allow blood sampling during microsphere injections. In this study, ligatures were guided around the LAD and tied securely and permanently to produce a chronic occlusion.

Each beagle was allowed to recover for a different time period: 4 hours, 2 days and 1 week. The animal studied at 1 week was included in Chapter 2 (Figure 2-8). Two hours before sacrifice, ^{201}Tl was injected as a measure of myocardial viability and 90 minutes before sacrifice a mixture of ^{111}In-DTPA and Gd-DTPA (bolus of 0.3 mmol/kg, infusion of 0.006 mmol/kg/min) was infused until the end of the study. As before, the study was timed to end at the occlusion period shown. For example, in the 4 hour occlusion the animal was sacrificed at 4 hours and the infusion of ^{111}In-DTPA/Gd-DTPA was started 90 minutes prior to this. Measurements of regional blood flow using radioactively labelled microspheres were made in all animals just before sacrifice.

After sacrifice, the status of the ligating suture was confirmed visually and the excised hearts were imaged at 1.5T using a high resolution 3D FLASH sequence (TR/TE 22/10ms, 40° flip angle) to map the distribution of Gd-DTPA. The hearts were sectioned,

using the images as a guide and counted for radioactivity and the radioactive counts used to determine blood flow, ^{201}Tl uptake and λ of Gd-DTPA as previously outlined.

4.3 Results

Microsphere blood flow results showed that flow was reduced in the LAD perfusion territory at the time of sacrifice in the 4 hour to 1 week occlusion periods. Flow as a percentage of flow in normal tissue was 6.6% in the 4 hour animal, 22% in the 2 day animal and 29.8% in the 1 week animal. In the infarcted regions, subendocardial flow was 33%,7% and 27% that of subepicardial flow respectively.

In all groups but the 4 hour occlusion animals strong relationships between λ and normalized ^{201}Tl uptake were seen ($r = -0.94$, 2 days; -0.77, 1 week; both $p<0.0001$). A graph of λ vs ^{201}Tl uptake from the dog studied at 1 week of reperfusion are contained in Figure 2-8 (Chapter 2). A representative graph of λ *vs* ^{201}Tl uptake at 2 days is shown in Figure 4-1. In tissue sections with very low (less than 0.3) ^{201}Tl uptake, there appeared to be a decrease in λ but the values of λ were still on the order of 1.0 ml/g. In the 4 hour animal the correlation coefficient between λ and ^{201}Tl uptake was very small ($r=-0.29$, $p=0.013$) (Figure 4-2) and below a ^{201}Tl uptake of 0.4, λ began to decrease. If only tissue sections with ^{201}Tl uptake above 0.4 were included, a correlation coefficient of –0.75 ($p<0.0001$) was calculated and for those below 0.4 a positive correlation coefficient of 0.79 ($p<0.0001$) was calculated.

Images of the excised hearts from 2 days and 1 week showed uniform enhancement of the infarcted region (Figure 4-3a). After 4 hours of occlusion a faintly

discernible region of increased signal intensity could be detected and the periphery of the infarct was very slightly enhanced (Figure 4-3b).

4.4 Figures

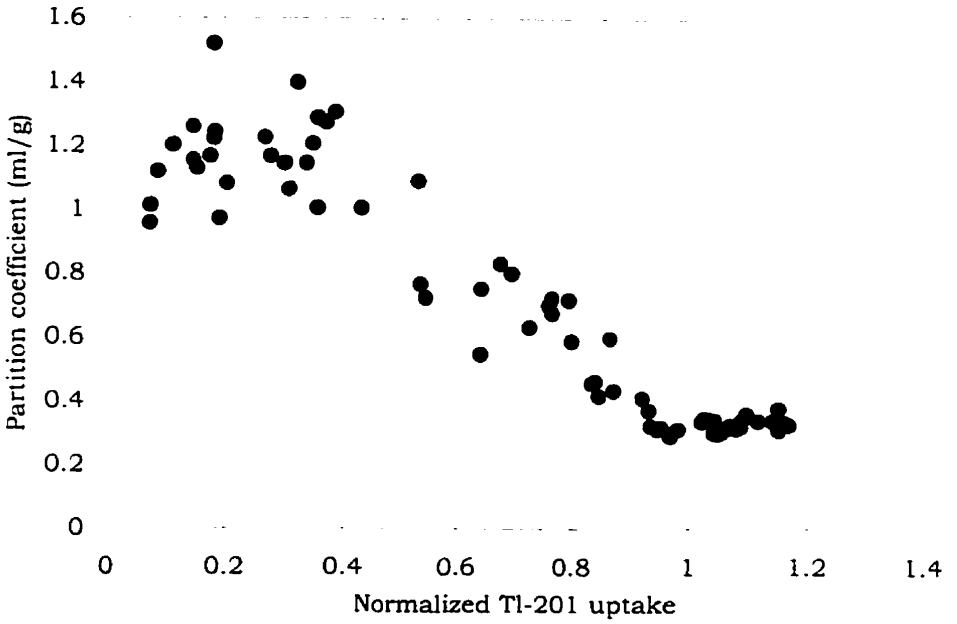

Figure 4-1 λ *vs* ^{201}Tl uptake after 2 days of chronic coronary artery occlusion

There was a significant correlation between λ and ^{201}Tl uptake (-0.94, $p<0.0001$). Some points with very low ^{201}Tl uptake appear to have slightly lower λ; this was most likely due to impaired delivery of ^{111}In-DTPA to these regions. However, λ is still substantially increased in these regions, indicating infarcted tissue.

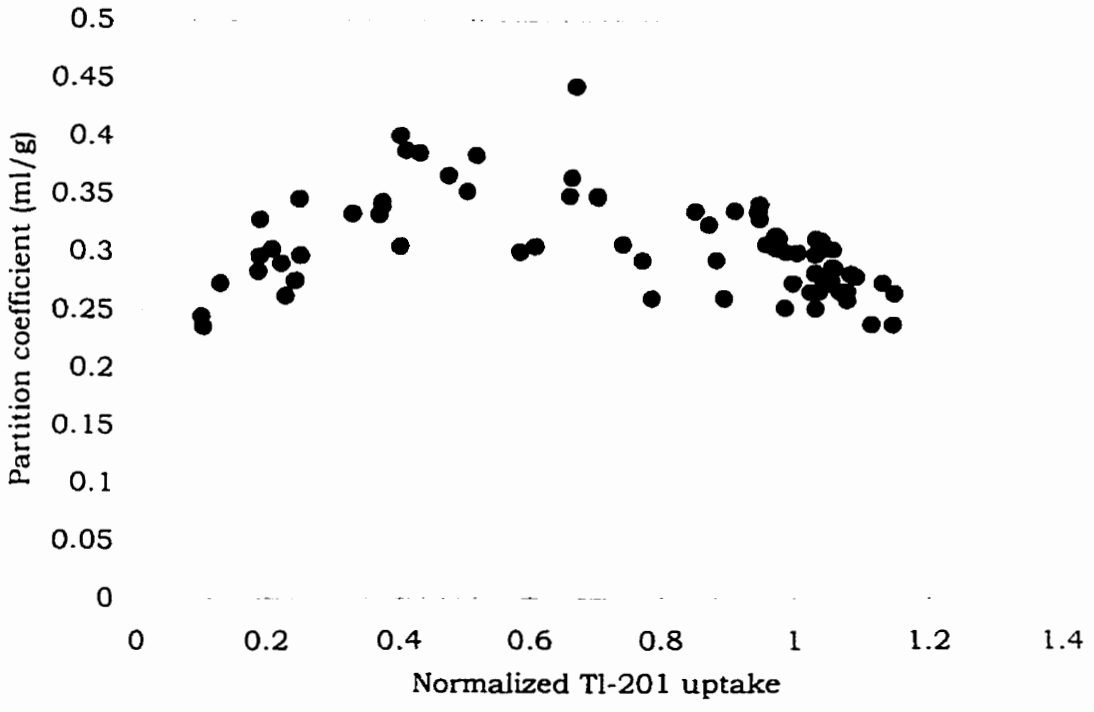

Figure 4-2 λ vs ^{201}Tl uptake 4 hours after chronic coronary artery occlusion

Although the correlation coefficient between λ and ^{201}Tl uptake was insignificant ($r = -0.28$, $p=0.013$) there appeared to be a linear relationship above ^{201}Tl uptake of 0.4; a correlation coefficient of –0.75 ($p<0.0001$) was calculated using tissue sections with ^{201}Tl uptake above 0.4. For tissue sections with ^{201}Tl uptake below 0.4 the correlation coefficient was 0.78 ($p<0.0001$), suggesting that impairment of flow to these regions resulted in inadequate tracer delivery.

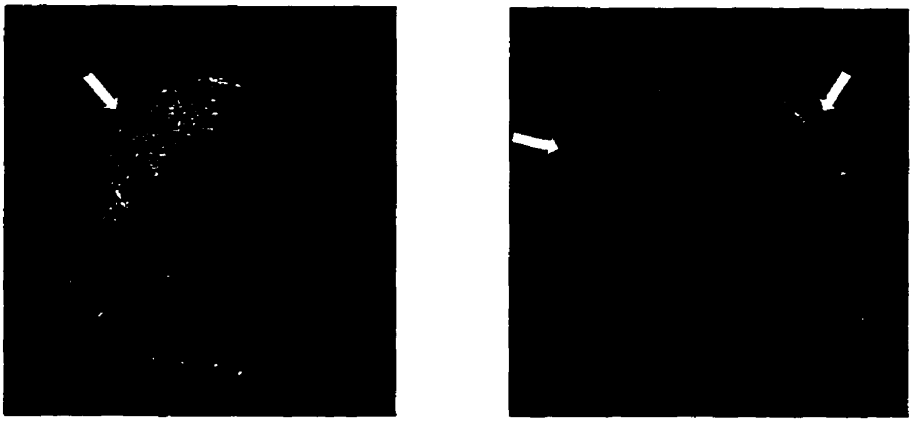

a) b)

Figure 4-3 Representative images of excised hearts

T_1-weighted images of excised hearts after a 90 minute constant infusion of Gd-DTPA. a)After 2 days of occlusion of a coronary artery a homogeneously increased region of signal intensity was detected (arrow). Similar results were seen at 1 week. b)After only 4 hours of occlusion, a faintly discernible region could be detected and the periphery of the infarcted region appeared to be slightly enhanced (between arrows).

4.5 Discussion

The results presented here showed that in the setting of a permanent coronary artery ligation enhancement following administration of Gd-DTPA can still occur. Thus, over this time period (2 days to 1 week), MRI with Gd-DTPA has the potential to determine myocardial viability regardless of whether reperfusion was attempted or was successful. This is potentially very important in the case of hibernating myocardium, where tissue is viable but blood flow is chronically reduced. If viable tissue can be found then further revascularization therapy is strongly indicated and may be very beneficial to the patient.

These results are consistent with previous results in both canine models of permanent occlusion (19-21) and human patients with occluded coronary arteries (23-25) that have shown hyperenhancement in infarcted tissue. In the clinical situation, in contrast to animal models, the true success of reperfusion or length of occlusion is often unknown. The results presented here indicate that even without complete reperfusion of the main coronary artery supplying a perfusion territory, increases in signal intensity in damaged tissue will be seen after contrast administration.

Flow to the occluded region increased with time after reperfusion. Nonetheless, based on the results of the 4 hour occlusion animal, flow was decreased for at least 4 hours and most of the tissue in the severely ischemic region of risk would have been irreversibly damaged at that point (26,27). Previous studies in the canine model have shown that immediately after occlusion of the main coronary artery supplying a territory, flow to that perfusion bed is severely reduced but increases gradually due to recruitment of collateral flow. By 24 hours post occlusion substantial increases in flow to occluded perfusion beds have occurred (28-31). In addition, these studies have shown that the increases are mainly due to increases in epicardial flow while endocardial flow stays the

same or decreases and our blood flow results were consistent with this observation. However, images of excised hearts at 2 days and 1 week showed homogeneous regions of signal enhancement and there were no tissue sections with abnormally low λ and low ^{201}Tl uptake which would indicate insufficient delivery of tracer. Thus, even these extremely low values of flow allowed sufficient delivery of Gd-DTPA to the infarcted tissue. In addition, in previous studies of chronic occlusion, when 15 μm microspheres were not delivered to the occluded territory, there was evidence of accumulation of diffusible tracers such as ^{86}Rb demonstrating residual collateral flow (32,33). Consequently, even in the setting of chronic coronary occlusion there would be a path for Gd-DTPA to enter the damaged region.

In the dog studied after 1 week of occlusion, one sample showed greatly increased λ with normal ^{201}Tl (Chapter 2, Figure 2-8). This may be evidence of enhancement in hibernating myocardium but the result was not seen in any of the other tissue sections at this or any time points. Thus, it is also possible that this point may be the result of a systematic error or improper tissue handling. The data in Figure 4-1 show a slight decrease in λ values in sections with ^{201}Tl uptake below 0.3. This decrease was most likely due to reduced delivery of ^{111}In-DTPA to regions with severely reduced blood flow. Nonetheless, λ in these sections was still over 1.0 ml/g which was 3 times greater than that in normal tissue. In the dog studied at 4 hours of occlusion impairment of tracer delivery to the damaged region most likely played a role in the results shown in Figure 4-2 and the image in Figure 4-3b. In the tissue sections with very low blood flow the ratio of tissue to blood concentrations may not be at equilibrium and thus may not truly represent λ. In this figure, the slope of the points above ^{201}Tl uptake of 0.4 appeared to

be lower than that in Figure 4-1 and in our previous studies of reperfusion (Chapters 2 and 3). This may be due to either tracer delivery or to evolving cell membrane damage similar to that seen very early after the start of reperfusion (Chapter 3). At low values of ^{201}Tl uptake in severely ischemic tissue, not enough Gd-DTPA could be delivered. Diesbourg *et al* (21) found similar results in a model of 1 to 4 days chronic ischemia during a 25 minute constant infusion; although λ was increased in most infarcted tissue sections, in some section with very low flow λ was severely decreased. In our study, at 2 or more days λ was increased in all infarcted tissue and this may have been due to the length of our constant infusion (90 minutes) which would have allowed more time for tracer delivery. Of course, more extensive studies need to be carried out to fully examine the relationship between λ and viability during chronic coronary artery occlusion.

This chapter shows that in the setting of chronic coronary artery occlusion, increases in λ in infarcted tissue can be expected when the occlusion period exceeds 2 days. This was important in determining the optimal timing for MR imaging during the clinical trial presented in Chapter 5.

4.6 References

1. M.C.G. Horrigan, E.J. Topol, Direct angioplasty in acute myocardial infarction. State of the art and current controversies. *in* "The Treatment of Acute Myocardial Infarction" (Kleiman, N.S, Ed.) *Cardiology Clinics* **13,** 321-338 (1995).
2. H.V. Anderson, Role of angiography. *in* "The Treatment of Acute Myocardial Infarction" (Kleiman, N.S, Ed.) *Cardiology Clinics* **13**, 407-419 (1995).
3. D.A. Whalen, D.G. Hamilton, C.E. Ganote, R.B. Jennings, Effect of a transient period of ischemia on myocardial cells. I. Effects on cell volume regulation. *Am. J. Pathol.* **74**, 381-398 (1974).
4. K.A. Reimer, R.B. Jennings, R.B., M.L. Hill, Total ischemia in dogs, *in vitro*. 2. High energy phosphate depletion and associated defects in energy metabolism, cell volume regulation, and sarcolemmal integrity. *Circ. Res.* **49**, 901-911 (1981).
5. R.A. Kloner, R.E. Rude, N. Carlson, P.R. Maroko, L.W.V. DeBoer, E. Braunwald, Ultrastructural evidence of microvascular damage and myocardial cell injury after coronary artery occlusion: which comes first? *Circulation* **62(5)**, 945-952 (1980).
6. R.B. Jennings, K.A. Reimer, K.A., Lethal myocardial ischemic injury. *Am. J. Pathol.* **102**, 241-255 (1981).
7. A. Maseri, L. Araujo, M.L. Finocchiaro, Collateral development and function in man. *in* "Collateral Circulation. Heart, Brain, Kidney, Limbs" (W. Schaper, J. Schaper, Eds.) p.381 Kluwer Academic Publishers, Boston, 1993.
8. R.W. Kass, M.N. Kotler, S. Yazdanfar, S., Stimulation of coronary collateral growth: Current developments in angiogenesis and future clinical applications. *Am. Heart J.* **123**, 486-496 (1992).
9. S. Sasayama, M. Fujita, M., Recent insights into coronary collateral circulation. *Circulation* **85**, 1197-1204 (1992).
10. M.P. Maxwell, D.J. Hearse, D.M. Yellon, D.M., Species variation in the coronary collateral circulation during regional myocardial ischaemia: a critical determinant of the rate of evolution and extent of myocardial infarction. *Card. Res.* **21**, 737-746 (1987).
11. J. Schaper, J. Weihrauch, Collateral vessel development in the porcine and canine heart. Morphology revisited. *in* "Collateral Circulation. Heart, Brain, Kidney, Limbs" (W. Schaper, J. Schaper, Eds.),p.65, Kluwer Academic Publishers, Boston, 1993.
12. R.C. Paternak, E. Braunwald, B.L. Sobel, Acute myocardial infarction. *in* "Heart Disease: A Textbook of Cardiovascular Medicine" (E. Braunwald, Ed),p.1200, W.B. Saunders, Toronto, 1992.
13. R. Bolli, Myocardial 'stunning' in man. *Circulation* **86**, 1671-1691 (1992).
14. W.D. Nitzberg, H.P. Nath, W.J. Rogers, W.P. Hood, P.L. Whitlow, R. Reeves, W.A. Baxley, Collateral flow in patients with acute myocardial infarction. *Am. J. Cardiol.* **56**, 729-736 (1985).
15. T.J. Brady, M.R. Goldman, I.A. Pykett, F.S. Buonanno, J.P. Kistler, J.H. Newhouse, C.T. Burt, W.S. Hinshaw, G.M. Pohost, G.M., Proton nuclear magnetic resonance imaging of regionally ischemic canine hearts: Effect of paramagnetic proton signal enhancement. *Radiology* **144**, 343-347 (1982).

16. T. Masui, M. Saeed, M.F. Wendland, C.B. Higgins, Occlusive and reperfused myocardial infarcts: MR imaging differentiation with nonionic Gd-DTPA-BMA. *Radiology* **181**, 77-83 (1991).
17. D. Tscholakoff, C.B. Higgins, U. Sechtem, M. McNamara, Occlusive and reperfused myocardial infarcts: Effect of Gd-DTPA on ECG-gated MR imaging. *Radiology* **160**, 515-519 (1986).
18. M. Saeed, M.F. Wendland, Y. Takehara, T. Masui, C.B. Higgins, c.B.. Reperfusion and irreversible myocardial injury: Identification with a nonionic MR imaging contrast medium. *Radiology* **182**, 675-683 (1992).
19. C.Y. Tong, F.S. Prato, G. Wisenberg, T.-Y. Lee, S.E. Carroll, D. Sandler. J. Wills. D.J. Drost, Measurement of the extraction efficiency and distribution volume for Gd-DTPA in normal and diseased canine myocardium. *Magn. Reson. Med.* **30**. 337-346 (1993).
20. G.E. Wesbey, C.B. Higgins, M.T. McNamara, B.L. Engelstad, M.J. Lipton. R. Sievers, R.L. Ehman, J. Lovin, R.C. Brasch, Effect of gadolinium-DTPA on the magnetic resonance relaxation times of normal and infarcted myocardium. *Radiology* **153**, 165-169 (1984).
21. L.D. Diesbourg, F.S. Prato, G. Wisenberg, D.J. Drost, T.P. Marshall, S.E. Carroll. B. O'Neill, Quantitation of myocardial blood flow and extracellular volumes using a bolus injection of Gd-DTPA: Kinetic modelling in canine ischaemic disease. *Magn. Reson. Med.* **23**, 239-253 (1992).
22. M.R. Goldman, T.J. Brady, I.A. Pykett, C.T. Burt, F.S. Buonanno, P. Kistler, J.H. Newhouse, W.S. Hinshaw, G.M. Pohost, Quantification of experimental myocardial infarction using nuclear magnetic resonance imaging and paramagnetic ion contrast enhancement in excised canine hearts. *Circulation* **5**, 1012-1016 (1982).
23. A.C. Van Rossum, F.C. Visser, M.J. van Eenige, M. Sprenger, J. Valk, F.W.A. Verheught, J.P. Roos, Value of gadolinium-diethylene-triamine pentaacetic acid dynamics in magnetic resonance imaging of acute myocardial infarction with occluded and reperfused coronary arteries after thrombolysis. *Am. J. Cardiol.* **65**. 845-851 (1990).
24. F. Fedele, T. Montesano, M. Ferro-Luzzi, E. Di Cesare, P. Di Renzi, F. Scopinaro. L. Agati, M. Penco, F. Serri, A. Vitarelli, A. Dagianti, Identification of viable myocardium in patients with chronic coronary artery disease and left ventricular dysfunction: Role of magnetic resonance imaging. *Am. Heart J.* **128**, 484-489 (1994).
25. C. Yokota, H. Nonogi, S. Miyazaki, Y. Goto, M. Maeno, S. Daikoku, A. Itoh. K. Haze, N. Yamada, Gadolinium-enhanced magnetic resonance imaging in acute myocardial infarction. *Am. J. Cardiol.* **75**, 577-581 (1995).
26. K.A. Reimer, J.E. Lowe, M.M. Rasmussen, R.B. Jennings, R.B., The wavefront phenomenon of ischemic cell death. 1. Myocardial infarct size *vs.* duration of coronary occlusion in dogs. *Circulation* **5**, 786-794 (1977).
27. K.A. Reimer, R.B. Jennings, The "wavefront phenomenon" of myocardial ischemic cell death. II Transmural progression of necrosis within the framework of ischemic bed size (myocardium at risk) and collateral flow. *Lab. Invest.* **40**, 633-644 (1979).

28. S.P. Bishop, F.C. White, C.M. Bloor, Regional myocardial blood flow during acute myocardial infarction in the conscious dog. *Circ. Res.* **38**, 429-438 (1976).
29. H.O. Hirzel, G.R. Nelson, E.H. Sonnenblick, E.S. Kirk, Redistribution of collateral blood flow from necrotic to surviving myocardium following coronary occlusion in the dog. *Circ. Res.* **39**, 214-222 (1976).
30. M. Fukunami, D.M. Yellon, Y. Kudoh, M.P. Maxwell, R.K.H. Wyse, D.J. Hearse, Spatial and temporal characteristics of the transmural distribution of collateral flow and energy metabolism during regional myocardial ischemia in the dog. *Can. J. Cardiol.* **3**, 94-103 (1987).
31. Y.-T. Shen, D.R. Knight, D.R. Canfield, S.F. Vatner, J.X. Thomas. Progressive change in collateral blood flow after coronary occlusion in conscious dogs. *Am. J.Physiol.(Heart Circ. Physiol.* **25)**, H478-H485 (1989).
32. S. Yoshida, S. Akizuki, D. Gowski, J.M. Downey, Discrepancy between microsphere and diffusible tracer estimates of perfusion to ischemic myocardium. *Am. J. Physiol.* **249**, H255-H264 (1985).
33. M.P. Maxwell, D.J. Hearse, D.M. Yellon, D.M., Is there a component of coronary collateral flow which cannot be detected by radiolabelled microspheres?. *Card. Res.* **21**, 747-754 (1987).

5 Report on Clinical Study on the Use of Gd-DTPA as a Marker of Myocardial Viability in Acute Reperfused Myocardial Infarction[1]

5.1 Introduction

The final step in developing any diagnostic imaging test is evaluating its potential and feasibility in the clinical setting. Animal experiments provide a well characterized model in terms of occluded coronary artery territory, blood flow, and infarct areas. In the clinical situation neither the true extent of damage nor residual regional blood flow are known and other methods must be used to indirectly ascertain the damage to the heart. These methods were mentioned in the introduction, and include techniques such as ^{18}FDG PET, ^{201}Tl SPECT and dobutamine echocardiography. In reality, the best clinical indicator of viability is return of contractility to a non-contracting region either with or without revascularization and these techniques have been shown to be fairly accurate in this respect (1-5). Since no clinically applied techniques have the same spatial resolution as MRI we had to compare our technique to one of the currently used standards. Then, if our MRI technique was accurate in detecting infarcted tissue compared to these techniques we would know that it was at least as and most likely better due to its higher resolution.

Based on the canine results presented in the previous three chapters, we were certain that we would see signal enhancement in damaged tissue at least 2 days after the start of occlusion, even if reperfusion was not attempted or was not successful. Thus, we performed the MR study approximately one week after presentation to the emergency

---

[1] The contents of this chapter will be submitted for publication when more patients have been studied. The results presented here are those obtained to date and have confirmed our hypothesis that damaged *human* tissue has increased values of λ as was seen in dogs. The protocol was developed by myself with the aid of Drs. Prato, Wisenberg and Ken Yvorchuk. The ^{201}Tl SPECT studies were carried out by the Department of Nuclear Medicine at St. Joseph's Health Centre and I have been performing the MRI studies.

department. As a gold standard for myocardial viability, we performed a rest-redistribution ^{201}Tl SPECT study (1,6). The most important aspect of the MRI study was imaging at equilibrium during a constant infusion of Gd-DTPA but we also performed a qualitative evaluation of regional blood flow using first pass imaging of a bolus of Gd-DTPA (7-9). In addition, we administered a dobutamine stress test using cine MRI to evaluate regional wall motion as an additional test for viability (10-12).

5.2 Methods

To date we have completed studies of 7 patients, 6 of whom received thrombolytic therapy (five with tissue plasminogen activator (tPA), one with streptokinase followed by tPA) following presentation to the emergency room with acute myocardial infarction. The MR study was performed 8.9 ± 1.1 days after presentation to the emergency department and 6 patients were receiving β-blocking medication at the time of the study.

As a gold standard for myocardial viability patients underwent a rest-redistribution ^{201}Tl SPECT study. 74 MBq of ^{201}Tl was injected at rest and SPECT images were acquired at 20 minutes and 3½ hours post injection.

The following day the MRI study was performed on a 1.5T Siemens Vision (Siemens, Erlangen Germany). The patients were placed in a four element phased-array body coil and the infarcted region was located using cine MRI (TR/TE 10/4.8ms, α = 30°, 13-21 cardiac phases (view-shared), rectangular field of view (128-196 × 256), in-plane resolution 1.4-1.9 mm) to detect wall motion abnormalities and T_2-weighted turbo spin echo images (fast spin echo) sequences (TR = 2 × R-R interval, $TE_{effective}$ = 57-76

ms) to detect regional changes in myocardial T_2 values produced by increases in extracellular water in infarcted tissue. The acquisitions were ECG triggered and acquired during a breath-hold to eliminate breathing artefacts.

Once the infarcted region was located, 1-2 image planes containing the region were selected and a bolus of Gd-DTPA (0.1 mmol/kg) was injected. A fast imaging sequence sensitive to Gd-DTPA concentration was used to follow the passage of contrast agent through the myocardium. This sequence, a saturation recovery turboFLASH (srTFL) consisted of a 90° pulse followed by a recovery period of 20 ms and then a turboFLASH acquisition (TR/TE 2.4/1.2 ms, α = 15°, 64-80 × 128 , 2.3-3.1 mm in plane resolution 10 mm slice thickness) (13). 100-150 images were acquired with a time resolution of once per heartbeat (60-85 beats per minute). We did not expect to be able to quantitate absolute blood flow with such a high concentration of contrast agent (13) but rather we were looking for qualitative differences in regional perfusion which would appear as differential enhancement patterns *ie:* lack or delay of signal intensity change as the bolus arrived at the myocardium would indicate reduced blood flow (7.8.9).

Immediately after the bolus a constant IV infusion of Gd-DTPA (0.004 mmol/kg/min) was started and continued for the rest of the study. Thirty minutes after the start of the infusion, high-resolution T_1-weighted MR images were acquired to map the distribution of Gd-DTPA (cine MRI, T_1 turbo spin echo with $TE_{effective}$ = 32 ms; all other parameters were the same as above). In addition, in six of the seven patients the saturation recovery turboFLASH was used to quantify λ as described in Chapter 3.

Finally, a low dose dobutamine stress study was performed in the MR system. Two short axis image planes containing non-contractile tissue were chosen and baseline

cine images were acquired. Each image took approximately 18-25 sec (one breathhold) followed by a 30 sec – 1 min recovery period. After the baseline images were acquired the dobutamine infusion was started at a rate of 5 μg/kg/min. Six min later the cine images were repeated and the infusion was then changed to 10 μg/kg/min. At 13 min the images were repeated and the infusion was stopped at 14 min. Six min after the end of the infusion, recovery images were taken.

Regions of interest were drawn in the damaged and normal regions on the srTFL images taken during bolus passage. ROIs were shifted between images as necessary to account for movement of the heart due to breathing. Signal intensity *vs* time curves were generated for each ROI and examined qualitatively for differences in enhancement patterns indicating differences in perfusion.

To compare the infarcted region detected by SPECT and MRI, redistribution SPECT slices were matched with their corresponding MRI slices; in each patient between 1 and 6 slices were of sufficient quality for this analysis. The left ventricular wall in each slice was divided into 16 segments. In the infarcted regions on the SPECT images the wall was sometimes not easily visualized; in these cases the shape of the wall was approximated based on the shape of the visible ventricle. The anterior intersection of the left and right ventricular wall was used as a landmark for the first segment on the MR images. This landmark was faintly visible on the more basal SPECT images. SPECT signal intensity in each slice was normalized to the average of three contiguous segments containing the highest signal intensity segment. MRI signal intensity was normalized to the average of the same three segments on the MR images.

Partition coefficient was estimated using the method mentioned in Chapter 3. Briefly, regions of interest were drawn in pre-contrast and equilibrium srTFL images and then λ was estimated using the equation:

$$\lambda = \frac{\Delta SI_{tissue}}{\Delta SI_{blood}} \text{ where } \Delta SI = SI_{equilibrium} - SI_{pre-contrast}.$$

Regional wall motion was analyzed using ARGUS software supplied by Siemens Canada. The end-systolic and end-diastolic contours of the four sets of cine images (baseline, 5 μg/kg/min, 10 μg/kg/min, recovery) were traced and then wall thickness (WT) was determined (14). Wall thickening index (WTI) was calculated:

$$WTI = \frac{WT_{ES} - WT_{ED}}{WT_{ED}}\%$$

where WT_{ES} and WT_{ED} were the wall thicknesses at end-sytole and end-diastole respectively.

5.3 Results

Representative signal intensity *vs* time curves are shown in Figure 5-1 for two of the patients. In patient #1 the damaged and normal regions showed similar enhancement patterns indicating similar perfusion (Figure 5-1a). In patient #2 the damaged region showed a decreased rate of enhancement in the infarcted inferior subendocardial region (Figure 5-1b) and a signal void was present in this region on the turboFLASH images (Figure 5-1c) taken approximately 30 seconds after the peak of the bolus in the left ventricle.

In all patients the delayed (redistribution) SPECT images showed signal intensity deficits indicative of infarcted tissue and in all cases these regions corresponded very

closely with regions of increased signal intensity on the high resolution T_1-weighted images. Representative images are shown in Figures 5-2 and 5-3. The quantitative comparison between ^{201}Tl uptake and MR signal is shown in Figure 3-4 and a negative correlation between ^{201}Tl uptake and MR signal intensity was seen in all individuals ($r = -0.66$ to -0.92, $p<0.05$ for all). In patient 2 the high resolution images were not of high enough quality for this analysis. In patients 3 and 6 some inferior segments with decreased Tl uptake did not show increased MR signal intensity. Since regional wall motion deficits could not be detected in these segments, they most likely represented breast attenuation artefacts.

A cutoff value of 60% of normal was set for ^{201}Tl uptake; segments with uptake below this value were considered infarcted. This cutoff value was chosen due to the results in patients who had a subendocardial infarcts by MRI. Some previous studies (1,6) have used cutoff values of 50% but there were no regions in some patients with ^{201}Tl uptake below 50%, most likely due to partial volume effects in voxels with mixtures of damaged and normal tissue. Mean ^{201}Tl uptake was determined in the segments below the cutoff value and in the corresponding segments on the MR images. Segments above 90% were considered viable. A comparison of the mean values is shown in Figure 5-5. Mean ^{201}Tl uptake was $40 \pm 16\%$ in infarcted segments and $98 \pm 6\%$ in non-infarcted segments ($p < 0.0001$). In the corresponding MRI segments, mean signal intensity was $177 \pm 42\%$ in infarcted segments and $106 \pm 12\%$ in non-infarcted segments ($p < 0.0001$).

In all patients except for patient #1 λ was determined *in vivo* using MR image signal intensities (Figure 5-6). In damaged tissue, λ had an average value of 0.83 ± 0.24

ml/g while in normal tissue it was 0.36 ± 0.05 ml/g (p=0.001) which compared well with the values from our previous animal studies (Chapters 2 and 3).

Finally, Figure 5-7 shows the change in WTI from baseline to the 10 μg/min/kg dobutamine infusion rate; this measure (change from baseline instead of absolute WTI) was chosen since some patients had preserved contractility at baseline and the change in WTI would show how the dobutamine affected the initial contractility independent of the initial WTI. In the damaged segments dobutamine infusion resulted in a non significant decrease of 3 ± 9.3% (p=0.32, paired difference t-test *vs* baseline) which was significantly lower than that in normal segments which experienced a significant increase in contractility of 22.2 ± 8.5% (p<0.0001).

5.4 Figures

a)

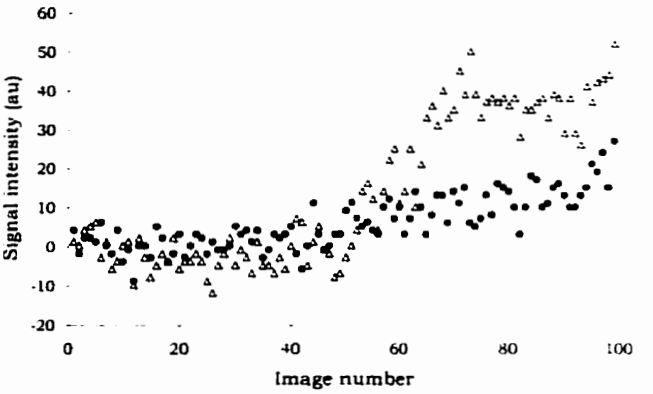

b)

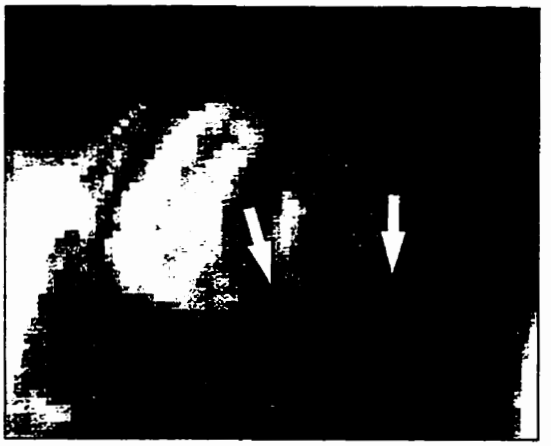

c)

Figure 5-1 Representative signal intensity *vs* time curves and contrast-enhanced images during first pass bolus tracking of Gd-DTPA

In (a) patient 4 with an inferior infarct no regional differences in perfusion were seen, *ie:* the enhancement patterns in normal anterior (△)and damaged inferior (●) regions were similar. In (b) patient 2 the inferior subendocardial region (●) showed slower uptake than normal tissue (△) and a signal void could be seen in this region on the turboFLASH images (c, arrows; acquired approximately 30 seconds after the peak of the bolus in the left ventricle).

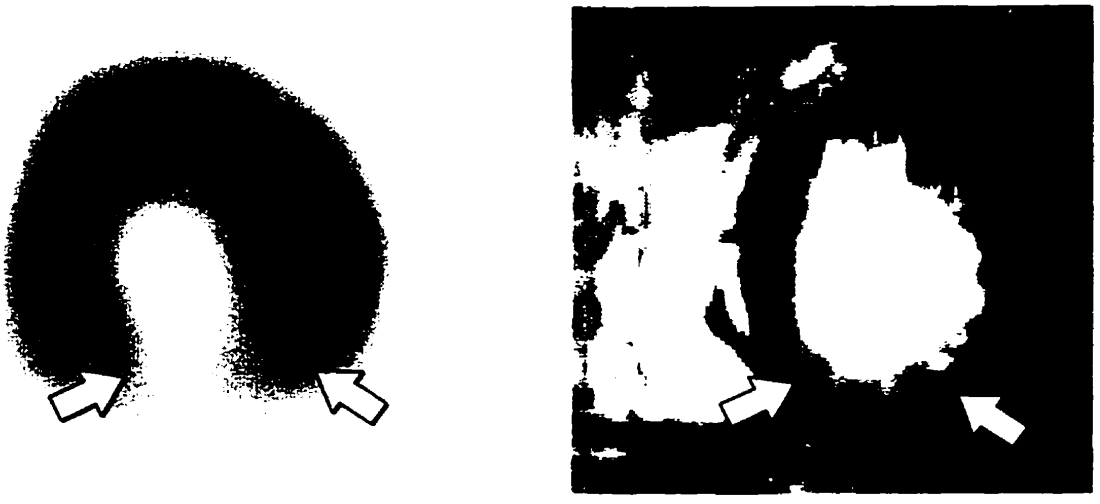

Figure 5-2 Representative ^{201}Tl SPECT and equilibrium Gd-DTPA images from a patient with a non-transmural infarct

Redistribution SPECT and contrast-enhanced T_1-weighted MR images from patient 1. There is a signal void in the inferior wall which corresponds very closely with a non-transmural region demonstrating increased signal intensity on the MR image.

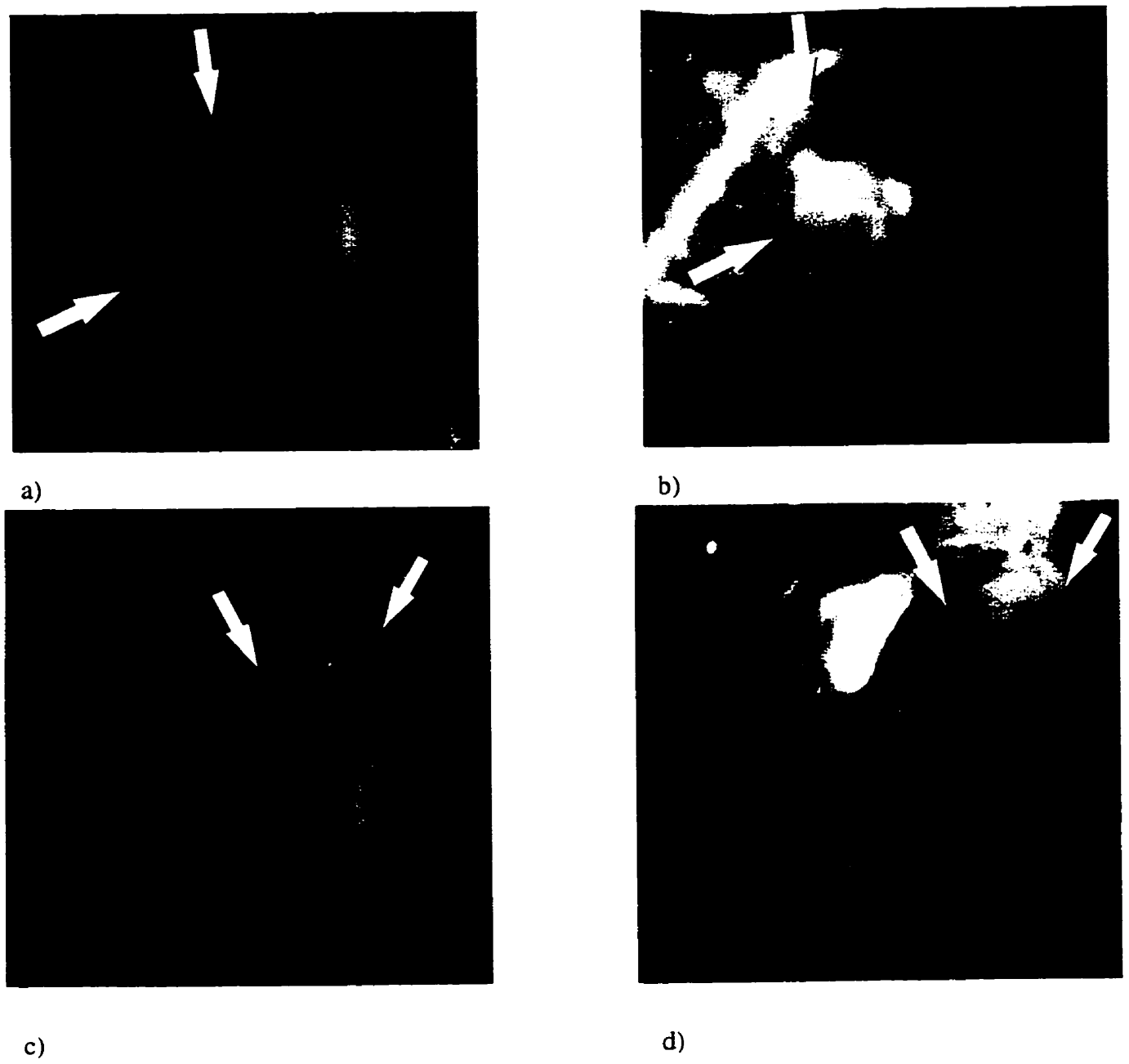

Figure 5-3 Representative ^{201}Tl SPECT and equilibrium Gd-DTPA images

Redistribution SPECT(a,c) and MRI (b,d) images from patient 3, who had an anterior infarct, showing excellent correspondence between SPECT signal void and MRI signal enhancement. The drop in signal intensity in the inferior region of the short axis SPECT image (a) may have been due to attenuation since no corresponding region of increased signal intensity or decreased contractility was seen on the MR images.

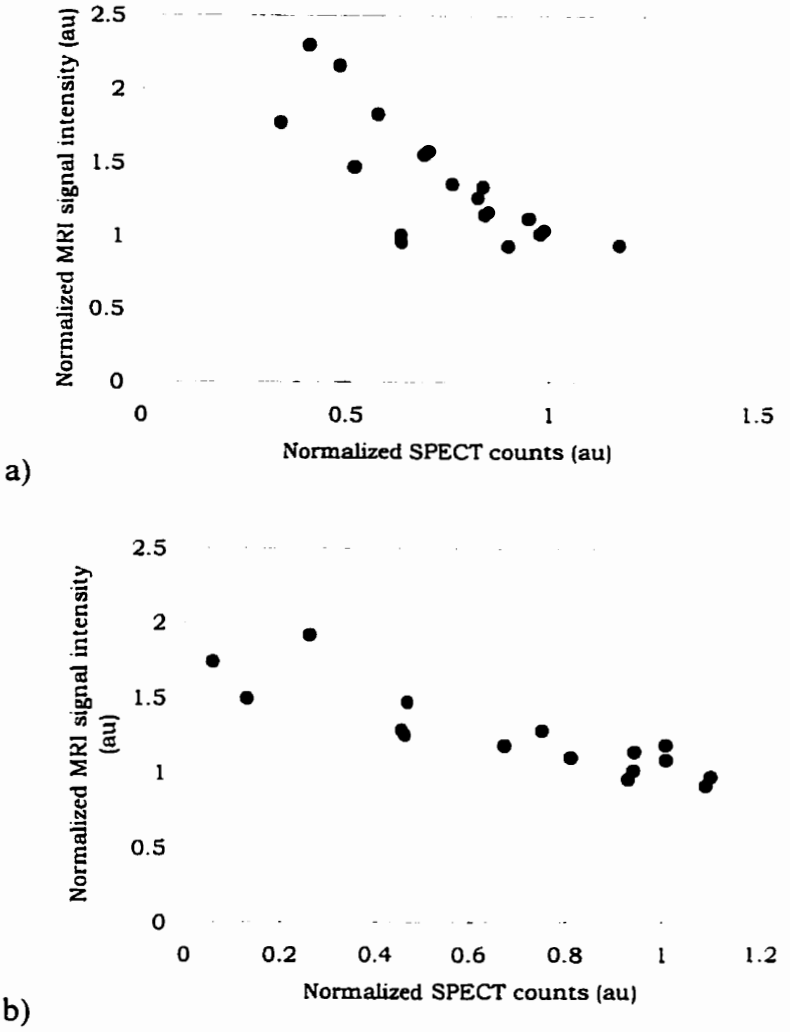

Figure 5-4 Correlation between ^{201}Tl uptake and MRI signal intensity in human subjects

Representative segmental comparison between normalized ^{201}Tl SPECT counts and MRI signal intensity in patient 3 (a, note the two points at a Tl uptake of approx. 0.65 with normal MRI values; these were likely due to an attenuation artifact along the inferior wall of this patient) and patient 4 (b). In each of these patients a negative correlation was calculated between ^{201}Tl counts and MRI signal (-0.76 and –0.88 respectively, both $p < 0.05$).

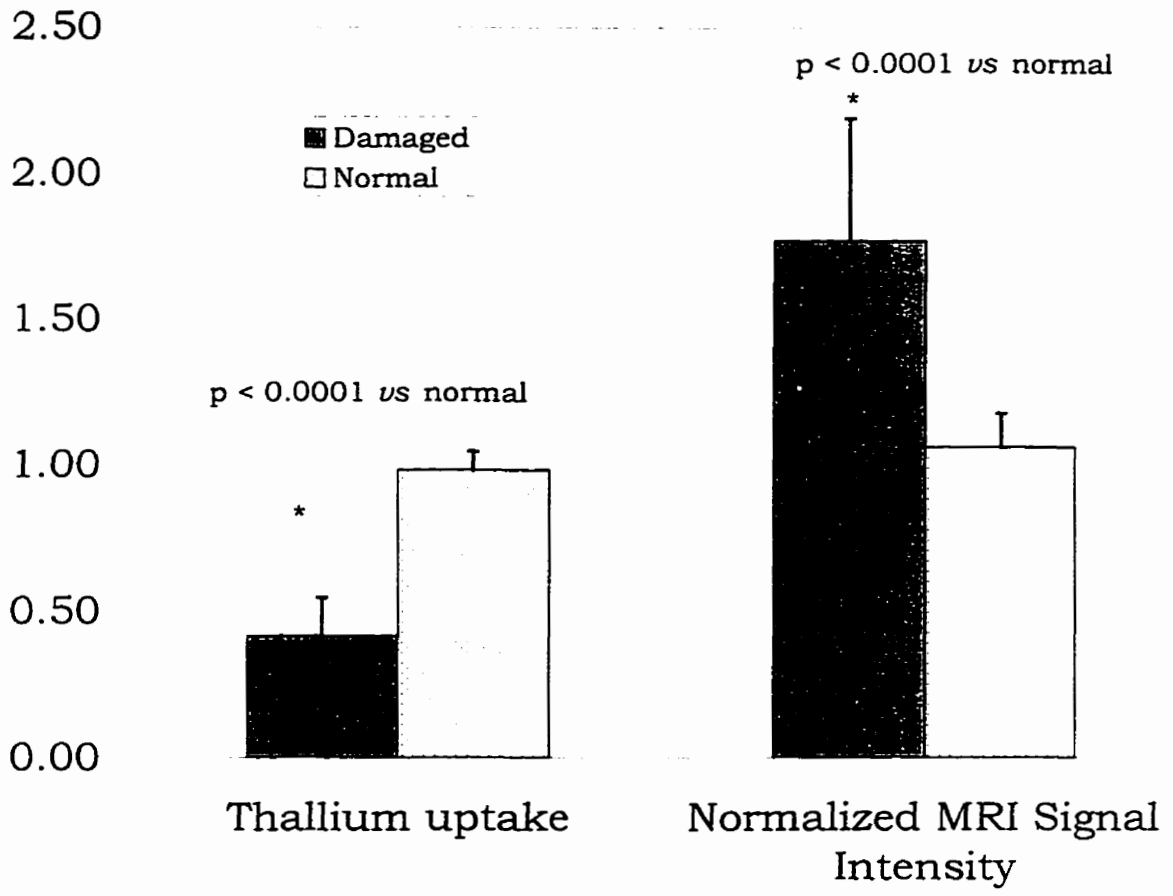

Figure 5-5 Comparison of ^{201}Tl uptake and MRI signal intensity in normal and damaged tissue

Average ^{201}Tl counts and MRI signal intensity in groups of segments designated as damaged or normal based on ^{201}Tl uptake. Damaged tissue included segments that had ^{201}Tl uptake below 60% of normal remote tissue and normal tissue had ^{201}Tl uptake above 90%. MRI segments considered damaged had 67% greater signal intensity than those considered normal ($p < 0.0001$).

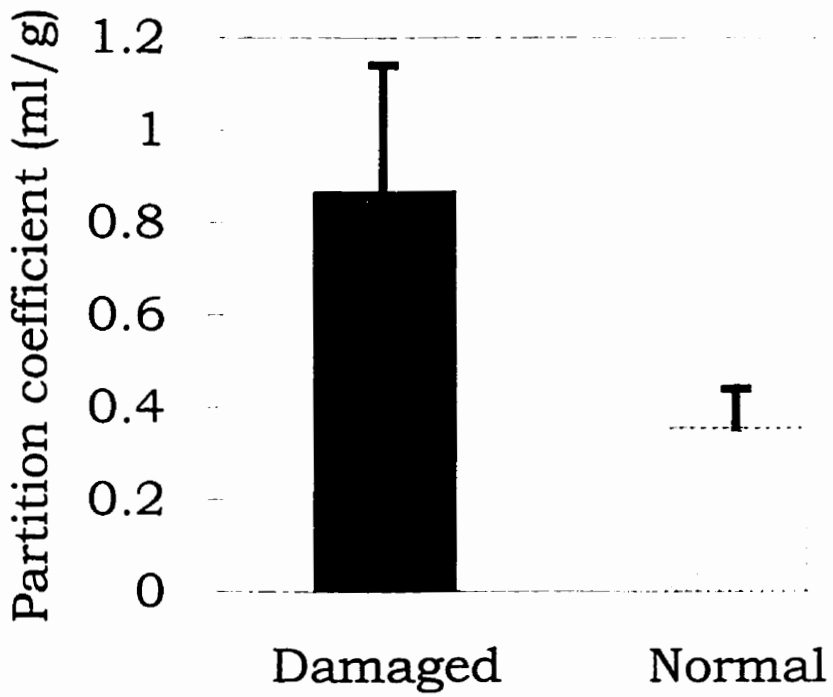

Figure 5-6 ***In vivo*** **partition coefficient values**

Partition coefficient in damaged and normal tissue for all patients except patient 1. Average λ in damaged tissue was 0.86 ± 0.23 ml/g, significantly greater than normal tissue where λ was 0.36 ± 0.05 ml/g (p=0.001).

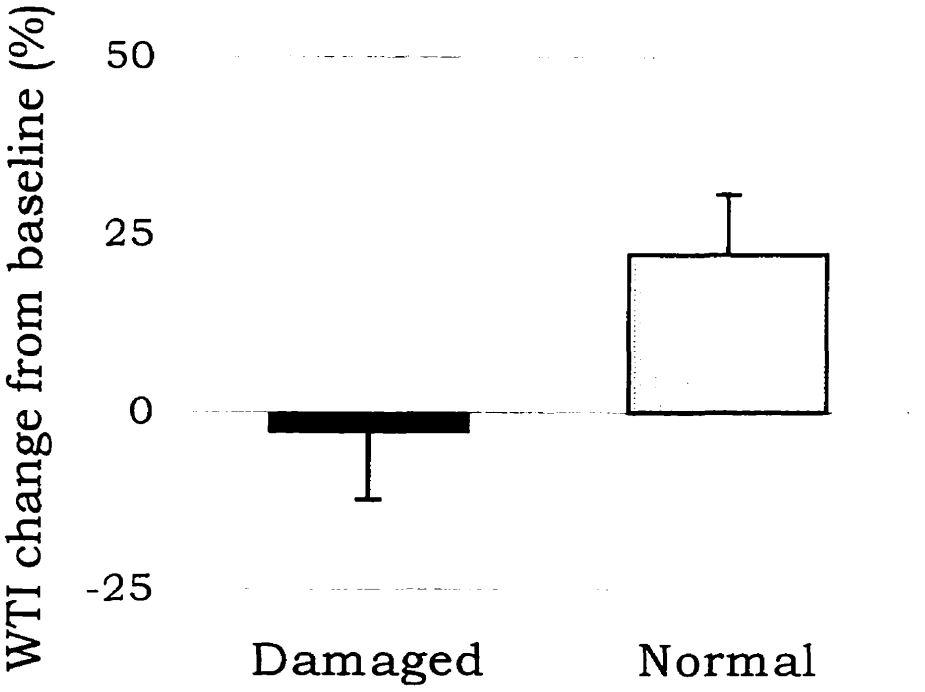

Figure 5-7 Wall thickening results

Change in WTI for all patients from baseline to the highest infusion rate of dobutamine (10 μg/kg/min). At the highest infusion rate normal tissue contractility increased by 22.2 ± 8.5% ($p<0.0001$) while damaged tissue decreased insignificantly by 3.0 ± 9.3% ($p = 0.32$).

5.5 Discussion

The results indicate that MRI during a constant infusion of Gd-DTPA has a valuable role in the clinical setting. In these patients the region of increased signal intensity corresponded well with ^{201}Tl uptake patterns and response to dobutamine stress. In patients with subendocardial infarcts *ie*: non-transmural infarcts, MRI offered more information than SPECT or contractility studies alone; in this case, SPECT may have called these regions viable (depending on the cutoff value chosen) while a resting wall motion study may have decided it was still viable due to preserved baseline contractility. The MRI study showed that both the slightly higher ^{201}Tl uptake and preserved baseline contractility may have been due to the residual viable tissue. Thus, MRI has the potential to play a very important role in the detection of myocardial viability.

In this study we examined perfusion qualitatively by looking for deficits in regional enhancement. We did not attempt to quantify regional blood flow absolutely since the arterial input curve was most likely inaccurate due to saturation of the peak of the curve at the concentration we used (0.1 mmol/kg) (13). Since the shape of a signal intensity *vs.* time curve was dependent on the input function as well as tissue parameters such as blood flow and partition coefficient, we did not use a semi-quantitative method to estimate perfusion (15). The bolus of Gd-DTPA was injected by hand and took approximately 20 seconds which was fairly long and would have decreased the accuracy of the results. However, the results of the bolus injection were consistent with the location of the infarct in the patients *ie*: perfusion deficits, if present, were in the same region as eventual hyperenhancement during the constant infusion. As an approximation of regional perfusion this qualitative method may be adequate but a quantitative measure of blood flow would be preferable. To do this, we need to measure the input function

accurately, either by injecting less contrast agent (13,16) or by using an imaging technique with greater dynamic range with respect to contrast concentration (17, 18)

The use of rest-redistribution ^{201}Tl SPECT imaging is widely accepted as a diagnostic test for myocardial viability. Since measurements are only done at rest this protocol does not give as much information about regional ischemia as a stress-redistribution protocol but it has shown accuracy for the detection of viability comparable to ^{18}FDG PET (1,2). Two of our SPECT studies in patients with anterior or antero-septal infarcts showed slight defects in the posterior wall which decreased the correlation between ^{201}Tl uptake and MRI. However, none of these segments had ^{201}Tl uptake less than 60% nor did they show increased signal intensity on the MR images. Thus, they were considered to be breast attenuation artefacts.

Dobutamine stress testing, either using echocardiography (19-24), cine MRI (11,12,25-27) or even gated SPECT (usually with ^{99m}Tc-labelled radiopharmceuticals due to their favourable imaging charcteristics) (28) has been shown to be quite sensitive in the detection of myocardium with the potential to regain contractility. If a segment contracts during dobutamine infusion, it is likely to contain enough viable tissue to regain its baseline contractility. In our study, increased signal intensity in a region during the infusion of Gd-DTPA (*ie*: infarcted tissue) was associated with a lack of contractility with dobutamine. Some patients with non-transmural enhancement had preserved contractility at baseline, presumably because the amount of remaining viable tissue was sufficient to allow contractility. In these patients however, no increase in contractility was seen during dobutamine infusion. In this study we saw no evidence of stunned myocardium (absent or reduced contractility at baseline in the absence of signal

enhancement) but we only examined two slices during dobutamine infusion. In a recent study by Dendale *et al* (1998) (29) patients were studied within two weeks after AMI using both contrast-enhanced MRI (Gd-DOTA) and a dobutamine stress test. Some regions with transmural enhancement showed both baseline contractility and response to dobutamine. They suggested that stunning may have played a role in this anomalous enhancement but since stunned tissue is still viable, it was unlikely that significant enhancement would have occurred in these regions. Since enhancement patterns after contrast administration are dependent on both flow and partition coefficient, perhaps the enhancement seen in this tissue could have been due to slow washout of contrast from ischemic yet viable tissue. Further studies of stunned myocardium need to be performed to examine this phenomenon. In addition, in our study, dobutamine was used as an alternate measure of viability. If we can prove that λ is related to myocardial viability then we would no longer need to perform the dobutamine test.

In 6 of the patients, β-adrenergic receptor blocking agents were being administered as part of their medical treatment. Since dobutamine acts on β receptors this may have decreased the effectiveness of the dobutamine test (30,31). Since this was just an initial clinical trial to determine the potential and feasibility of our protocol we felt that we could not justify withdrawing this very important medication. Nonetheless, even in these patients the dobutamine infusion, particularly at the 10 μg/kg/min level, had a marked effect on contractility in normal tissue. A more extensive clinical trial should withdraw medications such as this prior to the dobutamine test, as is generally done in the literature (19,25), in order to make the test as sensitive as possible.

The λ values we estimated *in vivo* in these patients corresponded very closely with those from our animal studies. λ in damaged tissue ranged from 0.6 to over 1.0 ml/g. Based on previous studies, the absolute value of λ may give some information about the severity of tissue damage or the length of occlusion in reperfused infarctions (32). Although in the clinical setting the true length of occlusion may be difficult to ascertain, the *in vivo* determination of λ, if it is related to the severity of tissue damage, may have some prognostic value and thus some impact on further treatment. In this limited number of patients, no relationship could be drawn between λ and the time between the onset of symptoms to the initiation of reperfusion therapy ($r = 0.27$, $p = 0.66$).

The time it took to complete this study, 1½ - 2 hours, was fairly long. The initial imaging before the bolus injection of Gd-DTPA took 30-40 minutes followed by a 35 minute wait during the constant infusion; then, equilibrium imaging and the dobutamine study took 40-50 minutes. The length of the study could be shortened in a number of ways. We have previously shown in humans and animals that 10-15 minutes is sufficient in order reach equilibrium in regions with blood flow at least 10% of normal; we chose to wait longer in order to be absolutely sure that equilibrium had been reached and thus, the 35 minute wait for equilibrium could be shortened. Alternatively, we could use that period to perform the dobutamine stress test which takes approximately 20 minutes. Since the dobutamine test was not the most important part of our protocol we did not want subjects to withdraw from the study due to discomfort during dobutamine before we performed equilibrium MR imaging. Finally, during the constant infusion, tissue concentrations are relatively stable so we could perform the initial part of the study which was done prior to the bolus injection, and then start the infusion outside of the magnet,

allowing another patient to be imaged. After an average study length of 30-45 minutes. the cardiac patient could be placed back into the magnet for equilibrium imaging. There are numerous possibilities for the protocol but the choice would depend on individual centres and would be based on the needs of the clinician and the availability of equipment.

The MR protocol we used here offers the promise of increased accuracy in the detection of myocardial viability. The extent of infarcted tissue with Gd-DTPA-enhanced MRI compared very closely with that using ^{201}Tl SPECT and the dobutamine study helped to confirm those results. The ability to exactly register both viability and contractility information (using cine MRI) would give the clinician increased flexibility in making decisions, particularly if a relationship between the transmural extent of infarction and the recovery of function existed. In addition, information about regional perfusion using a bolus injection of contrast agent is possible.

5.5.1 Summary

This study showed that a constant infusion technique is feasible in patients and that regions of increased signal intensity compared well with regions of decreased ^{201}Tl uptake. Thus, there is great potential for MRI with Gd-DTPA in the determination of myocardial viability. A more complete clinical trial is recommended in a larger number of patients.

5.6 References

1. V. Dilsizian, R.O. Bonow, Current diagnostic techniques of assessing myocardial viability in patients with hibernating and stunned myocardium. *Circulation* **87(1)**, 1-20 (1993).
2. R.O. Bonow, V. Dilsizian, A. Cuocolo, S.L. Bacharach, Identification of viable myocardium in patients with chronic coronary artery disease and left ventricular dysfunction. Comparison of thallium scintigraphy with reinjection and PET imaging with ^{18}F-fluorodeoxyglucose. *Circulation* **83,** 26-37 (1991).
3. C. Le Feurve, N. Baubion, N. Aubry, J.P. Metzger, P. de Vernejoul, A. Vacheron, Assessment of reversible dyssnergic segments after acute myocardial infarction: Dobutamine echocardiography versus thallium-201 single photon emission computed tomography. *Am. Heart. J.* **131**, 668-675 (1996).
4. A. Elhendy, G. Trocino, A. Salustri, J.H. Cornel, J.R.T.C Roelandt, E. Boersma, R.T. van Domburg, R.P. Krenning, G.M. El-Said, P.M. Fioretti, Low-dose dobutamine echocardiography and rest-redistribution thallium-201 tomography in the assessment of spontaneous recovery of left ventricular function after recent myocardial infarction. *Am. Heart J.* **131**, 1088-1096 (1996).
5. R. Sciagrà, G.M. Santoro, G. Bisi, P. Pedenovi, P.F. Fazzini, A. Pupi, A., Rest-redistribution thallium-201 SPECT to detect myocardial viability. *JNM* **39**, 384-390 (1998).
6. V. Dilsizian, P. Perrone-Filardi, J.A. Arrighi, S.L. Bacharach, A.A. Quyyumi, N.M.T. Freedman, R.O. Bonow, Concordance and iscordance between stress-redistribution-reinjection and rest-redistribution thallium imaging for assessing viable myocardium. Comparison with metabolic activity by positron emission tomography. *Circulation* **88**, 941-952 (1993).
7. W.J. Manning, D.J. Atkinson, W. Grossman, S. Paulin, R.R. Edelman, First-pass nuclear magnetic resonance imaging studies using Gd-DTPA in patients with coronary artery disease. *JACC* **18**, 959-965 (1991).
8. E.G. Walsh, M. Doyle, M.A. Lawson, G.G. Blackwell, G.M. Pohost, Multislice first-pass myocardial perfusion imaging on a conventional clinical scanner. *Magn. Reson. Med.* **34,** 39-47 (1995).
9. K. Lauerma, K. Virtanen, L.M. Sipilä, P. Hekali, H.J. Aronen, Multislice MRI in assessment of myocardial perfusion in patients with single-vessel proximal anterior descending coronary artery disease before and after revascularization. *Circulation* **96**, 2859-2867 (1997).
10. F.P. van Rugge, E.E. van der Wall, S.J. Spanjersberg, A. de Roos, N.A.A. Matheijssen, A.H. Zwinderman, P.R.M. Dijkman, J.H.C. Reiber, A.V.G. Bruschke, Magnetic resonance imaging during dobutamine stress for detection and localization of coronary artery disease. Quantitative wall motion analysis using a modification of the centerline method. *Circulation* **90**, 127-138 (1994).
11. F.M. Baer, E. Voth, C.A. Schneider, P. Theissen, H. Schicha, U. Sechtem, Comparison of low-dose dobutamine-gradient-echo magnetic resonance imaging and positron emission tomography with [^{18}F]fluorodeoxyglucose in patients with chronic

coronary artery disease. A functional and morphological approach to the detection of residual myocardial viability. *Circulation* **91,** 1006-1015 (1995).

12. F.M. Baer, E. Voth, E. LaRosée, C.A. Schneider, P. Theissen, H.J. Deutsch, H. Schicha, E. Erdmann, U. Sechtem, Comparison of dobutamine transesophageal echocardiography and dobutamine magnetic resonance imaging for detection of residual myocardial viability. *Am. J. Cardiol.* **78,** 415-419 (1996).
13. M. Jerosch-Herold, N. Wilke, A.E. Stillman, R.F. Wilson, Magnetic resonance quantification of the myocardial perfusion reserve with a Fermi function model for constrained deconvolution. *Med. Phys.* **25**, 73-84 (1998)
14. J.A.C. Lima, R. Jeremy, W. Guier, S. Bouton, E.A. Zerhouni, E. McVeigh, M.B. Buchalter, M.L. Weisfeldt, E.P. Shapiro, J.L. Weiss, Accurate systolic wall thickening by nuclear magnetic resonance imaging with tissue tagging: Correlation with sonomicrometers in normal and ischemic myocardium. *JACC* **21,** 1745-1751 (1993).
15. K. Lauerma, K.S. Virtanen, L.M. Sipilä, P. Hekali, H.J. Aronen, Multislice MRI in assessment of myocardial perfusion in patients with single-vessel proximal left anterior descending coronary artery disease before and after revascularization. *Circulation* **96**, 2859-2867 (1997).
16. J.-P.Vallée, H.D. Sostman, J.R. MacFall, R.E. Coleman, Quantification of myocardial perfusion with MRI and exogenous contrast agents. *Cardiology* **88**, 90-105 (1997).
17. C.Y. Tong, F.S. Prato, A novel fast T_1-mapping method. *JMRI* **4**, 701-708 (1994).
18. C.A. McKenzie, R.S. Pereira, Z. Chen, F.S. Prato, D.J. Drost, Dynamic range of a single shot T_1 mapping method. *Submitted to Magn. Res. Med.* (May 1998).
19. L.A. Piĕrard, M. DeLandsheere, C. Berthe, P. Rigo, H.E. Kulbertus, Identification of viable myocardium by echocardiography during dobutamine infusion in patients with myocardial infarction after thrombolytic therapy: Comparison with positron emission tomography. *JACC* **15,** 1021-1031 (1990).
20. G. Barilla, M. Gheorghiade, M. Alam, F. Khaja, S. Goldstein, Low-dose dobutamine in patients with acute myocardial infarction identifies viable but not contractile myocardium and predicts the magnitude of improvement in wall motion abnormalities in response to coronary revascularisation. *Am. Heart J.* **122**, 1522-1531 (1991).
21. S.C. Smart, S. Sawada, T. Ryan, D. Segar, L. Atherton, K. Berkovitz, P.D.V. Bourdilon, H. Feigenbaum, Low-dose dobutamine echocardiography detects reversible dysfunction after thrombolytic therapy of acute myocardial infarction. *Circulation* **88**, 405-415 (1993).
22. C.G. Cigarroa, C. deFilippi, E. Brickner, L.G. Alvarez, M.A. Wait, P.A. Grayburn, Dobutamine stress echocardiography identifies hibernating myocardium and predicts recovery of left ventricular function after coronary revascularization. *Circulation* **88,** 430-436 (1993).
23. I. Afridi, N.S. Kleiman, A.E. Raizner, W.A. Zoghbi, Dobutamine echocardiography in myocardial hibernation: Optimal dose and accuracy in predicting recovery of ventricular function after coronary angioplasty. *Circulation* **91**, 663-670 (1995).

24. P.A. Marcovitz, V. Shayna, R.A. Horn, A. Hepner, W.F. Armstrong, Value of dobutamine stress echocardiography in determining the prognosis of patients with known or suspected coronary artery disease. *Am. J. Cardiol.* **78**, 404-408 (1996).
25. D.J. Pennell, Underwood, C.C. Manzara, H. Swanton, J.M. Walker, P.J. Ell, D.B. Longmore, Magnetic resonance imaging during dobutamine stress in coronary artery disease. *Am. J. Cardiol.* **70**, 34-40 (1992).
26. F.P. van Rugge, E.E. van der Wall, A. de Roos, A.V.G. Bruschke, Dobutamine stress magnetic resonance imaging for detection of coronary artery disease. *JACC* **22**, 431-439 (1993).
27. P.A.C. Dendale, P.R. Franken, G.-J. Waldman, D.G.E. De Moor, D.A.M. Tombeur, P.F.C. Block, De Roos, A., Low-dosage dobutamine magnetic resonance imaging as an alternative to echocardiography in the detection of viable myocardium after acute infarction. *Am. Heart J.* **130**, 134-140 (1995).
28. E.G. DePuey, A. Rozanski, Using gated technetium-99m-sestamibi SPECT to characterize fixed myocardial defects as infarct or artifact. *JNM* **36**, 952-955 (1995).
29. P. Dendale, P.R. Franken, P. Block, Y. Pratikakis, A. de Roos, Contrast enhanced and functional magnetic resonance imaging for the detection of viable myocardium after infarction. *Am. Heart J.* **135**, 875-880 (1998).
30. N.J. Weissman, M.W. Levangie, J.B. Newell, L. Guerrero, A.E. Weyman, M.H. Picard, Effect of β-adrenergic receptor blockade on the physiologic response to dobutamine stress echocardiography. *Am. Heart J.* **130**, 248-253 (1995).
31. N.J. Weissman, M.W. Levangie, J.L. Guerrero, A.E. Weyman, M.H. Picard, Effect of β-blockade on dobutamine stress echocardiography. *Am. Heart J.* **131**, 698-703 (1996).
32. J. Schwitter, M. Saeed, M.F. Wendland, N. Derugin, E. Canet, R.C. Brasch, C.B. Higgins, Influence of severity of myocardial injury on distribution of macromolecules: Extravascular versus intravascular gadolinium-based magnetic resonance contrast agents. *JACC* **30**, 1086-1094 (1997).

6 Summary

6.1 Conclusions

The objectives presented in the introduction were used to justify our hypothesis that increased λ is indicative of infarcted tissue in an animal model. In addition, the hypothesis was shown to be correct in human patients with acute myocardial infarction.

6.1.1 The determination of myocardial viability in acute reperfused myocardial infarction; animal studies (objectives i and ii)

While many previous studies have examined signal enhancement in damaged tissue in both animals and humans, my studies characterized the reasons behind signal enhancement, *ie*: increased λ and also the evolution of λ with time after reperfusion. During a constant infusion of Gd-DTPA, the regional tissue concentration of Gd-DTPA is related to the partition coefficient of Gd-DTPA; since MR signal intensity is dependent on Gd concentration, these regions with increased partition coefficient will appear as regions of increased signal intensity. The results of Chapters 2 and 3 showed that the partition coefficient of Gd-DTPA (λ) was inversely related to the uptake of ^{201}Tl, an accepted indicator of viability. In addition, λ in damaged tissue began to increase as early as 1 minute and stayed increased over normal tissue for 8 weeks after reperfusion. The studies suggested that beyond 6 weeks infarcted tissue still had increased λ but this was not discernible using tissue sections; however, high resolution T_1-weighted images of excised hearts at 8 weeks showed thin regions of increased signal intensity. The studies in Chapters 2 and 3 also showed that even in regions with very low blood flow, *ie*: less than 10% of normal values, increased λ was seen in damaged regions by one hour after the start of the constant infusion protocol. Thus, a high resolution assessment of myocardial viability is possible using MRI with Gd-DTPA.

In chapter 3 I validated a method to estimate λ *in vivo* from image signal intensities. Although this technique had been used previously by other groups it had not been validated using a technique such as radioactive counting of tissue samples (a technique that did not allow us to follow changes of λ *in vivo*).

6.1.2 Studies of chronic coronary artery occlusion (objective iii)

In Chapter 4, limited studies in a canine model of chronic coronary artery occlusion were described. The left anterior descending coronary artery was occluded for 4 hours, 2 days and 1 week in separate dogs. After 4 hours of occlusion no changes were seen in λ but after 2 days or more, substantial increases of λ in damaged tissue were seen. These results were similar to previous animal and human studies of non-reperfused infarctions. In our studies blood flow in the occluded territory increased with duration of occlusion, most likely due to collateral circulation; in the normal canine myocardium there is fairly extensive collateral circulation compared to the normal human myocardium. However, since most acute myocardial infarctions occur in the setting of coronary arteries gradually narrowed by atherosclerosis the collateral circulation in these patients may be extensive (1, 2) and similar to that in the normal canine myocardium (3). Therefore, even patients without reperfusion could be expected to have some flow to territories in which the main coronary artery is blocked which would allow the entry of Gd-DTPA.

6.1.3 The clinical evaluation of myocardial viability (objective iv)

The final step in the development of any diagnostic test is evaluating its clinical utility. Chapter 5 contained results from 7 patients studied 8.9 ± 1.1 days after presentation to the emergency room with acute myocardial infarction (AMI). Six of these patients received thrombolytic therapy. A rest-redistribution ^{201}Tl SPECT study was

performed as a gold standard for myocardial viability. The following day the MRI study was performed; it consisted of a bolus injection of Gd-DTPA to examine qualitative differences in regional blood flow and then equilibrium imaging during a constant infusion of Gd-DTPA to locate regions of infarcted myocardium. Finally, a stress study using cine MRI with dobutamine was administered as a further confirmation that the distribution volume of Gd-DTPA could characterize tissue viability.

The results of ^{201}Tl SPECT and MRI agreed very well both qualitatively (visual examination of infarct location and size) and quantitatively (correlation of MRI and SPECT signal intensities in corresponding segments). The correlation coefficients in the quantitative evaluation were quite similar to those calculated during the animal studies in chapters 2 and 3. λ was estimated *in vivo* and the values in damaged and normal tissue, 0.83±0.20 ml/g *vs* 0.36±0.05 ml/g respectively ($p = 0.002$), were very similar to those determined in the animal studies. The dobutamine stress test showed that in regions of myocardium with increased MRI signal intensity, wall thickening index (WTI, a measure of myocardial contractility) failed to increase during dobutamine infusion while in normal myocardium WTI increased significantly (-3.0±9.4 %, $p=0.32$,22.2±8.5%, $p<0.0001$). Thus, the results of this study showed that increased signal intensity on MRI images during a constant infusion of Gd-DTPA was related to myocardial viability detected by both ^{201}Tl SPECT and dobutamine stress testing.

6.2 Implications and Future Work

MRI has great potential for all aspects of cardiac imaging and recent advances in hardware and software have increased the speed and quality of the images that are produced. The information required by a cardiologist will depend on the patient in question but it is conceivable that much of this information may be available in a single

MR examination rather than a combination of many diagnostic tests. An integrated MRI cardiac exam could include the determination of cardiac anatomy or morphology, function and functional reserve, regional blood flow, and viability.

6.2.1 Cardiac Imaging for Acute Myocardial Infarction

6.2.1.1 Morphology

MR imaging is recognized for its ability to assess cardiac anatomy. Using MRI techniques, ventricular size and mass can be determined accurately even if the ventricle is deformed or misshapen. With newer techniques, the entire heart can be imaged within a few breath-holding periods. Recently, techniques for MR coronary angiography have been developed (4); although still in the development stage, the addition of this test would greatly enhance the value of an MRI cardiac exam.

6.2.1.2 Function

Echocardiography is the most widely used technique to determine myocardial function due to its portability and ease of use (5). However, cine MRI, as used in chapter 5, is a powerful technique for analyzing myocardial function due to the quality of the MR images. Using cine MRI, wall thickening and ejection fraction can be accurately assessed and quantitated (6). In addition, MR tissue tagging offers new possibilities for quantitating myocardial function (7). These techniques can be combined with dobutamine either to look for contractile reserve in stunned or hibernating tissue or to detect tissue with critical stenoses (using high doses of dobutamine as mentioned in the introduction) (8).

6.2.1.3 Regional Myocardial Blood Flow

Although not addressed directly in this thesis the determination of absolute myocardial blood flow is very important. As mentioned previously, hibernating tissue arguably has the most to benefit from revascularization since stunned tissue already has

adequate blood flow and will recover spontaneously. In addition, the determination of absolute myocardial blood flow may have important implications in deciding on patient care or evaluating treatment. In Chapter 5 we used enhancement patterns on signal intensity *vs* time curves after a bolus injection of Gd-DTPA to qualitatively evaluate perfusion deficits. Other groups have related semi-quantitative measures of enhancement curves (*eg*: initial slope or time to peak signal intensity) to flow or flow reserve with some success (9). Unfortunately, tissue enhancement patterns are dependent not only on regional blood flow but also on partition coefficient and the shape of the arterial input curve so in order to accurately determine flow, tracer kinetic modelling taking all of these parameters into account, must be used. Several groups have developed promising tracer kinetic models for myocardial tissue and these are under investigation (10, 11). However, there is an additional problem that the pulse sequence used must have adequate dynamic range; the signal intensity of such a sequence must behave linearly with the large range of contrast agent concentrations during bolus transit. Current imaging sequences have limited dynamic range which limits the accuracy and/or precision of data and hence the fitted parameters (11). Our group and others have developed imaging sequences that show promise in this regard but their utility remains to be proven (12-14).

6.2.1.4 Viability

Finally, the determination of myocardial viability using a constant infusion of Gd-DTPA was the major goal of the work presented in this thesis. The benefits of a constant infusion protocol were clear in regards to viability determination. A constant infusion protocol will remove the confounding effects of regional blood flow from the determination of myocardial viability. After a bolus injection, Gd-DTPA is cleared from the blood so signal intensity will be dependent on both regional blood flow and partition

coefficient (15). At equilibrium during a constant infusion, signal intensity is dependent primarily on λ and hence viability.

The use of MRI offers the potential for a high resolution assessment of viability and this may have important implications for patient treatment and prognosis. There are no currently available methods to detect the extent of infarcted tissue with this resolution. As mentioned in the introduction there is evidence that the transmural extent of an infarct may relate to its ability to contract (16). Although most current revascularization procedures attempt to reperfuse large territories (*ie*: angioplasty or bypass surgery revascularize entire coronary artery territories), newer techniques such as trans-myocardial laser revascularization seek to restore blood flow to more limited areas (17). It may be quite important to avoid unnecessary stress to a patient caused by revascularizing an infarcted area using such an invasive technique. However, the real potential for MRI has not yet been realized. Future work needs to be focussed on the clinical implications of extent of damage, *eg*: what degree of myocardial damage is inconsistent with patient survival? These questions will most likely need to be answered using larger scale clinical trials involving multiple centres in order to have the necessary patient base to complete the studies in a reasonable amount of time.

6.2.2 Future Work

These results should apply to any extracellular tracer as long as it is inert (*ie*: not involved in metabolism). There have been studies of contrast enhancement between normal and infarcted tissue using other extracellular tracers (15,18-22). We chose Gd-DTPA since it was a widely studied tracer which has been administered to a large number of patients with few ill effects (23). However, Gd-DTPA is ionic and transient

hemodynamic effects have been shown to occur during bolus administration (24). It might be beneficial to use a non-ionic agent to avoid these effects.

The detection of viable myocardium in territories with greatly reduced blood flow, as in Chapter 4, is very important since these areas have the greatest potential to benefit from revascularization treatment (tissue referred to as hibernating myocardium as opposed to stunned myocardium which recovers spontaneously) (25). Future work should examine changes in λ and the detection of these changes with MRI and Gd-DTPA in tissue with chronically reduced blood flow to determine the value of λ in hibernating versus infarcted myocardium.

Finally, the non-invasive estimation of λ *in vivo* may have clinical importance since there is currently evidence to suggest that the absolute magnitude of λ may be related to the severity of damage in reperfused infarcted tissue (26,27). Additional studies need to be performed to evaluate the importance of the absolute value of λ in terms of tissue damage and clinical decision making.

6.3 Summary of Thesis

This thesis examined whether the partition coefficient of Gd-DTPA (λ) was related to myocardial viability in myocardial tissue damaged by acute and chronic coronary artery occlusion. During a constant infusion of Gd-DTPA the tissue concentration of the agent is primarily related to λ. In a canine model λ was increased in damaged tissue as early as 1 minute after reperfusion and stayed increased for at least 6 weeks. This increased λ in infarcted regions results in increased signal intensity on MR images. In addition, a technique to estimate λ *in vivo* was validated. A limited clinical trial of the technique which compared contrast-enhanced MRI to established methods of assessing viability

such as rest-redistribution ^{201}Tl SPECT and dobutamine stress testing showed that MRI with Gd-DTPA was accurate in detecting viability after coronary artery occlusion with or without reperfusion. Larger scale trials of the clinical utility of the technique in order to demonstrate its diagnostic and prognostic potential still need to be carried out but MRI with Gd-DTPA shows great promise in the non-invasive determination of myocardial viability.

6.4 References

1 W.D. Nitzberg, H.P. Nath, W.J. Rogers, W.P. Hood, P.L. Whitlow, R. Reeves, W.A. Baxley, Collateral flow in patients with acute myocardial infarction. *Am. J. Cardiol.* **56,** 729-736 (1985).

2 S. Sasayama, M. Fujita, Recent insights into coronary collateral circulation. *Circulation* **85,** 1197-1204 (1992).

3 M.P. Maxwell, D.J. Hearse, D.M. Yellon, Species variation in the coronary collateral circulation during regional myocardial ischaemia: a critical determinant of the rate of evolution and extent of myocardial infarction. *Card. Res.* **21,** 737-746 (1987).

4 P.G. Danias, R.R. Edelman, W.J. Manning, Coronary MR angiography. *in* "Cardiac Magnetic Resonance Imaging" (Reichek, N., Ed), *Cardiology Clinics* **16(2),** 207-225 (1998).

5 E.A. Geiser, Echocardiography: Physics and instrumentation. *in* "Cardiac Imaging" (D.J. Skorton, H.R. Schelbert, G.L. Wolf, .H. Brundage, Eds), p.273, W.B. Saunders, Toronto 1996.

6 R.M. Peshock, W.G. Hundley, D.L. Willett, D.E. Sayad, M.P. Chwialkowski, Quantitative magnetic resonance imaging of the heart. *in* "Cardiac Imaging" (Skorton, D.J., Schelbert, H.R, Wolf, G.L., Brundage, B.H, Eds), p.759, W.B. Saunders, Toronto, 1996.

7 E. McVeigh, Regional myocardial function. *in* "Cardiac Magnetic Resonance Imaging" (Reichek, N., Ed), *Cardiology Clinics* **16(2),** 189-206 (1998).

8 T. Ryan, Stress Echocardiography *in* "Cardiac Imaging" (D.J. Skorton, H.R. Schelbert, G.L. Wolf, .H. Brundage, Eds), p.503, W.B. Saunders, Toronto, 1996.

9 K. Lauerma, K. Virtanen, L. Sipilä, P. Hekali, H.J. Aronen, Multislice MRI in assessment of myocardial perfusion in patients with single-vessel proximal anterior descending coronary artery disease before and after revascularization. *Circulation* **96,** 2859-2867 (1997).

10 R.K. Singal, T.-Y. Lee, H.A. Razvi, H. Mosalei, J.D. Denstedt, S.S. Chun, J. Bennett, W. Romano, M. Toll, Evaluation of doppler ultrasonography and dynamic contrast-enhanced CT in acute and chronic renal obstruction. *J. Endourol.* **11,** 5-13 (1997).

11 M. Jerosch-Herold, N. Wilke, A.E. Stillman, R.F. Wilson, Magnetic resonance quantification of the myocardial perfusion reserve with a Fermi function model for constrained deconvolution. *Med. Phys.* **25,** 73-84 (1998)

12 C.Y. Tong, F.S. Prato, A novel fast T_1-mapping method. *JMRI* **4,** 701-708 (1994).

13 C.A. McKenzie, R.S. Pereira, Z. Chen, F.S. Prato, D.J. Drost, Dynamic range of a single shot T_1 mapping method. *Submitted to Magn. Res. Med.* (May 1998).

14 S. Ding, S.D. Wolff, F.H. Epstein, Improved coverage in dynamic contrast-enhanced cardiac MRI using interleaved gradient-echo EPI. *Magn. Reson. Med.* **39,** 514-519 (1998).

15 R.M. Judd, C.H. Lugo-Olivieri, M. Arai, T. Kondo, P. Croisille, J.A.C. Lima, V. Mohan, L.C. Becker, E.A. Zerhouni, Physiological basis of myocardial contrast

enhancement in fast magnetic resonance images of 2-day old reperfused canine infarcts. *Circulation* **92,** 1902-1910 (1995).

16 A.N. Lieberman, J.L. Weiss, B.I. Jugdutt, L.C. Becker, B.H. Bulkley, J.H. Garrison. G.M. Hutchins, C.A. Kallman, M.L. Weisfeldt, Two-dimensional echocardiography and infarct size: Relationship of regional wall motion and thickening to the extent of myocardial infarction in the dog. *Circulation* **63,** 739-745 (1981).

17 M. Mirhoseini, S. Shelgikar, M.M. Cayton, New concepts in revascularization of the myocardium. *Ann. Thorac. Surg.* **45,** 415-420 (1988).

18 M. Ovize, D. Revel, M. de Lorgeril, J.-B. Pichard, G. Dandis, J. Delaye, R. Renaud, M. Amiel, Quantitation of reperfused myocardial infarction by Gd-DOTA-enhanced magnetic resonance imaging. An experimental study. *Invest. Radiol.* **26,** 1065-1070 (1991).

19 R.M. Judd, C.H. Lugo-Olivieri, M. Arai, T. Kondo, P. Croisille, J.A.C. Lima, V. Mohan, L.C. Becker, E.A. Zerhouni, Physiological basis of myocardial contrast enhancement in fast magnetic resonance images of 2-day-old reperfused canine infarcts. *Circulation* **92,** 1902-1910 (1995).

20 J.A.C. Lima, R.M. Judd, A. Bazille, S.P. Schulman, E. Atalar, E.A. Zerhouni. Regional heterogeneity of human myocardial infarcts demonstrated by contrast-enhanced MRI: Potential mechanisms. *Circulation* **92,** 1117-1125 (1995).

21 E.R. Holman, A.C. van Rossum, T. Doesburg, E.E. van der Wall, A. de Roos, C.A. Visser, Assessment of acute myocardial infarction in man with magnetic resonance imaging and the use of a new paramagnetic contrast agent gadolinium-BOPTA. *Magn. Res. Imag.* **14,** 21-29 (1996).

22 P. Dendale, P.R. Franken, P. Block, Y. Pratikakis, A. de Roos, Contrast enhanced and functional magnetic resonance imaging for the detection of viable myocardium after infarction. *Am. Heart J.* **135,** 875-880 (1998).

23 H.A. Goldstein, F.K. Kashanian, R.F. Blumetti, W.L. Holyoak, F.P. Hugo, D.M. Blumenfield, Safety assessment of gadopentetate dimeglumine in US clinical trials. *Radiology* **174,** 17-23 (1990).

2424 A. Mühler, M. Saedd, R.C. Brasch, C.B. Higgins, Hemodynamic effects of bolus injection of gadodiamide injection and gadopentetate dimeglumine as contrast media at MR imaging in rats. *Radiology* **183,** 523-528 (1992).

25 E. Braunwald, J.D. Rutherford, Reversible ischemic left ventricular dysfunction: Evidence for the "hibernating myocardium". *JACC* **8,** 1467-1470 (1986).

26 J. Schwitter, M. Saedd, M.F. Wendland, N. Derugin, E. Canet, R.C. Brasch, C.B. Higgins, Influence of severity of myocardial injury on distribution of macromolecules: Extravascular versus intravascular gadolinium-based magnetic resonance contrast agents. *JACC* **30,** 1086-1094 (1997).

27 M.F. Wendland, M. Saeed, E. Canet, C.B. Higgins, Potential measurement of viable cell fraction in reperfused myocardial infarction using Gd-enhanced IR-EPI. *in* "Proceedings of 5th Annual Meeting of ISMRM", 1997, Vancouver, BC, Canada, p.846.

Appendix A Copyright Release from the journal *Magnetic Resonance in Medicine*

St Joseph's Health Centre
London

268 Grosvenor St., London, Ontario N6A 4V2
Telephone (519) 646-6100 Ext. 4328

Department of Nuclear Medicine & Magnetic Resonance

July 22 1998
(519) 646 6100 x.4682
FAX: (519) 646 6135
rpereira@lri.stjosephs.london.on.ca

Carol Richman
Permission and Copyright
Williams and Wilkins
351 Camden Street
Baltimore MD 21201-2436

Ms. Richman,

I am writing to request copyright releases for two articles of which I am first author and would like to include in my Ph.D. thesis. One article has been published in *Magnetic Resonance in Medicine* and the second article has been accepted pending revisions. The papers are:

MRM-98-3742
Assessment of myocardial viability using MRI during a constant infusion of Gd-DTPA; further studies at early and late periods of reperfusion.
Raoul S. Pereira, Frank S. Prato, Jane Sykes, Gerald Wisenberg
(Revisions currently under review)

MRM-95-2585
The determination of myocardial viability using Gd-DTPA in a canine model of acute myocardial ischemia and reperfusion.
Raoul S. Pereira, Frank S. Prato, Gerald Wisenberg, Jane Sykes
(Published November 1996).

Would it be possible to have these releases faxed to me at the above number since I need them before August 12 1998. Otherwise, they can be mailed to Raoul Pereira, Department of Nuclear Medicine, St. Joseph's Health Centre, London, Ontario, Canada N6A 4V2.

Thank you very much for your help

Raoul Pereira

Raoul Pereira
Ph.D. Candidate
Department of Medical Biophysics

Permission granted
Provided a reference
line is placed.

Debbie Heise
7-27-98

Appendix B Animal Experimentation Ethics Approvals 1993-1998

The UNIVERSITY *of* WESTERN ONTARIO

University Council on Animal Care
Animal Use Subcommittee

August 27, 1998

Dear Dr. Prato:

Your "Application to Use Animals for Research or Teaching" entitled:

"Magnetic Resonance Imaging of Ischemic Heart Disease "
Funding Agency– MRC

has been approved by the University Council on Animal Care. This approval expires in one year on the last day of the month. The number for this project is 98194-08 and replaces 97153-7 .

1. This number must be indicated when ordering animals for this project.
2. Animals for other projects may not be ordered under this number.
3. If no number appears please contact this office when grant approval is received.
   If the application for funding is not successful and you wish to proceed with the project, request that an internal scientific peer review be performed by the Animal Use Subcommittee office.
4. Purchases of animals other than through this system must be cleared through the ACVS office. Health certificates will be required.

ANIMALS APPROVED

Canine	-	Beagle, 1-3 yrs., M/F	-	25

STANDARD OPERATING PROCEDURES

Procedures in this protocol should be carried out according to the following SOPs. Please contact the Animal Use Subcommittee office (661-2111 ext. 6770) in case of difficulties or if you require copies. SOP's are also available at http://www.uwo.ca/animal/acvs

310 Holding Period Post Admission
320 Euthanasia
322 Criteria for Early Euthanasia - Non-rodent

REQUIREMENTS/COMMENTS

Please ensure that individual(s) performing procedures on live animals, as described in this protocol, are familiar with the contents of this document.

1. 3 stage surgical prep to be used.

After hours emergency contact is: J. Sykes - 293-3310

c.c. Approved Protocol - F. Prato, J. Sykes, D. Forder
Approval Letter - J. Sykes, D. Forder

The UNIVERSITY *of* WESTERN ONTARIO

University Council on Animal Care
Animal Use Subcommittee

July 10, 1997

Dear Dr. Prato:

Your "Application to Use Animals for Research or Teaching" entitled:

"Magnetic Resonance Imaging of Ischemic Heart Disease""
Funding Agency: MRC

has been approved by the University Council on Animal Care. This approval expires in one year on the last day of the month. The number for this project is # 97153-7. This replaces #96122-7.

1. *This number must be indicated when ordering animals for this project.*
2. *Animals for other projects may not be ordered under this number.*
3. *If no number appears on this approval please contact this office when grant approval is received. If the application for funding is not successful and if you wish to proceed with the project, request that an internal scientific peer review be performed by the Animal Use Subcommittee office.*
4. *Purchases of animals other than through this system must be cleared through the ACVS office. Health certificates will be required.*

ANIMALS APPROVED

Canine	–	*Beagles, 1-2 yrs., 10-12 kgs., F*	–	*25*

REQUIREMENTS/COMMENTS

Please ensure that individual(s) performing procedures on live animals, as described in this protocol, are familiar with the contents of this document.

1. Please ensure that the old protocol number (#96122-7) is replaced by the new protocol number (#97153-7) on all pertinent animal records, cards, door signs, etc. All personnel ordering animals must also be informed of this new protocol number.

c.c. *Approved Renewal* – *L. Prato, J. Sykes, P. Schoffer*
Approval Letter – *J. Sykes, P. Schoffer*

The UNIVERSITY of WESTERN ONTARIO

University Council on Animal Care
Animal Use Subcommittee

June 13, 1996

Dear Dr. Prato:

Your "Application to Use Animals for Research or Teaching" entitled:

"Magnetic Resonance Imaging of Ischemic Heart Disease"
Funding Agency: MRC

has been approved by the University Council on Animal Care. This approval expires in one year on the last day of the month. The number for this project is # 96122-7. This replaces #95147-7.

1. This number must be indicated when ordering animals for this project.
2. Animals for other projects may not be ordered under this number.
3. If no number appears on this approval please contact this office when grant approval is received. If the application for funding is not successful and if you wish to proceed with the project, request that an internal scientific peer review be performed by your animal care committee.
4. Purchases of animals other than through this system must be cleared through the ACVS office. Health certificates will be required.

ANIMALS APPROVED

Dogs	-	Beagles, 8-15 kg., females	20

REQUIREMENTS/COMMENTS

Please ensure that individual(s) performing procedures, as described in this protocol, are familiar with the contents of this document.

c.c. Approved Renewal - F. Prato, P. Schoffer
Approval Letter - P. Schoffer

The UNIVERSITY of WESTERN ONTARIO

Council on Animal Care • Animal Care and Veterinary Services
Director - Michele M. Bailey, D.V.M.
Clinical Veterinarian - Susan H. Fussell, D.V.M.

July 30, 1995

Dear Dr. Prato:

Your "Application to Use Animals for Research or Teaching" entitled:

"Magnetic Resonance Imaginf of Ischaemic Heart Disease"

Funding Agency: MRC - M316C8

has been approved by the University Council on Animal Care. This approval expires in one year on the last day of the month. The number for this project is #95147-7. This replaces #94179-7.

1. This number must be indicated when ordering animals for this project.
2. Animals for other projects may not be ordered under this number.
3. If no number appears on this approval please contact this office when grant approval is received. If the application for funding is not successful and if you wish to proceed with the project, request that an internal scientific peer review be performed by your animal care committee.
4. Purchases of animals other than through this system must be cleared through the ACVS office. Health certificates will be required.

ANIMALS APPROVED

Dogs - Beagles - 20

REQUIREMENTS/COMMENTS

Please ensure that individual(s) performing procedures, as described in this protocol, are familiar with the contents of this document.

c.c. Approved Renewal - F. Prato, P. Schoffer
Approval Letter - P. Schoffer, Office of Research Services

MBailey

Health Sciences Centre • London, Ontario • Canada • N6A 5C1 • Telephone: (519) 661-3034 • Fax: (519) 661-2028

The UNIVERSITY *of* WESTERN ONTARIO

Council on Animal Care • Animal Care and Veterinary Services
Director - Michele M. Bailey, D.V.M.
Clinical Veterinarian - Susan H. Fussell, D.V.M.

July 25, 1994

Dear Dr. Prato:

Your "Application to Use Animals for Research or Teaching" entitled:

"Magnetic Resonance Imaging of Ischaemic Heart Disease"

has been approved by the University Council on Animal Care. This approval expires in one year on the last day of the month. The number for this project is # 94179-7

1. This number must be indicated when ordering animals for this project.
2. Animals for other projects may not be ordered under this number.
3. If no number appears on this approval please contact this office when grant approval is received. If the application for funding is not successful and if you wish to proceed with the project, request that an internal scientific peer review be performed by your animal care committee.
4. Purchases of animals other than through this system must be cleared through the ACVS office. Health certificates will be required.

ANIMALS APPROVED

Dogs – Beagles – 25

REQUIREMENTS/COMMENTS

Please ensure that individual(s) performing procedures, as described in this protocol, are familiar with the contents of this document.

SURTIA – September 14, 1993 – Approved.

c.c. D. Hill
P. Schoffer

MBailey

Health Sciences Centre ••London, Ontario ••Canada ••N6A 5C1 ••Telephone: (519) 661-3034 ••Fax: (519) 661-2028

The UNIVERSITY *of* WESTERN ONTARIO

Council on Animal Care • Animal Care and Veterinary Services
Director - Michele M. Bailey, D.V.M.
Clinical Veterinarian - Susan H. Fussell, D.V.M.

October 12, 1993

Dear Dr. Prato:

Your "Application to Use Animals for Research or Teaching" entitled:

"Magnetic Resonance Imaging of Ischaemic Heart Disease"

has been approved by the University Council on Animal Care. This approval expires in one year on the last day of the month. The number for this project is # 93280-10

1. This number must be indicated when ordering animals for this project.
2. Animals for other projects may not be ordered under this number.
3. If no number appears on this approval please contact this office when grant approval is received. If the application for funding is not successful and if you wish to proceed with the project, request that an internal scientific peer review be performed by your animal care committee.
4. Purchases of animals other than through this system must be cleared through the ACVS office. Health certificates will be required.

ANIMALS APPROVED

Dogs – Beagles – 15

REQUIREMENTS/COMMENTS

Please ensure that individual(s) performing procedures, as described in this protocol, are familiar with the contents of this document.

The Committee would like to thank you for your clearly written "lay summary".

c.c. **D. Hill**
P. Schoffer

Health Sciences Centre • London, Ontario • Canada • N6A 5C1 • Telephone: (519) 661-3034 • Fax: (519) 661-2028

Appendix C Human Experimentation Protocol Approval

IMAGE EVALUATION
TEST TARGET (QA-3)

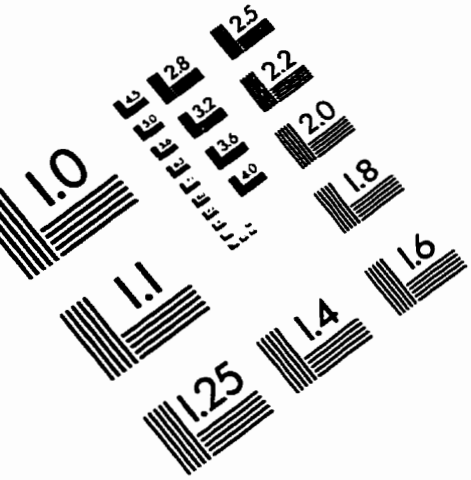

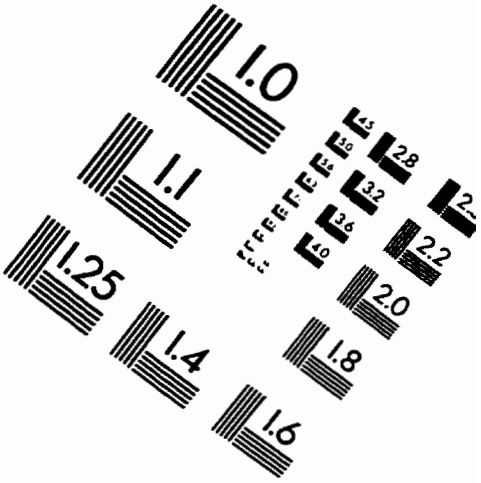

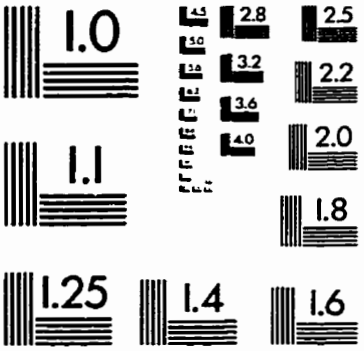

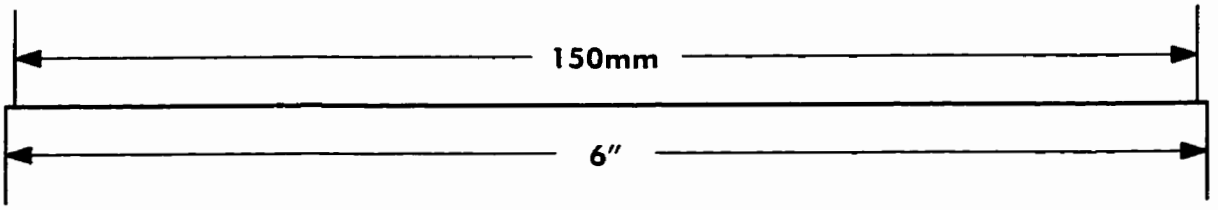

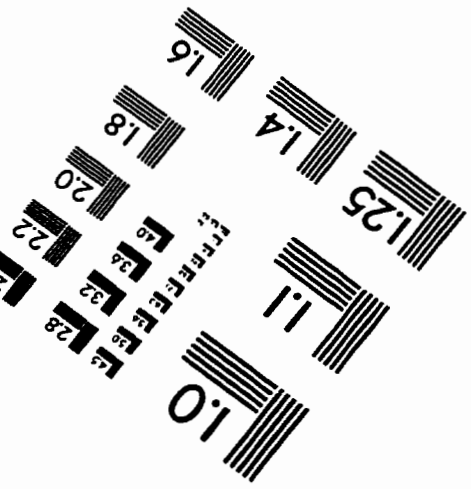

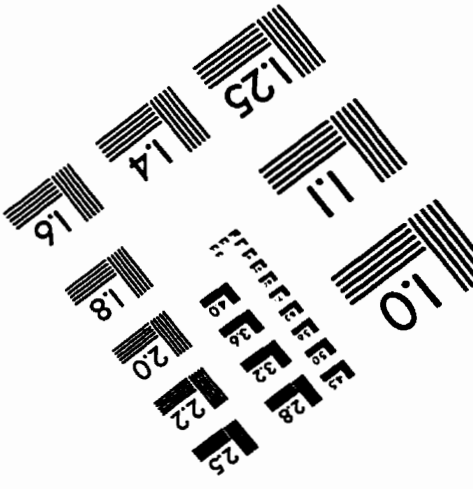

APPLIED IMAGE, Inc
1653 East Main Street
Rochester, NY 14609 USA
Phone: 716/482-0300
Fax: 716/288-5989